# Probabilistic design of settling basins for environmental compliance

## Development and evaluation of a risk-based approach

**Master's thesis**
William de Lange
Delft, 8 April 2011

Delft University of Technology

# Probabilistic design of settling basins for environmental compliance
## Development and evaluation of a risk-based approach

Master's thesis

William de Lange
8 April 2011

### Graduation committee

| | |
|---|---|
| Prof.drs.ir. J.K. Vrijling | Delft University of Technology (chairman) |
| Dr.ir. G.J. de Boer | Delft University of Technology |
| Dr.ir. P.H.A.J.M. van Gelder | Delft University of Technology |
| Ir. C. den Heijer | Delft University of Technology |
| Dr.ir. M. van Koningsveld | Van Oord Dredging and Marine Contractors BV |
| Dr.ir. Z.B. Wang | Delft University of Technology |

### Student

Name: William de Lange
Student number:
Email:

Faculty of Civil Engineering and Geosciences · Delft University of Technology

The work in this thesis was supported by Van Oord Dredging and Marine Contractors BV. Their cooperation is hereby gratefully acknowledged.



Typesetting: LaTeX

Cover photo: Settling basins in [redacted]
Images: Matlab, Van Oord, Inkscape

# Preface

This thesis is the result of my graduation project and concludes the Master of Science programme at the Faculty of Civil Engineering and Geosciences at Delft University of Technology. This study was initiated by Van Oord Dredging and Marine contractors bv.

I would like to thank my graduation committee for their supervision, advice and support. I would also like to thank prof.dr.ir. L.C. van Rijn and dr.ir. J.C. Winterwerp for their valuable advices and dr.ir. M. van Koningsveld for providing the frame work of the model and for his comments and suggestions. Further I would like to thank my colleagues from the environmental department of Van Oord for answering my questions and the nice working environment.

In particular, I thank my parents, family and friends for their interest and support.

Delft, 1st April 2011

William de Lange

# Summary

There is an increasing public awareness for the potential negative environmental effects of dredging and reclamation projects. Therefore, almost every project requires an environmental impact assessment (EIA). These EIA's usually provide strict environmental requirements that must be taken into consideration in the design and execution of a project. These environmental requirements can form a high risk for contractors because the inability to meet the environmental requirements can result in large fines or downtime. The determination of the environmental impacts of these projects includes large uncertainties. This results in stringent environmental requirements and a conservative approach by the contractor. Understanding these uncertainties leads to a more realistic view of the situation and provides a better basis for establishing the environmental requirements.

The environmental impacts caused by the release of suspended sediments are often an important issue in an EIA. The insight into the released amount of suspended sediment particles is an important link in the investigation into the environmental impacts caused by this release. These impacts can be an increased turbidity due to the suspended sediment. Especially corals are very vulnerable for increased levels of turbidity and it also causes a reduction of photosynthesis by marine life. This study is restricted to provide insight into the emission of suspended sediment particles due to the release of return water. This water is used to pump dredged material to the disposal area after which the excess water is released. Settling basins can be used to remove fines particles from the return water.

The settling of the suspended sediment particles in a settling basin takes time. The remaining concentration of suspended particles in the outflowing water and the discharge give the emission of suspended sediment particles. This outflow concentration is hard to predict due to varying circumstances (e.g. wind, discharge and inflow concentration) and uncertainties in the settling process (e.g. agglomeration of clay particles). A probabilistic approach is a powerful method to incorporate uncertainties. It provides insight into the propagation of these uncertainties in the outflow concentration.

This requires an efficient model (*the project model*) that takes into account the relevant physical processes in a simplified way. With an one-dimensional modelling of the flow profile, the transport of suspended sediment in the two dimensional vertical plane is simulated. Besides the turbulent mixing also processes such as flocculation (agglomeration of clay particles) and secondary flow are included. This enables the project model to provide the concentration of suspended sediment in the vertical plane. Due to its efficiency, the project model is suitable for performing a large number of simulations which is needed for probabilistic calculations.

The project model is compared with measurement data and existing solutions. The results of the comparison with the measurement data are in the same order of magnitude. Although these data are not suitable for calibration, it gives a good indication of the suitability of the model. The project model is also compared with an existing model that is not suitable for probabilistic analysis. This gives similar values for the outflow concentration. The vertical concentration distribution of the models shows a significant difference. The results of the project model are considered most appropriate as the vertical distribution is also taken into account in the transport of suspended sediment. The project model also gives satisfactory results for comparison with an analytical solution of the suspended sediment concentration in the vertical plane.

In order to enable the probabilistic calculation of the outflow concentration a number of statistical distributions is determined for the varying circumstances and uncertainties in the settling process. Therefore, these values are not fixed but have a certain probability of occurrence and represent the uncertainty. A probabilistic analysis of a case study provides insight into the main sources of uncertainty in the outflow concentration. Besides the discharge and the inflow concentration the wind has a significant impact on the outflow concentration due to the additional turbulent mixing and the influence of secondary flows. Especially a direction that is opposite to the flow direction has a negative influence. Furthermore, it appears that the processes related to the clay particles (minimal settling velocity and flocculation) are very decisive. The parameters of these processes are therefore proposed as calibration parameters. There appears to be an optimal basin depth. This is the optimum between the residence time and turbulent mixing. When the basin is deeper than this optimal basin depth the positive effect of the longer residence time is eliminated by the larger turbulent mixing that is caused by the increased depth.

By expressing the environmental risk of the contractor in a financial risk, it is possible to determine an economic optimal design of a settling basin. As the area available for a settling basin can hardly vary within a certain project, the economic optimum is only determined for the basin depth and the discharge (the latter can be considered as the choice of equipment). Because of the limited construction costs of a settling basin, the *economic* optimal basin depth is almost equal to the basin depth for an optimal outflow concentration. For the optimal choice of equipment the costs of equipment also play an important role. In this case, the optimum is between the minimal production costs at an acceptable risk. For this risk, time effects and the time period over which the risk can be spread, play an important role. Finally, the profitability of wind protection for settling basins is investigated. For the case study the risk reduction, appears to be roughly equal to the additional construction costs. For projects with a higher risk, the use of wind protection can be profitable.

The availability of a probabilistic model for determining the outflow concentration of settling basins offers interesting possibilities for the probabilistic analysis of environmental impacts of dredging and reclamation projects. This is because not only emissions are quantified but also insight is provided into the uncertainties and the sources of these uncertainties. This also enables the determination of an economically optimal design of a settling basin and provides insight in the associated financial risks.

# Samenvatting

Er is een steeds groter maatschappelijk bewustzijn voor de mogelijke negatieve effecten van bagger- en landaanwinningprojecten voor de omgeving. Daarom vereist vrijwel ieder project een milieu effect rapportage (MER). Hieruit volgen meestal strikte milieueisen die in acht genomen moet worden bij het ontwerp en de uitvoering van een project. Deze milieueisen kunnen voor aannemers een groot risico vormen, omdat het schenden van de milieueisen kan leiden tot hoge boetes of het stilleggen van de werkzaamheden. De bepaling van de milieueffecten van deze projecten bevat grote onzekerheden. Dit resulteert in strenge milieueisen en een conservatieve aanpak door de aannemer. Inzicht in deze onzekerheden leidt tot een realistischer beeld van de situatie en vormt een betere basis voor het opstellen van de milieueisen.

De milieueffecten die veroorzaakt worden door het vrijkomen van gesuspendeerde sedimentdeeltjes vormen vaak een belangrijk onderdeel van een MER. Het inzichtelijk maken van de vrijkomende hoeveelheid gesuspendeerde sedimentdeeltjes is een belangrijke schakel in het onderzoek naar de milieueffecten die hierdoor veroorzaakt worden. Hierbij kan gedacht worden aan verhoogde troebelheid door de aanwezige sedimentdeeltjes. Vooral koraal is hier erg gevoelig voor en het heeft ook een negatieve invloed op de fotosynthese van het zeeleven. Deze studie beperkt zich tot het inzichtelijk maken van de hoeveelheid gesuspendeerde sedimentdeeltjes die vrijkomen bij het lozen van retourwater. Dit water wordt gebruikt voor het verpompen van baggerspecie naar de stortplaats, waarna het overtollige water wordt geloosd. Sedimentatiebassins kunnen worden gebruikt om de fijne deeltjes uit het retourwater te verwijderen.

Het bezinken van de gesuspendeerde sedimentdeeltjes in het sedimentatiebassin kost veel tijd. De nog aanwezige concentratie van gesuspendeerde deeltjes in het uitstromende water geeft, samen met het debiet, de vrijkomende hoeveelheid gesuspendeerde sedimentdeeltjes weer. Deze uitstroomconcentratie is moeilijk te voorspellen door de onzekerheden in zowel de omgevingscondities (bijv. wind, instroomdebiet en instroomconcentratie) als in het bezinkproces (bijv. samenklontering van kleideeltjes). Met behulp van probabilistische methoden is het mogelijk om de doorwerking van deze onzekerheden in de uitstroomconcentratie inzichtelijk te maken.

Hiervoor is een efficiënt model (*het projectmodel*) opgezet dat de relevante fysische processen op vereenvoudigde wijze simuleert. Met een eendimensionale bepaling van het stroomprofiel, wordt het transport van gesuspendeerd sediment in het tweedimensionale verticale vlak gesimuleerd. Naast de turbulente menging worden ook processen als flocculatie (samenklontering van kleideeltjes) en secundaire stroming meegenomen. Hierdoor kan met het projectmodel de concentratie van gesuspendeerd sediment in het verticale vlak worden bepaald. Door de efficiëntie is het projectmodel geschikt voor het uitvoeren van een groot aantal simulaties dat nodig is voor probabilistische berekeningen.

Het project model is vergeleken met meetdata en bestaande oplossingen. De resultaten van de vergelijking met de meetdata liggen in dezelfde orde van grote. Hoewel deze meetdata niet geschikt is voor kalibratie, geeft het een goede indicatie van de geschiktheid van het model. Daarnaast is het projectmodel ook vergeleken met een bestaand model dat niet geschikt is voor probabilistische analyses. Dit geeft vergelijkbare waarden voor de uitstroomconcentratie. De verticale concentratieverdeling van de modellen vertoont een groot verschil, maar de resultaten van het projectmodel worden beter geacht omdat dit model de verticale verdeling volledig simuleert. Het projectmodel geeft ook bevredigende resultaten voor de vergelijking met een analytische oplossing van de gesuspendeerde sedimentconcentratie in het verticale vlak.

Voor de probabilistische berekening van de uitstroomconcentratie wordt een aantal omgevingscondities en het bezinkproces bepaald op basis van statistische verdelingen. Deze waarden liggen dus niet vast maar hebben een bepaalde kans op voorkomen en vertegenwoordigen hiermee de onzekerheid. Een probabilistische analyse aan de hand van een casus geeft inzicht in de grootste bronnen van de onzekerheid in de uitstroomconcentratie. Naast het debiet en de instroomconcentratie blijkt de wind een behoorlijk grote invloed te hebben. Enerzijds door de extra turbulente menging en anderzijds onder invloed van secundaire stroming. Vooral een windrichting die tegengesteld is aan de stromingsrichting heeft een negatieve invloed. Verder blijken de processen met betrekking tot de kleideeltjes (minimale valsnelheid en flocculatie) erg bepalend. De parameters van deze processen worden daarom voorgesteld als kalibratieparameters. Er blijkt een optimale bassindiepte te zijn. Dit is het optimum tussen de verblijftijd en de turbulente menging. Wanneer het bassin dieper is dan dit optimum, dan wordt het positieve effect van de langere verblijftijd teniet gedaan door de turbulente menging die groter is in diepere bassins.

Door het milieurisico voor de aannemer uit te drukken in een financieel risico is het mogelijk om te komen tot een economisch optimaal ontwerp van een sedimentatiebassin. Daar het oppervlak van het bassin vrijwel altijd bepaald wordt door het project, is dit economische optimum alleen bepaald voor de bassindiepte en het debiet (deze laatste kan worden gezien als de materieelkeuze). Omdat de aanlegkosten van een bassin beperkt zijn, is het *economische* optimum voor de bassindiepte vrijwel gelijk aan de bassindiepte met de optimale uitstroomconcentratie. Voor de optimale materieelkeuze spelen de materieelkosten ook een belangrijke rol. Hier ligt het optimum bij minimale productiekosten tegen een aanvaardbaar risico. Voor dit risico kunnen tijdseffecten en de tijd waarover het risico gespreid kan worden, een belangrijke rol spelen. Ten slotte is de winstgevendheid van windbescherming voor sedimentatiebassins onderzocht. Voor de casus blijkt het risicoverlagende effect ongeveer gelijk te zijn aan de extra aanlegkosten. Voor projecten met een groter risico kan het gebruik van windbescherming zelfs winstgevend zijn.

De beschikbaarheid van een probabilistisch model voor het bepalen van de uitstroomconcentratie van sedimentatiebassins biedt interessante mogelijkheden voor het probabilistisch analyseren van milieueffecten bij bagger- en landaanwinningprojecten. Dit omdat niet alleen de emissie wordt gekwantificeerd, maar ook inzicht wordt gegeven in de onzekerheden en de bronnen van deze onzekerheden. Hierdoor is het ook mogelijk om te komen tot een economisch optimaal ontwerp van een sedimentatiebassin met inzicht in de bijbehorende financiële risico's.

# Contents

# List of Figures

# List of Tables

# Chapter 1

# Introduction

## 1.1 Reason for the research

### Background information

Over the last decades the sustainable reconciliation of economic demands and the natural environment receives increased attention. Public concern for environmental values has grown as a consequence of past negative impacts associated with economic demands. Integration of these concerns in national as well as international policies has made sure that environmental aspects have become a fully recognised part of decision making processes related to large infrastructure. Dredging and reclamation projects are also confronted with these increased environmental interests, as these projects are often executed in sensitive areas that provide habitat to a large variety of flora and fauna. For many developed countries and financiers of dredging projects, an environmental impact assessment (EIA) is a strict requirement that has to be taken into account in the design of the project in order to meet environmental restrictions given by law. This usually results in environmental requirements for the design and execution of the project. For contractors these environmental requirements can form a significant risk as the inability to meet these environmental requirements can have serious financial consequences. Besides a financial risk there also is a societal risk for the contractor, as non-sustainable work methods are likely to generate resistance with the general public.

The tendency to eliminate adverse environmental impacts as much as possible often results in stringent environmental requirements related to the realization of large dredging projects. Complying with these requirements is an important issue for contractors in both the design and execution phase. Prediction of environmental compliance is often difficult due to varying circumstances and uncertainties. This leads to a conservative approach that might be positive from a ecologic perspective, but negative from a budget perspective. Furthermore the investment associated with achieving environmental compliance may result in limited environmental benefits only, where investment of the same amount of money in a different way may provide more beneficial results. Increased insight in the uncertainties associated with large dredging projects enables a more realistic approach. On the one hand it may lead to more realistic environmental impact assessments; an interesting study into the uncertainties of ecological effects is done by van Kruchten (2008). On the other hand it allows contractors to develop risk based execution methods that allow for economic optimization. A probabilistic approach is a powerful method to incorporate uncertainties.

### Environmental impacts of dredging and reclamation

The environmental impacts of dredging and reclamation projects are very project dependent. A number of impacts are directly related to the construction activities such as the removal or burial of habitat. A second direct effect is the increased turbidity due to suspended sediments caused by the dredging or reclamation activities. This can be harmful to bed vegetation. The sedimentation of these fine sediments can result in a layer of fine sediments on the bed that can influence the bottom dwelling organisms. A third effect is the whirling up of organic matter that serves as nutrients for some species and that facilitates the dispersion of species. Impacts which are indirect related to the construction activities are mainly caused by the release of substances into the water and the changes in de hydrography. The substances of the bed can be contaminated and their release can form a risk for aquatic organisms and pollution of the food chain. Changes in hydrography can create different flow patterns and sedimentation rates. In coastal areas also the salinity can be influenced by dredging activities. These changes also can created opportunities for different species which were unable to survive under the natural conditions.

The influence of these effects on the environment is highly dependent on the natural conditions and variations. As long as the natural variation in space and time is of the same order as the variation caused by the dredging activities, the effects can be considered as small, because of the fact that the effects also could be caused by for instance a regular storm. Even in the case of a major impact on the environment, the effect does not have to be considered as unacceptable, because in nature extreme events occur as well. These events are mentioned in ecology as disturbances (Begon et al., 2006). Such disturbances in the ecology as for instance floods or extreme storms can give opportunities for new species. In general, disturbances are a part of ecologic system and should not always be prevented, because of the human origin of the disturbance. Despite the vision that disturbances also occur in nature, still many aspects of dredging activities are considered as a degradation of the environment and should therefore be treated as such.

A small overview of possible relations between dredging related activities and the environment is given in the cause and effect based DPSIR-scheme (Figure 1.2). More information about the environmental aspects of dredging can be found in IADC/CEDA (2008).

#### Increased turbidity

Although there is a large variety of environmental impacts, limitation of increased turbidity due to suspended sediments appears to be an important environmental requirements for contractors in practice (Nieuwaal, 2001). Especially corals are very vulnerable for increased levels of turbidity. Increased turbidity also cause a reduction of photosynthesis by marine life. This can have a negative influences on the growth of for instance algae, that form the base for several food chains. The negative effects on the growth of algae due to suspended sediments was an important issue at the land reclamation project Maasvlakte 2. Suspended sediment concentration (TSS or Total Suspended Solids) is the measurement of the dry-weight mass of sedimentary material that is suspended in the water per unit of volume of water. The relation between the suspended sediment concentration and the turbidity depends on the composition of the sediments and has to be determined on site.

There are different sources of suspended sediments at dredging and reclamation projects. The removal of the sediment with the dredging equipment can cause emission of suspended sediments due to disturbance of the bed. In case of a suction dredger, return water that is used to transport the dredged material contains a lot a fine sediments which take time to settle. Especially when this return water is used to transport fine material and is released near shore, this can form a serious risk for the environment. This is for instance the case at land reclamations or onshore disposal of the dredged material. Finally, the offshore disposal of the dredged material can also result in emissions of suspended sediments.

The mitigation of the impacts of suspended sediments due to disturbance of the bed can be done by careful selection of the working method, investigation of the currents or for instance the use silt screens. The impact of offshore release of return water can be mitigated by careful selection of the location and the actual currents. The same holds for offshore disposal of dredged material for which a suitable location can be chosen in order to minimize the effects. In case of nearshore releases of return water the options for optimizing the location are mostly limited. Therefore a frequently used method to mitigate the impacts of the return water is the construction of a settling basin. This is an artificial basin, through which the return water will flow. The large surface and large cross section result in very low flow velocities inside the basin, which gives the fine sediment particles the opportunity to settle.

#### Settling basins

Figure 1.1 gives a example of the use of settling basins at a project in Ireland with onshore disposal of the dredged material. It gives an overview of the whole process, from the dredging of bed material with a cutter suction dredger to the emission of suspended sediment and the possible impact on a sensitive receiver (in this case migrating salmon). The first basin was used as a dumping ground which could be filled from various locations. The larger factions and undissolved clay balls will stay in this basin, as they settle quickly. The suspended sediments flow through the weir box into the settling basin and the majority will settle due to the low flow velocity. The same holds for the next settling basin. Due to the low suspended sediment concentration, the impact on the bed level of the settling basins is usually limited. As these basins mainly contain fine sediments, they are also called silt ponds. The use of one or more settling basins results in a emission of suspended sediments that is far lower than in case of direct release.

The design of these settling basins includes many uncertainties as the way particles settle is hard to predict. Also processes like flocculation (agglomeration of clay particles) and the influence of the wind contain high uncertainties and make it hard to predict the emission of suspended sediments. Quantification of this emission and its uncertainty is essential to investigate the environmental impacts due to the emission of these suspended sediments. It also gives a realistic picture of the situation for both engineers and ecologists. This realistic picture of the emission of suspended sediments is valuable information in the decision process of environmental issues and can also be used for economic optimization purposes.

The purpose of this project is to use probabilistic methods for the design of settling basins in order to fulfill environmental requirements of dredging and reclamation projects. Within this study only environmental requirements related to the emission of suspended sediments will be taken into account. A model will be developed that represents the relevant physical processes that influence the emission of suspended sediments. This model will be referred to in the report as the *project model*. The emission is determined by the discharge through the basin and the actual concentration of suspended sediments of the discharged water. The environmental requirements that come from the EIA are assumed to represent the environmental risk for flora and fauna. Therefore within this project the environmental risk will be considered from the contractors point of view and represents the financial risk of the inability to meet the environmental requirements. This environmental risk is considered as downtime of the equipment or penalties. Taking into account these risks enables economic optimization using probabilistic methods. This results in the following objective and associated research questions:

## 1.2 Objective

> Development and evaluation of a probabilistic approach to quantify the outflow concentration of settling basins on dredging and reclamation works, in order to enable environmental risk based design optimization.

### 1.2.1 Research questions

I How can the outflow concentration of suspended sediments (TSS) at settling basins be determined?

II How does the project model perform for measurement data and compared to existing solutions?

III What are the main sources of uncertainties in case of probabilistic calculation of the outflow concentration of suspended sediments?

IV What is the economic optimal design of a settling basin accounting for uncertainties?

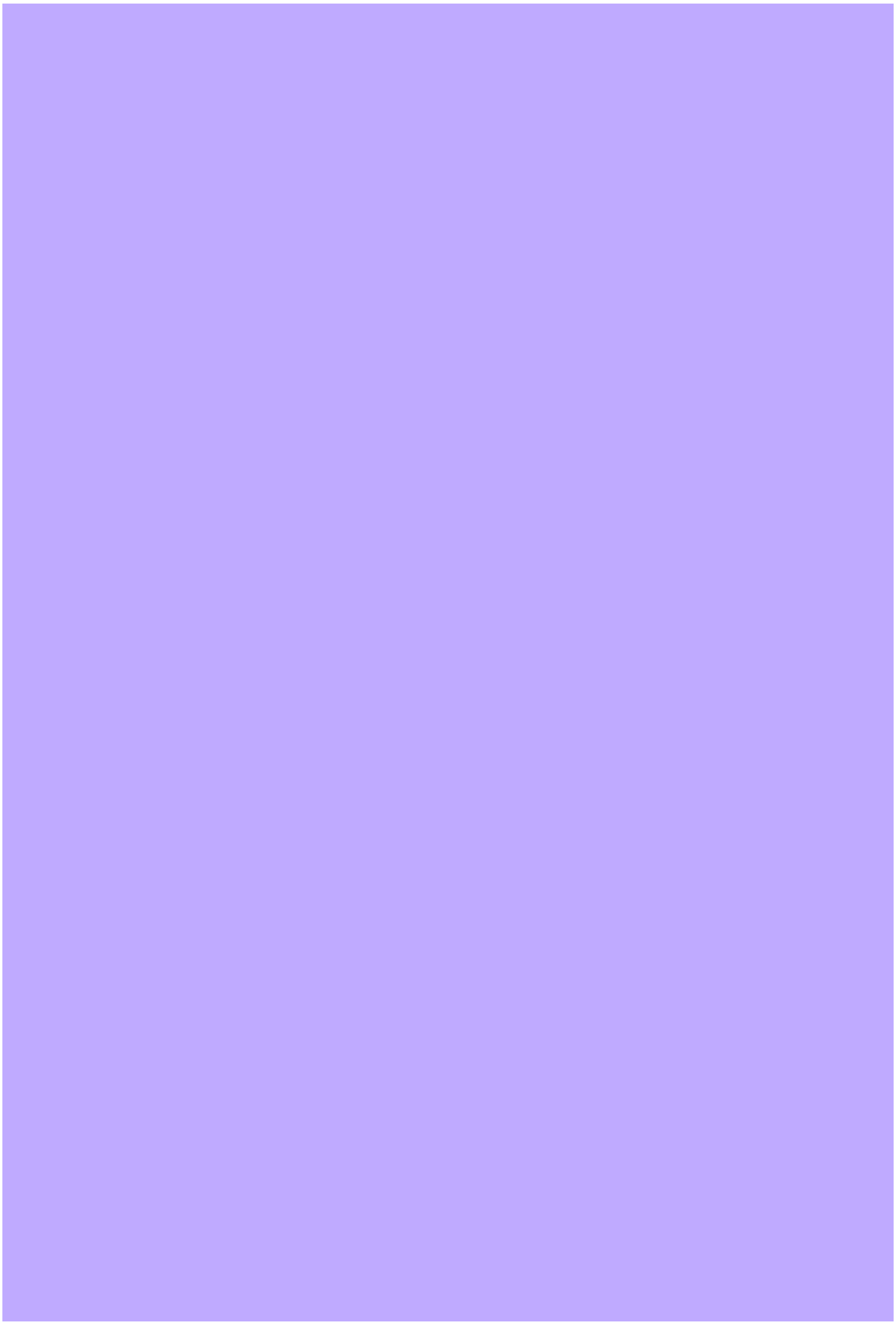

Figure 1.1: Situation sketch [redacted]

### 1.2.2 Research approach

Based on a literature review, existing tools and expert judgement, a simplified and efficient suspended sediment transport model is developed to determine the outflow concentration of a settling basin, for given conditions and input parameters. Due to its simplicity, the project model is able to do large number of calculations which is required for probabilistic methods. Furthermore, processes like flocculation and wind can be specified by the user.

This deterministic model is evaluated with measurement data, an existing model and an analytical solution. Both model uncertainties and parameter uncertainties can be implemented in the model which enables probabilistic calculations and analysis of the uncertainties.

Interviews with cost estimators of Van Oord gave a first impression of environmental risks. These interview were also the basis for the identification of the *decision variables* within the design of a settling basin. This enables economic optimization of the basin design and gives possibilities for the reduction of the environmental risks. The novel character of the probabilistic approach developed in this study unfortunately means that insufficient field data is available to illustrate the entire process with actual project data. To enable quantification and visualization of the difference between a deterministic and a probabilistic calculation an arbitrary case study is defined and used throughout this study.

### 1.2.3 Framework principles

The project model is developed for given input parameters as discharge, inflow concentrations, fraction distribution and wind distribution. It is appropriate for both stationary and instationary situations, although within this project only stationary situations are taken into account to enable proof of concept and to increase the understandability of the model outcomes. Only low concentrations of suspended sediments can be applied as sediment-fluid interactions are not taken into account. As environmental damage due to emission of suspended sediments is very dependent on the project, an arbitrary *limit value* is chosen. Within the probabilistic design, exceedance of this limit is assumed to have an undesirable environmental impact and is defined as failure. For the contractor, this failure results in downtime or a penalty.

## 1.3 Report structure

Chapter 2 gives the determination of the outflow concentration of suspended sediment. It describes the relevant physical processes in a settling basin for both the modelling of the flow as for the modelling of the transport of suspended sediments. Important processes as the particle fall velocity and the influence of flocculation are described in detail. Also the influence of the wind shear stress on both the flow profile and turbulence is explained. Finally, numerical aspects on boundary conditions and computational requirements are described.

Chapter 3 gives a number a deterministic calculations of the project model for different sediment distributions and compares these results with existing solutions and measurement data. It is intended to be an evaluation of the performance of the project model. The available measurement data is compared with deterministic calculations of the project model. Although the data is not suitable for calibration, the comparison with the project model results is promising. The bed boundary condition and the development of the vertical suspended sediment concentration profile of the project model is compared with an analytical solution in order the compare the numerical results of the project model with this analytical solution.

The following chapter, Chapter 4, aims to be an answer to the research question about the sources of uncertainty. It gives an overview of the different parameters and the corresponding uncertainties. A arbitrary limit value for the outflow concentration is defined to quantify the probability of failure. The design point is determined with both the first order reliability method (FORM) and the Monte Carlo based *center of gravity* method. The influence coefficients for the different parameters are determined which both methods. Finally, a number of Monte Carlo simulations with variations of the most important parameters is done, showing the influence of these parameter on the outflow concentration.

The implementation of the environmental risks is explained in Chapter 5. This resulted in the most economic choice for both equipment and basin depth. For the choice of equipment also the time effects are taken into account. Finally the profitability of wind protection for settling basins is investigated.

Conclusions of this study are stated in Chapter 6. This chapter also gives recommendations for the way the project model should be used for environmental compliance and economic optimization in future projects. Finally, recommendations for improvement of the project model and for the modelling of environmental impacts on dredging and reclamation works are given.

### Driver

- human needs/economic development
  - e.g. dredging of harbours
  - land reclamation
- human health (environmental dredging)
  - pollution of food chain
  - prevention of spreading
- ...

### Pressures

- emission of suspended sediments
- disturbance of the bed
- change in bathymetry
- use of heavy equipment
- removal of polluted sediment
- ...

### Status

- temporary increased turbidity
  - light attenuation
- change of bed material
- covering of the bed with sediments
- noise
- cleaner bed
- changes in currents
- extra nutrients
- ...

### Impacts

- interference with marine fauna
  - interference with respiration and (filter-)feeding of (shell)fish
  - impediment to mobility
  - irritation to tissue
- interference with benthic flora and fauna
  - disturbance of the bed
  - physical contact with dredging equipment
- less spreading of pollutants
- dispersion of species
- ...

### Response

- investigation of natural variation
  - comparison between natural variation and human activities
- identification of possible impacts due to human activities
- valuation of impacts
  - modelling of impacts
  - time needed to restore
- control of emissions
- limitation of activities
- compensation measurements
- prevention of future pollution
- ...

Figure 1.2: DPSIR-scheme

# Chapter 2

# Deterministic modelling

The determination of the outflow concentration of suspended sediments starts which the calculation of the flow pattern. The flow pattern varies over the basin. [redacted] performed a comprehensive literature study into this subject. [redacted] This enables one dimensional modelling over the horizontal axis (1DH) in the direction of the mean flow. Also ASCE (2008) states that one dimensional modelling is sufficient for the modelling of settling basins. Therefore for the modelling of the flow in the settling basin, the shallow water equations are used. This results in a horizontal flow profile in an very efficient way. The use of the shallow water equations also creates possibilities for non-stationary calculations and is general applicable.

For the modelling of the suspended sediment concentration over the basin, 1DH-modelling is not sufficient as the suspended sediment concentration can exhibit significant gradients over the vertical due to the settling of suspended particles. Therefore, the vertical axis is also taken into account resulting in a two dimensional modelling in the vertical plane (2DV). The vertical distribution of the flow velocity can be approximated very good with the logarithmic velocity profile. Therefore, the 2DV-flow pattern, which is required for the modelling of the suspended sediment concentration, is calculated from the mean flow according to the logarithmic velocity profile. This results in a very efficient derivation of the 2DV-flow pattern. This flow pattern is used in de 2DV-suspended sediment transport model. This results in a 2DV distribution of the suspended sediment concentration over the basin for given input parameters and basin dimensions.

## 2.1 1DH Flow modelling

The shallow water equations come from a number of simplifications which are applied on the general equations for conservation of momentum and the continuity (Equation B.1 to B.4). First of all, uniform flow in the horizontal direction will be assumed. The effect of Coriolis will be neglected because of the limited area. For the vertical direction, hydrostatic pressure is assumed. Integrating over both the width and the depth, finally results in the shallow water equations which are given below. The full derivation of the shallow water equations is given in Appendix B.

$$\frac{\partial Q}{\partial x} + B\frac{\partial \eta}{\partial t} = 0 \tag{2.1}$$

$$\frac{\partial Q}{\partial t} + \frac{\partial}{\partial x}\left(\alpha_2 \frac{Q^2}{A_s}\right) = -gA_s\frac{\partial \eta}{\partial x} - c_f B_s \frac{Q|Q|}{A_s^2} \tag{2.2}$$

With:

| | |
|---|---|
| $x$ | horizontal coordinate [m] |
| $Q$ | discharge [m$^3$/s] |

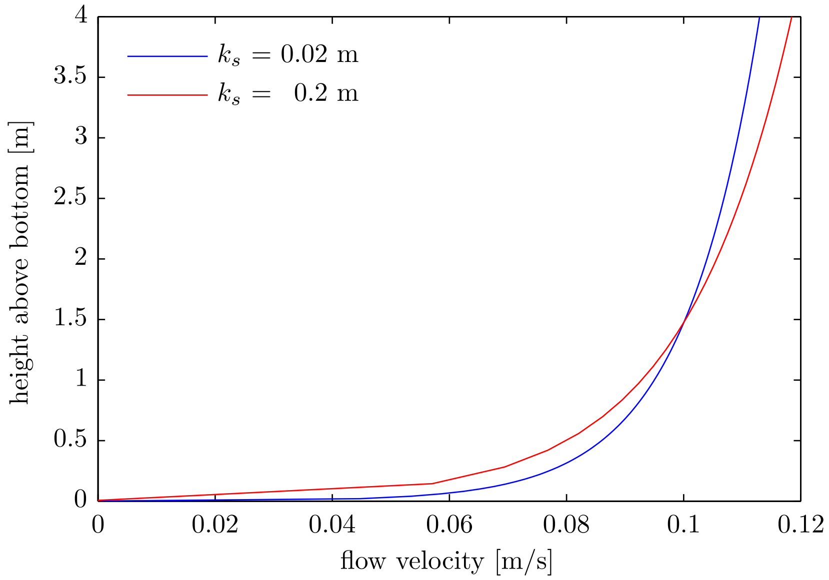


Figure 2.1: Logaritmic velocity profile at mean flow velocity of 0.1 m/s

| | |
|---|---|
| $B$ | storage width [m] |
| $\eta$ | water level [m] |
| $t$ | time [s] |
| $A_s$ | channel cross section [m$^2$] |
| $g$ | gravitational accelerations [m/s$^2$] |
| $c_f$ | bottom friction coefficient [m] |
| $B_s$ | channel width [m] |
| $\alpha_2$ | $= \frac{\overline{u^2}}{\overline{u}^2}$ |

## 2.2 2DV Flow pattern

With the shallow water equations and a upstream and downstream boundary, it is possible to derive the flow velocities along the horizontal axis of the basin. In the stationary situations, which is the scope of this project, a equilibrium flow situation is reached after a number of iterations. This flow velocity is averaged over the cross section. This flow velocity will be distributed over the vertical axis according to the logarithmic velocity profile (van Rijn, 1993).

$$u(z) = \frac{u_*}{\kappa} \ln\left(\frac{z}{z_0}\right) \tag{2.3}$$

With:

| | |
|---|---|
| $u$ | horizontal velocity [m/s] |
| $z$ | vertical coordinate [m] |
| $u_*$ | friction velocity [m/s] |
| $\kappa$ | Von Karman constant (0.4) [-] |

In this equation $z_0$ is the level at which the theoretical flow velocity is zero. The flow is assumed to be hydraulic rough, because of the natural conditions. This is confirmed by typical settling basin calculations. Therefore this value can be determined by $z_0 = 0.033 \cdot k_s$, in which $k_s$

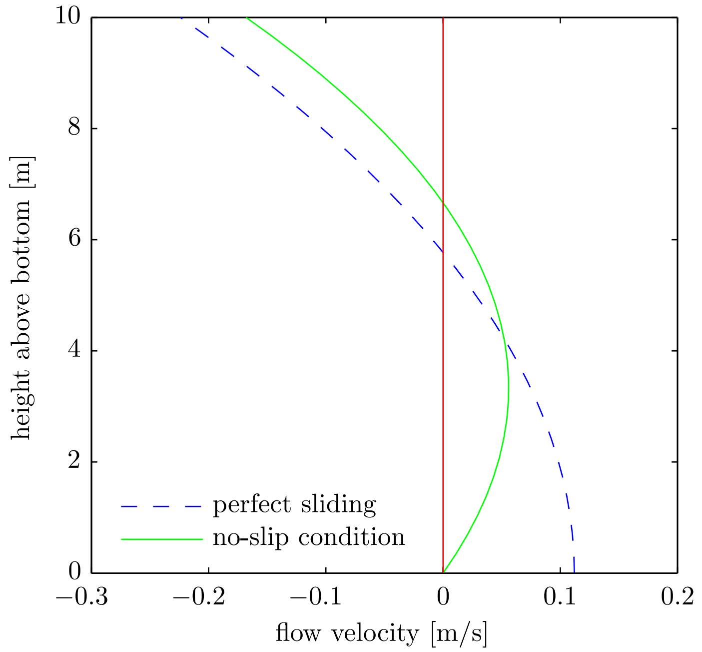


Figure 2.2: Horizontal secondary flow at a windspeed of 20 m/s

is the roughness height according to Nikuradse. After determination of the vertical velocity profile over the whole horizontal axis, a velocity profile over longitudinal section of the basin is created. Figure 2.1 gives an example of a logarithmic velocity profile for two different Nikuradse roughness heights.

### 2.2.1 Wind effects

Wind can have an effect on the flow pattern and the transport of suspended sediment in the settling basin. Two different types of influence are taken into account. The first type of influence are secondary flows due to the wind. The second effect is additional turbulence due to the wind shear stress on the surface. This effect will be treated in Subsection 2.3.3. The effect of wind waves is neglected as typical wind waves calculations for settling basins show only small waves with short wave lengths compared to the water depths, due to limited fetch lengths. Therefore the wave generated bed shear stress is negligible.

The effect of secondary flows due to wind is modeled as was the basin a lake. Only secondary flows in the vertical plain between the inflow and outflow are taken into account as this is the most relevant plain for the sediment concentration profiles. The concentration profiles are assumed to be constant over the width of the basin and therefore a horizontal flow has no effect on the concentration profiles. The effect of vertical secondary flows over the width is only local and is not taken into account in particular. The sediment mixing due to secondary flows over the width of the basin is assumed to be included in the sediment mixing coefficient.

In the vertical plain between the inflow and outflow, the secondary flow is modelled as a two dimensional circulation in a non-stratified lake, because of the low mean flow velocity in the basin. For modelling this secondary flow, use is made of analytical formulations for lake circulations due to wind (Hutter et al., 2011). Figure 2.2 gives an example of the secondary flow for two different assumptions for the bottom boundary. For reasons of consistency a no-slip condition at the bottom is applied in order to be consistent with the no-slip condition of the mean flow. The secondary flow is assumed to be fully horizontal in the grid cells in the middle of the model because of modelling

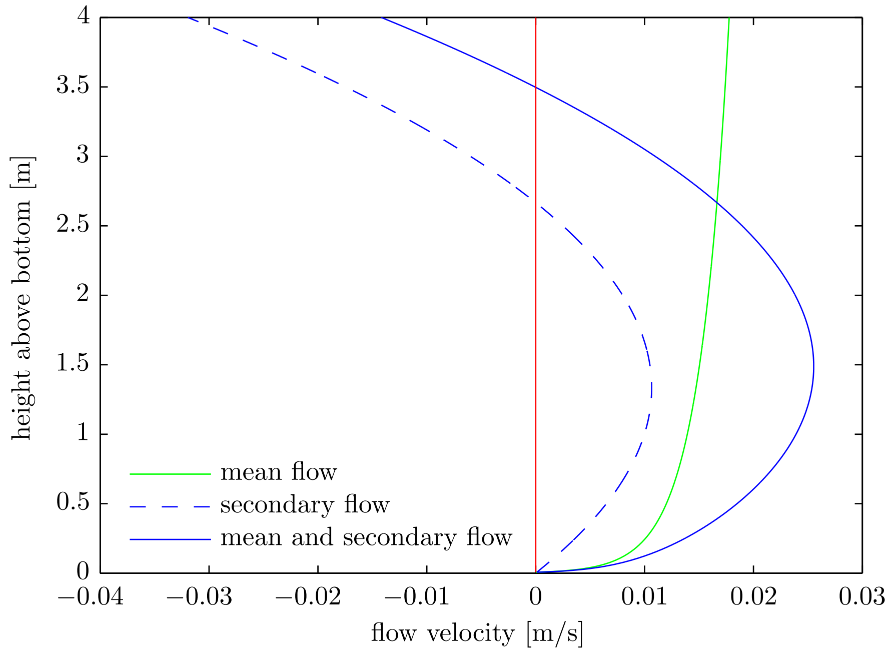


Figure 2.3: Horizontal flow at a wind speed of 15 m/s (no-slip condition) and a mean flow of 0.015 m/s

reasons. The vertical discharge is limited to the boundary grid cells, so all vertical flow goes through this grid cells. This is considered as an conservative assumption, as it will result in higher vertical velocities. Overall, the effect of vertical secondary flows is considered as small because the sediment mixing over the vertical due to turbulence is dominating at high wind speeds. This results in small vertical gradients in the suspended sediment concentration profiles and therefore the vertical flow only has small effects.

This secondary flow velocity is superposed on the mean flow velocity to get a resulting flow velocity field (see Figure 2.3). In the boundary grid cells only the mean flow is taken into account. Although the logarithmic velocity profile is influenced by the secondary flow, a super positioning of both components is considered as sufficient as the mean flow velocity is usually small and therefore this approach only creates small errors. Section B.3 gives a full overview of the formulations which are used in the model for wind induced currents.

## 2.3 2DV Sediment transport modelling

The scope of the transport of sediments within this project is limited to the transport of suspended materials, because the bed load transport is assumed to have no influence on the outflow concentration of suspended sediment that flows through the weir box. The transport of bed load materials is therefore not taken into account.

### 2.3.1 Interaction between the sediment and the fluid

The sediment concentration in the water can have an effect on the flow conditions of the fluid. Winterwerp and van Kesteren (2004) describes several interactions between the fluid and the suspended sediment in the fluid. The most important aspects for settling basins will be mentioned. First of all there is an influence on the bottom and therefore roughness of the bottom can change, which influences the flow pattern. Next, the falling particles create a upward return flow of the fluid. The last effect which will be mentioned is the effect of differences in density. The suspended sediment particles will result in an higher density of the suspension compared to water without suspended particles. Especially at high concentrations this will result in density driven currents, which can result in a totally different flow pattern and vertical density gradients. These vertical density gradients cause reduction of the turbulent mixing over the vertical, which finally changes the vertical velocity profile.

In the case of a settling basin at reclamation works, low and horizontal flow velocities are assumed. High concentrations of suspended sediment will only occur in the neighbourhood of the pipe in the dumping ground. Further away from the inflow the larger particles are settled and only the small particles, which need more time to settle, are present. This especially holds for the settling basins which usually come after the dumping ground. Therefore the influence of the sediment concentration is not taken into account in the flow calculations. For reasons of simplicity, also the bed roughness is not related to the effects of the suspended sediment, but based on expert judgement given local circumstances and sediment fractions.

### 2.3.2 Flow driven suspended sediment transport

Because of the above mentioned simplifications, the sediment transport rate is considered as a function of the flow velocity. Given the longitudinal velocity profile, a time varying mass balance for sediment is set up for each grid point in the following equation:

$$\frac{\partial c}{\partial t} + u\frac{\partial c}{\partial x} + \frac{\partial w_s c}{\partial z} - \frac{\partial}{\partial x}\left(\epsilon_{s,x}\frac{\partial c}{\partial x}\right) - \frac{\partial}{\partial z}\left(\epsilon_{s,z}\frac{\partial c}{\partial z}\right) = 0 \tag{2.4}$$

With:

| | |
|---|---|
| $x$ | horizontal coordinate [m] |
| $z$ | vertical coordinate [m] |
| $c$ | concentration of suspended sediments [kg/m$^3$] |
| $u$ | horizontal flow velocity [m/s] |
| $w_s$ | particle fall velocity [m/s] |
| $t$ | time [s] |
| $\epsilon_s$ | sediment mixing coefficient [m$^2$/s] |

This equation is solved for each sediment fraction independently (except for the fall velocity in case of hindered settling and flocculation, which is mentioned later), which results in suspended sediment concentration profiles over the vertical cross section in the direction of the mean flow. The derivation, including all boundary conditions, is given in Appendix C. Special care is given to the particle fall velocity $w_s$. This is the velocity at which the gravity force is equal to the fluid drag force. For natural sediment, van Rijn (1993) gives three formulations for different particle diameters. For each different fraction, the fall velocity is calculated by the model.

### 2.3.3 Sediment mixing coefficient

The turbulent flow in the basin causes turbulent diffusion, which highly influences the vertical concentration profile. The rate of this turbulence is related to the velocity gradients due to shear stresses. Therefore wind shear stress causes additional turbulence as mentioned in Subsection 2.2.1. A parabolic turbulent mixing coefficient is assumed due to the bed shear stress as this mimics the physics in the best way (van Rijn, 1984). The effect of additional mixing over the vertical due to the wind shear stress, will be taken into account by an extra component in de sediment mixing coefficient. This component is derived from the additional turbulent viscosity due to the wind generated turbulent kinetic energy (see Figure 2.4). This turbulent kinetic energy is determined with the *Algebraic closure model* (Deltares, 2010). Once the turbulent viscosity is calculated, it is possible to determine the (turbulent) eddy diffusivity by the *Prandtl-Schmidt number*. Finally the the sediment mixing coefficient can be calculated by taking into account the $\beta - factor$ (van Rijn,

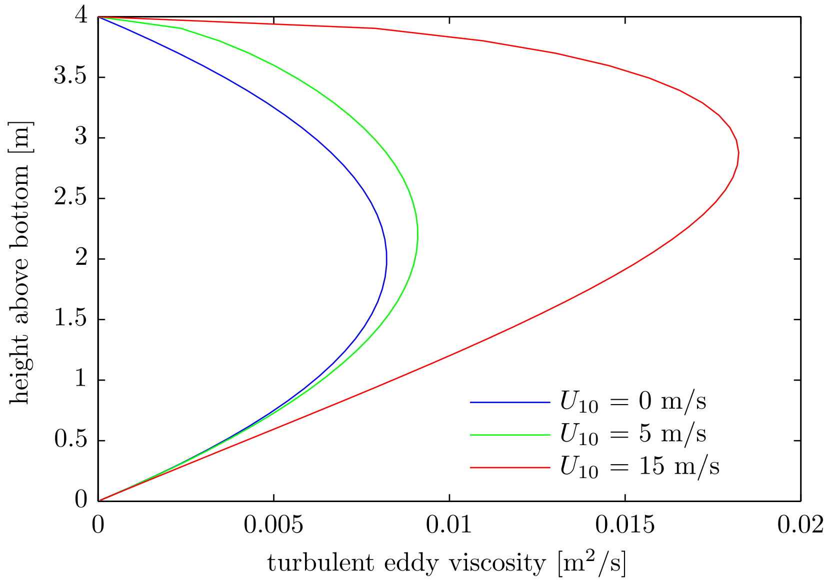


Figure 2.4: Turbulent viscosity profile for different wind speeds ($\overline{u}_{flow}$ = 0.25 m/s)

1984) which represents the difference between the eddy diffusivity of the fluid and the sediment mixing coefficient. The determination of the turbulent mixing coefficient due to the bed shear stress, based on the turbulent kinetic energy and the *Prandtl-Schmidt number* leads to the same expression as given bij van Rijn (1984). For reasons of consistency, the determination of the turbulent eddy diffusion is based in the turbulent kinetic energy. The complete derivation is given in Section C.5.

### 2.3.4 Particle fall velocity

**Hindered settling**

The above calculated fall velocity is the fall velocity in still water. This is a good approximation for low suspended sediment concentrations. At higher concentrations, near the point of inflow, a falling particle influences the flow, as mentioned above, and therefore influences the fall velocity of surrounding particles. For the flow calculation, this influence is neglected but the influence on the fall velocity can be significant. This behaviour is called hindered settling. Winterwerp and van Kesteren (2004) gives an overview of the processes that influence the fall velocity. The literature gives several different formulas to calculate this velocity ([redacted] Winterwerp and van Kesteren, 2004; van Rijn, 1993, 2007). The formula of van Rijn (2007) is chosen because its simplicity and it is also recently used in the sediment transport model TRANSPOR2006 (van Rijn, 2006). The effect on the viscosity is implicitly represented in this formula.

Hindered settling effects start to play a role at sediment concentrations in the order of 10 kg/m$^3$, which only will occur near the inflow point. Hindered settling effects are dominating for concentrations larger than 30 kg/m$^3$. At extreme high concentrations in the order of 100 kg/m$^3$ the settling velocity reduces drastic and a lutocline (a sharp step structure in suspended sediment concentration) can arise. These effects are outside the scope of this project as differences in density are no longer neglicible. These density differences create for instance density currents and damping of the turbulence due to buoyancy effects. The model is designed in such a way that hindered settling effects can also be neglected. Therefore is is possible to investigate the impact of hindered settling in each individual case.

### Flocculation

Small sediment particles have cohesive properties. Therefore these small particles can merge together when they collide and form larger flocs. These larger flocs have a larger fall velocity and they will settle faster than without merging. This process is called flocculation and it is governed by the following three processes (Winterwerp and van Kesteren, 2004):

1. Brownian motion is the seemingly random movement of particles suspended in a fluid which cause the particles to collide, resulting in the formation of aggregates.

2. Collisions between particles due to different particle fall velocities, resulting in the formation of aggregates.

3. Collisions due to turbulent eddies in the fluid, resulting in the formation of aggregates. Turbulent shear can also result in break up of already formed flocs, resulting in smaller particles.

These processes are also largely influenced by factors like salinity, suspended sediment concentration and temperature, which influences the viscosity of the fluid. The literature shows a strong relationship between salinity and flocculation as the cations in seawater neutralise the negative charges between the particles (Winterwerp and van Kesteren, 2004). Flocculation is assumed to be fully active for a salinity value larger than about 5 psu (van Rijn, 2007), so for seawater flocculation is always fully active. High sediment concentrations increase the probability of collisions between particles and therefore have an increasing effect on the fall velocity, until hindered settling start to plays a role. Turbulence increases the probability of collisions between particles but large shearing forces also cause break up of the flocs. This continuous process of flocculation and break up due to turbulence, results in a dynamic equilibrium. In still water (no turbulence) flocs may grow to larger sizes due to differential settling collisions. This continues until they break up due to the larger fluid shear as a result of the higher fall velocity.

Flocculation also takes time, as shown in Figure 2.5. This figure shows the ratio between the settling time and the flocculation time. When the flocculation time is longer than the settling time, no significant flocculation effects are expected. Indicative calculations show that in typical settling basin examples the flocculation time is longer than the settling time. Based on this calculations no strong flocculation effects are expected in the basin itself, but the fine sediments in the basin still form flocs. It is assumed that the size of the flocs is determined by the dredging process. High shear stresses in the dredging process can break up the flocs. Based on this assumption there is a certain minimum floc size which survives the dredging process. The size of this smallest floc is completely site specific. In order the be able to model this type of flocs it is suggested to formulate a certain minimum fall velocity which corresponds which the minimum floc size (J. C. Winterwerp, personal communication, December 12, 2010). This minimum floc size can be determined from water samples of the return water. This can be done in the field relatively easily with simple equipment and a well trained eye. A minimum fall velocity for flocs is also given in van Rijn (2007) in combination with flocculation.

Despite the knowledge about the several processes with influence the flocculation, it is still very difficult to determine if flocculation takes place and to formulate relationships between all these processes of flocculation. Simple empirical relationships do not underperform for more physical based relations ([redacted] . Therefore the simple empirical formulation of van Rijn (2007) is chosen, combined with a linear relationship between flocculation and salinity for the range in with flocculation if not fully active. The model is designed in such a way that a minimum fall velocity can be given for both flocculated and non-flocculated situations. Therefore is is possible to investigate the sensitivity for flocculation in each individual case.

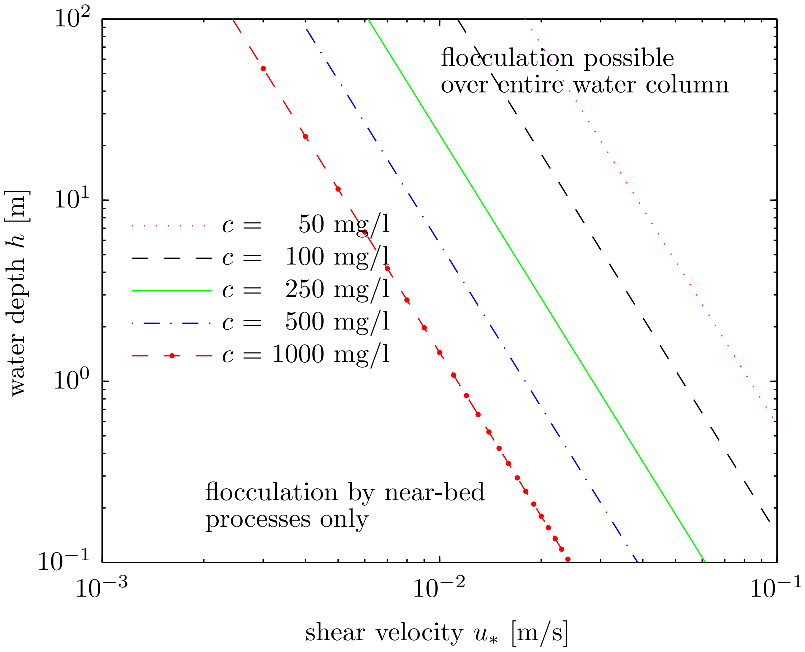


Figure 2.5: Relative flocculation time of mud flocs in water column (Winterwerp and van Kesteren, 2004)

### 2.3.5 Bed boundary conditions

#### Non-cohesive sediments

As mentioned in Section 2.3, the bed load transport in not taken into account. Therefore the level of transition between bed load and suspended load forms the boundary of the model domain. The transport of sediment below this level is assumed to be bed load transport. This level is called the reference level and is located at half the bed form height above the bed level with a minimum of $0.01 \cdot waterdepth$ (van Rijn, 1984). At the bed two types of boundaries may be applied. Either a concentration type boundary or a gradient type boundary can be applied (Wang, 1989). The former requires the indication of a fixed, but potentially time-varying, concentration value at the bed. The latter assumes that the bed concentration adjusts itself such that the concentration gradient near the bed at all times is equal to the concentration gradient under equilibrium conditions.

The gradient type boundary is considered to be the most appropriate, because the bed concentration can be different from the equilibrium concentration, but it still has the tendency to adapt to the equilibrium concentration profile. Therefore the local concentration gradient at the reference level is chosen to be equal to the gradient under equilibrium conditions. In the project model the bottom gradient for each available fraction is calculated according to the multi fraction method (van Rijn, 2006). For numerical purposes the reference level is chosen halfway between the two lowest vertical velocity points. This should be kept in mind by defining the levels of the vertical velocity points. The derivation of the gradient boundary condition is given in appendix C.2.

#### Cohesive sediments

Cohesive sediments behave in a different way compared to the non-cohesive sediments. This has also consequences for the boundary condition. In the classical view on cohesive sediments, as described by Winterwerp and van Kesteren (2004), erosion and deposition of cohesive sediments cannot occur simultaneously and there is a threshold for both erosion and deposition between which no sediment flux could take place. [redacted] describes the mechanism of cohesive sediment in a similar way. Experiments however, show that erosion and deposition can take place simultaneous. Winterwerp and van Kesteren (2004) concluded that the behaviour at the bed should be interpreted as a probability of resuspension instead of a mechanism of erosion and deposition and for low concentration engineering applications it is proposed only to use the sediment flux:

$$D = w_s \cdot c_b \tag{2.5}$$

in which $w_s$ is the characteristic settling velocity and $c_b$ is the near bed sediment concentration.

For the modelling purpose within this project it is decided to describe the sediment flux with Equation 2.5 instead of the more theoretical based processes like deposition and erosion. This downward sediment flux in combination with an upward flux due to turbulent mixing is used in the bed boundary condition in Equation C.7.

The near bed concentration is calculated with the multi fraction method for the reference concentration (van Rijn, 2007). Although further research is desirable for the fine sediment fractions, this method can be applied for the full size range of $8 - 2000$ $\mu m$. Depending on the bed shear stress, this will lead to an equilibrium background concentration or to full deposition when the settling time goes to infinity. For both numerical and physical purposes, there will be always an certain minimum background concentration.

### 2.3.6 Operational effects

#### Outflow concentration

As mentioned in Section 2.1, the model is based on one-dimensional flow. Especially near the outflow weir box (see Figure 2.6) this is an oversimplification, as is less likely that water from the bottom of the basin, with a higher suspended sediment concentration, will go through the weir box. Therefore only the upper part of the vertical concentration profile will be taken into account by determining the outflow concentration. The part which goes through the weir box has to be specified by the user and can be a calibration factor. This parameter is assumed to be a function of the ratio between the mean flow velocity and the velocity at the weir box $\frac{Uweir}{U_{mean}}$, and the sediment fall velocity $w_s$. It should be noted that the vertical concentration gradient for suspended fines is very small, so for these particles this parameter has a minor effect.

#### Clay balls

Under certain conditions, the sediment-water-mixture which comes through the inflow construction, is not fully suspended, but contains smaller or larger balls of clay. The fines in these balls do not have to settle individually but will settle immediately when they reach the dump site. Therefore the suspended sediment concentration decreases faster compared with the case of fully suspended sediments. The intensity of these balls can be expressed in a percentage of the total sediment flux. As a first assumption is it suggested to decreases the inflow concentration with the percentage of clay balls and to assume the settling of these balls in the direct neighborhood of the inflow, in order to model this effect. In this stage of the project the focus is on silt ponds and the settling of fine particles. Clay balls are therefore not taken into account within the project model.

## 2.4 Computational efficiency

Despite the fact that the computing power is increasing, it is a limitation in running large numbers of calculations. These large numbers of calculations are required for the probabilistic analyses. Therefore several measures had to be taken to limit the requested amount of computational resources to reasonable proportions. The most important measure is the simplification of the process. Several simplifications are described in this chapter and are listed here for completeness:

1. 1DH flow modeling instead of three dimensional (3D) flow modelling.

Figure 2.6: Weir box in settling basin in [redacted]

2. 2DV modelling of the transport of suspended instead of 3D modelling
3. The sediment-fluid interaction is not taken into account.
4. The turbulent mixing coefficient is taken as a constant over the horizontal axis.

The Matlab software, in which the project model is developed, has the ability to give insight in the time required to run the several stages of the simulation. This creates the possibility to focus on the most time consuming parts of the calculation. The flow calculations appears to be very efficient compared to the sediment transport calculation. This is because the sediment concentration is also calculated over the vertical. To improve the efficiency of this part of the simulation, quick versions of several routines are created, in which the process of defining the input parameters is optimized for doing large numbers of identical calculations. To avoid large numbers of loop calculations, several parts of the calculation process are vectorized, which is far more computational efficient. This finally leaded to a calculation process in which the time needed to solve the equations is dominating. This part cannot be improved by optimizing the calculation process as it is determined by the number of grid points in both horizontal and vertical direction and by the number of time steps which is executed in the sediment transport calculation.

## 2.5 Conclusions

The project model appears to be a simplified model for the quantification of the outflow concentration of suspended sediments. Based on a 1DH-flow calculation and a 2DV-calculation of the transport of suspended sediments, the distribution of the suspended sediment concentration is provided. From this distribution, the outflow concentration can be determined. The project model contains the relevant physical processes and almost all parameters can specified by the user, which enables a high degree of flexibility and transparency. Due to its efficiency it is able do large numbers of calculations that are required for probabilistic analyses.

# Chapter 3

# Deterministic analysis

## 3.1 Model evaluation

The evaluation of the model in this stage of the project is based on the expert judgement about the relevant processes and the behaviour of the project model under changing circumstances. This is especially done for flocculation (J. C. Winterwerp, personal communication, December 12, 2010), flow modelling (G. J. de Boer, personal communication, January 13, 2011) and sediment transport (L. C. van Rijn, personal communication, January 26, 2011). Besides this, also a comparison with an existing model is made and the project model is also executed with measurement data.

### 3.1.1 Comparison with [redacted]

Table 3.1: [redacted]

### 3.1.2 Comparison with [redacted]

### 3.1.3 Comparison with analytical solution

The project model is tested with a clean water discharge which develops a equilibrium suspended sediment concentration (see: Figure E.7). Hjelmfelt and Lenau (1970) has developed a analytical solution for this case, based on a constant concentration as bottom boundary. Despite some discontinuities in the simplifications, the results of both the project model and the analytical solution show similar concentrations. The concentrations of the project model show slightly smaller gradients over the horizontal which is probably caused by the horizontal diffusion, that is neglected in the analytical solution. The solutions of both the project model and Hjelmfelt and Lenau (1970) approach the well-known Rouse-profile with increasing distance as both solutions use the parabolic distribution for the sediment mixing coefficient. The dimensionless results of both the project model and the analytical solution are given in Figure 3.3 and 3.4, in which is $X$ a dimensionless

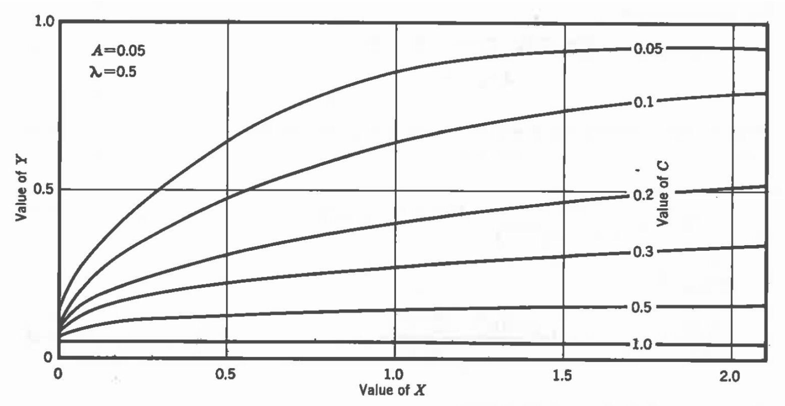


Figure 3.3: Dimensionless analytical results (Hjelmfelt and Lenau, 1970)

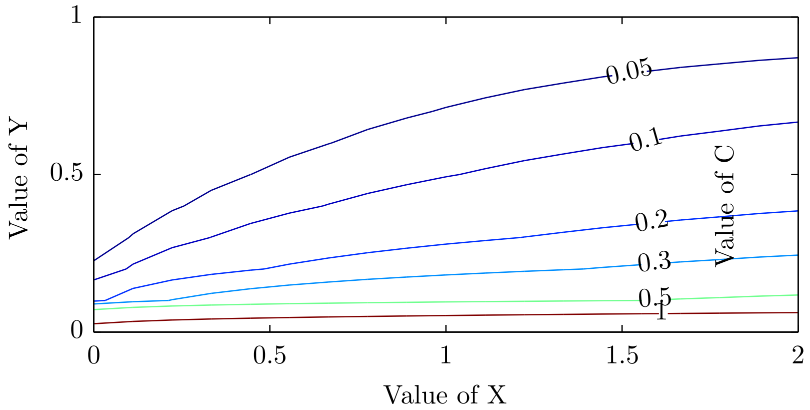


Figure 3.4: Dimensionless results project model; imitation analytical solution Figure 3.3

parameter of the horizontal position and the sediment mixing coefficient, $Y$ is the dimensionless vertical position and $C$ is the dimensionless suspended sediment concentration.

## 3.2 Case study

In order the analyse the sensitivity of the model a artificial case study is defined for which the project model. This case is defined in the following way. A cutter suction dredger has to dredge a trance in a coastal area (mean wind speed: 7 m/s). A dumping site will be used the catch the main part of the material. Based on a particle distribution analysis of the material which has to be dredged, the outflow concentration of the dumping site is estimated at 1 kg/m$^3$. The environmental impact assessment has identified two sensitive species, in the direct surrounding of of the emission of the return water, which are sensitive for irritation to tissue. These species can only survive if suspended sediment concentrations are below 100 mg/l. As lethal impacts on these species are considered as unacceptable, the environmental requirements of the project do not allow emissions of suspended sediments in concentrations, which are higher than 100 mg/l.

In order to fulfill this environmental requirements, the contractors chooses the construct a settling basin through which the outflow of the dumping site will flow. There maximum space available allows a basin of 200 meters long and 200 meters wide. The equipment which is used has a discharge of [redacted] m$^3$/s (e.g. Sliedrecht 34 on Figure 3.5) and the contractor wants to know if he can fulfill the environmental requirements for which the project model is used. This results in

Figure 3.5: Cutter suction dredger: Sliedrecht 34 (Van Oord)

| **parameter** | **quantity** | **unit** | **description** |
|---|---|---|---|
| $Q_{in}$ | [redacted] | $m^3/s$ | mean inflow discharge |
| $C_{in}$ | 1 | $kg/m^3$ | estimated inflow concentration |
| $k_s$ | 0.25 | m | roughness height (Nikuradse) |
| $S$ | 35 | psu | salinity |
| $U_{10}$ | 10 | m/s | wind speed; conservative assumption |
| $angle$ | 180 | degree | wind angle opposite to flow direction (worst case) |
| $Part_{Outflow}$ | 1 | - | part of vertical profile (see Subsection 2.3.6) |
| $floc$ | off | - | no flocculation (worst case) |
| $w_{s,min}$ | 5e-5 | m/s | minimum fall velocity (floc size about 8 $\mu m$) |

Table 3.2: Input parameters case study

the input parameters given in Table 3.2 and 3.3.

The model results show that a basin with a depth of 4 meter in this conservative simulation does not fulfill the requirements as the outflow concentration is 129 mg/l. Assuming only the highest 10 percent of the vertical concentration profile will result in a outflow concentration of 127 mg/l. So the influence of this parameter is very limited as the vertical gradients in the suspended sediment concentration are small. Neglecting the influence of the wind results in a total different picture as the mean concentration at the end of the basin is 37 mg/l. The highest 10 percent of the vertical concentration profile is in this case only 4 mg/l. This indicates significant vertical gradients in the suspended sediment concentration. It can be concluded that wind causes serious mixing over the vertical. Table 3.4 gives an overview of the outflow concentration for various wind speeds and various directions. This table shows that tailwind even has as positive effect on the outflow concentration.

The influence of the water depth depends on the situation as several processes are dependent on it. If the vertical mixing is dominant compared to the settling of the particles, the vertical gradients in the suspended sediment concentration are small. In this case the influence of the water depth is limited, as the bottom extracts a certain amount of sediment from the water by the bed boundary condition (see Equation 2.5). The expected benefit of a longer residence time, is strongly reduced by the vertical mixing which disables the particles to settle. The bed boundary

| fraction | percentage |
|---|---|
| 0 - 4 | 16 % |
| 4 - 12 | 30 % |
| 12 - 20 | 35 % |
| 20 - 40 | 12 % |
| 40 - 100 | 7 % |

Table 3.3: Fraction distribution case study

Table 3.4: Outflow concentration of suspended sediments for various wind speeds and directions in the case study

extracts the same amount of sediment from the water, independent of the water depth, as the water flux and the suspended sediment concentration on a specific point are almost constant for all water depths. Deep basins can even have a negative influence on the outflow concentration as deeper basins also have extra mixing over the horizontal due to turbulence and secondary currents.

### 3.2.1 Deterministic design

The design of the basin of the above described case study has to fulfill the environmental requirements. As a lot of parameters are uncertain, a number of assumptions have to be done in order to determine the outflow concentration. Especially for wind parameters, this will result in a conservative assumption for the wind speed of 10 m/s, which is only exceeded 20% of the time. For the wind direction the worst case senario of head wind (wind direction is opposite to the flow direction) is assumed. Also the behaviour of the fines is uncertain. This results in conservative assumptions for both flocculation and the minimum fall velocity. Flocculation is therefore assumed to do not take place and the minimum floc size is assumed to be about 8 $\mu m$. Finally also the behaviour of the flow near the outlet is uncertain so the whole vertical concentration profile is taken into account to determine the outflow concentration. This results in a outflow concentration of 129 mg/l. Figure 3.6 shows the model results of this deterministic design.

As this design does not fulfill the environmental requirements, it has to be modified within a limited number of variables in order to ensure environmental compliance. A significant reduction of the wind speed in needed to meets the requirements. This can for instance been achieved by executing the project in a certain period of the year. Also a reduction of the discharge to [redacted] $m^3/s$, by using different equipment, results in a outflow concentration which is lower than 100 mg/l.

## 3.3 Conclusions

The project model is evaluated in various ways. Several experts are consulted for the modeling of the different physical processes in the model. This resulted in a model with a number of parameters

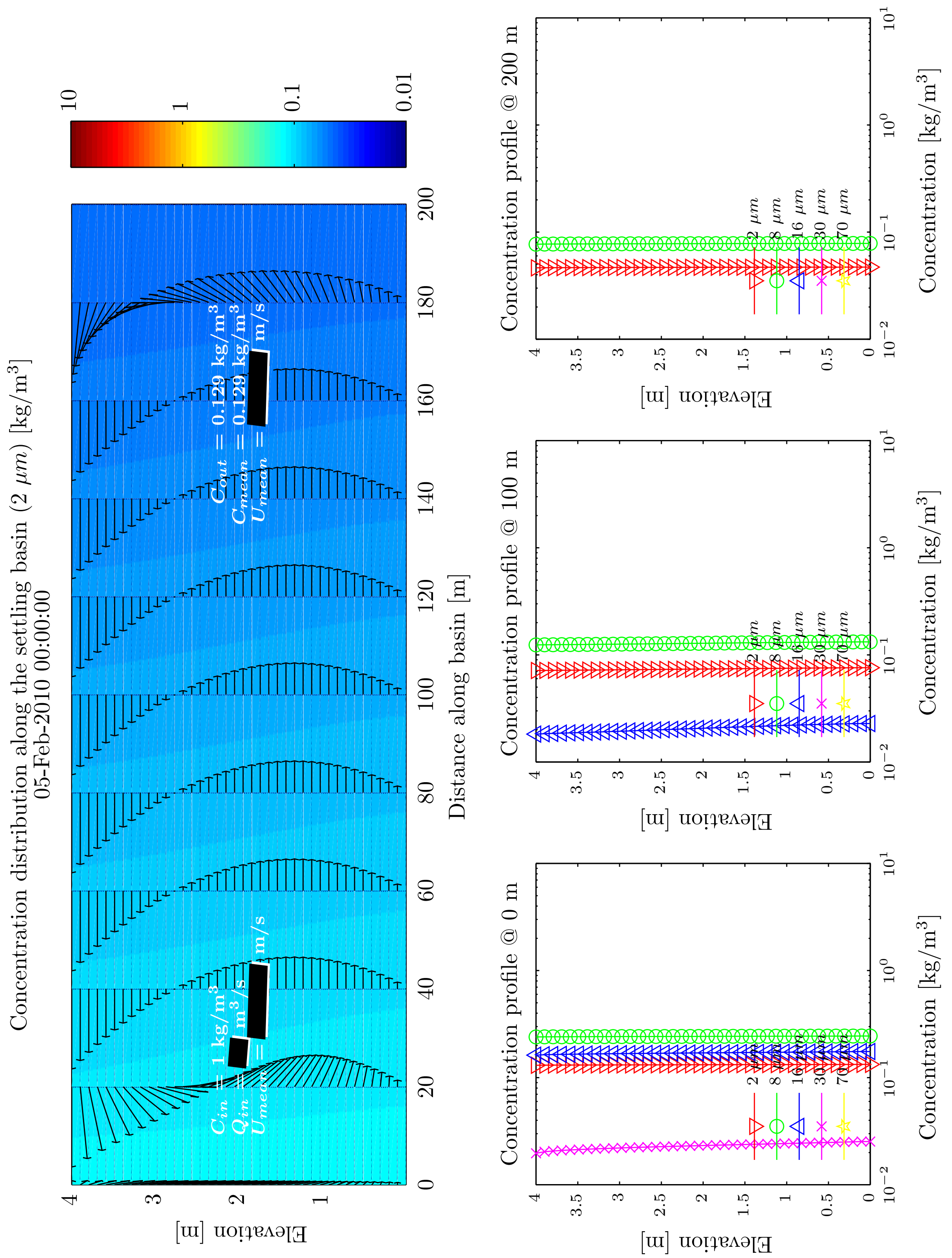


Figure 3.6: Model results case study

which is compared to a existing model and measurement data. For both comparisons, the model appears to give realistic quantities and to behave in a realistic way. The bed boundary and the development of a vertical concentration profile corresponds with a analytical solution in a very good way, expert the influence of some horizontal diffusion.

The definition of a case study enables the design of a basin and gives insight in the behaviour of the model. The basin depth appears to have a minor influence of the outflow concentration as vertical gradients in the suspended sediment concentration are small. Due to the large uncertainties, conservative assumptions will be done, which results in a high outflow concentration, without giving any insight in the propagation of these conservative assumptions in the results.

The assumption for the minimum floc size is conservative and has a large influence on the model results as follows from [redacted] As it is assumed that the dredging process mainly determines the minimum floc size and therefore the minimum fall velocity, field data of the minimum fall velocity is essential to validate this parameter and is also needed to investigate if flocculation occurs in the basin.

# Chapter 4

# Probabilistic analysis

## 4.1 Probabilistic approach

Modelling of the outflow concentration of a settling basins involves many uncertainties due to lack of knowledge and statistical variations. It is therefore impossible to determine a single answer as a result of the outflow concentration. The single answers, as calculated in Subsection 3.2.1, are based on a number of assumptions, which mostly results in a conservative answers, as assumptions are chosen on the safe side. The uncertainty in the input parameters propagates in the results of the project model and are uncertain as well. Therefore the model output should not be a single answer, but a probability distribution of possible outcomes. By investigation of all the relevant uncertainties, it is possible to determine the elaboration of these uncertainties in the final results.

### 4.1.1 Uncertainties

Uncertainties can be divided in various categories. Van Gelder (2000) mentions two primary categories of uncertainty. These are the inherent uncertainties, which represent randomness or the variations in nature, and epistemic uncertainties, which are caused by lack of knowledge of all the causes and effects in physical systems, or by lack of sufficient data. These latter uncertainties are divided in statistical and model uncertainties.

#### Inherent uncertainty in space and time

The inherent uncertainties in time within the project model are the variations over time which cannot be predicted. This is the case for the wind speed $U_{10}$ and the direction of the wind. Although the distributions of these parameters can be investigated in great detail, the actual value still has its uncertainty. The same holds for salinity, but its variation over time is limited.

The composition of the dredged material has a variation in space due to the origin of the material. This variation in space has an influence on the minimum floc size and therefore on the minimum fall velocity $w_{s,min}$. Also the possibilities for flocculation can vary over space. The composition of the dredged material also has a effect on the inflow concentration $C_{in}$ and a limited influence on the effective roughness height $k_s$ of the basin.

#### Statistical uncertainty

The statistical uncertainties that are taken into account in the model to describe the variations of input parameters like discharge and inflow concentration. These parameters are strongly related to the equipment and the operator. Investigation of these parameters can be to expensive or impossible due to lack of sufficient data. Therefore these parameters entail an uncertainty. So, besides a inherent variation in time, the inflow concentration also has a statistical uncertainty.

#### Model uncertainty

The model uncertainty is caused by the lack of knowledge about all the physical processes that are involved or caused by simplifications, needed for computational efficiency, which is treated in Section 2.4. The uncertainties within this project are caused by one-dimensional modelling of the flow and by the uncertainties in the modelling of the suspended sediment concentration profile. Also the outflow concentration through the outflow construction is uncertain. As stated is Section 2.3, the part of the vertical concentration profile which represents the outflow concentration, is an input parameter. This parameter has a large uncertainty which has to be taken into account.

The uncertainty in the settling of sediment particles is a combination of the uncertainty of both the fall velocity and the turbulent mixing. This is especially important for the small fractions for which the upward flux due to turbulence is in the same order as the vertical flux due to gravity. These fractions mainly determine the outflow concentration. Therefore it is decided to only model the uncertainty of the minimum fall velocity and the probability of flocculation.

The influence of the wind also causes uncertainties in the model as the relation between the actual wind speed and the surface shear stress (the wind-drag coefficient) is hard to determine. However, the statistical variation in the wind speed is very broad and this wind speed is dominating the surface shear stress. Therefore it is assumed that the uncertainty in wind speed is dominating the uncertainty in the surface shear stress and the uncertainty in the wind-drag coefficient is not taken into account separately.

### 4.1.2 First order reliability method

The first order reliability method (FORM) calculates the probability of failure based on a linearisation around the design point in the reliability function. Despite the neglect of the higher order effects, this method gives valuable information about the influence of the different parameters on the final results. For each parameter an influence coefficient ($\alpha$-values) is calculated, which provides insight in the relative influence of the different parameter (CUR, 1997).

These calculations according to the FORM are executed with a routine[1] from *OpenEarth* (van Koningsveld et al., 2010). After defining the input parameters with corresponding distributions, the influence coefficients and the probability of failure according to a reliability function, can be calculated.

### 4.1.3 Monte Carlo method

A Monte Carlo simulation (CUR, 1997) gives a very good insight in the elaboration of uncertainties. This method makes a large number of calculations with samples taken from the distributions of the input parameters. Eventual dependencies between certain parameters should be taken into account. If the number of samples is sufficient, the distribution of the calculation results will approach the exact distribution, for the given input distributions.

These calculations are also executed with a routine[2] that is made available by *OpenEarth*. This routine enables the user to vary all the input parameters over several statistical distributions and is able to calculate the probability of failure for a given reliability function. It also shows all the outcomes of the simulation, which makes it possible the investigate the distribution of these results. These realizations from also give possibilities to analyse the influence of each different parameter.

[1] https://repos.deltares.nl/repos/OpenEarthTools/trunk/matlab/applications/probabilistic/engines/FORM/FORM.m

[2] https://repos.deltares.nl/repos/OpenEarthTools/trunk/matlab/applications/probabilistic/engines/MonteCarlo/MC.m

| input | distribution | parameters | | α-value | description |
|---|---|---|---|---|---|
| $Q_{in}$ | normal | $\mu =$ [redacted] | $\sigma =$ [redacted] | -0.2966 | inflow discharge [m$^3$/s] |
| $C_{in}$ | normal | $\mu = 1.0$ | $\sigma = 0.10$ | -0.4932 | input concentration [kg/m$^3$] |
| $k_s$ | normal | $\mu = 0.25$ | $\sigma = 0.05$ | -0.0646 | roughness height [m] |
| $S$ | normal | $\mu = 35$ | $\sigma = 2$ | -0.0001 | salinity of the water [psu] |
| $U_{10}$ | Weibull | $\lambda = 7.896$ | $k = 2$ | -0.6972 | wind speed at 10 meter [m/s] |
| $angle$ | uniform | $a = 0$ | $b = 360$ | 0.1844 | wind angle [degree] |
| $Part_{Out}$ | normal | $\mu = 0.45$ | $\sigma = 0.05$ | -0.0033 | part of concentration profile [-] |
| $floc$ | Bernoulli | $p = 0.25$ | | 0.0000 | occurrence of flocculation |
| $w_{s,min}$ | normal | $\mu = 7e^{-5}$ | $\sigma = 7e^{-6}$ | 0.3801 | minimum fall velocity [m/s] |

| | |
|---|---|
| normal distribution: | $\mu$ = mean, $\sigma$ = standard deviation |
| Weibull distribution: | $\lambda$ = scale parameter, $k$ = shape parameter |
| uniform distribution: | $a$ = minimum, $b$ = maximum |
| Bernoulli distribution: | $p$ = success probability |

Table 4.1: Distibution and $\alpha$-values of case study

## 4.2 Sensitivity analysis Case study

The input parameters of the model are uncertain and are therefore given as a statistical distribution in the model. The results is a distribution of the model output, which is in this case the suspended sediment concentration of the outflowing water. The way this output distribution reacts on a individual input parameter varies strongly between the different parameters. For instance in low concentration simulations, without flocculation and hindered settling, the outflow concentration is linear related to the inflow concentration, which means that a doubling a the input concentration results in a doubling of the outflow concentration. Within the probabilistic calculations a exceedance of a limit value is defined as **failure**. This results in the following reliability function for which failure is defined as $z < 0$.

$$Z = c_{limit} - c_{outflow} \tag{4.1}$$

With:

| | |
|---|---|
| $Z$ | reliability function (failure: $Z < 0$) |
| $c_{limit}$ | limit value of the outflow concentration of suspended sediments [kg/m$^3$] |
| $c_{outflow}$ | outflow concentration of suspended sediments [kg/m$^3$] |

The FORM gives insight in the mutual proportions between the different input parameters by the so called influence coefficients. Table 4.1 gives an overview of the influence coefficients for a probabilistic simulation of the case study which is described in Section 3.2. The nine input parameters are varied over different statistical distributions, for which the parameters are assumed. The normal distributed parameters contain a uncertainty in the quantity of the parameter, which is the result of a large number of mostly unknown variables. According to the central limit theory (CUR, 1997), such parameters are normal distributed. The wind speed is distributed according a Weibull distribution for coastal conditions (Wiering and Rijkoort, 1983, pg. 135) in the Netherlands with an average wind speed[3] of 7 m/s. The wind direction is uniformly distributed as a first assumption, because this depends on the basin orientation and location. Finally occurrence of flocculation is modelled with a Bernoulli distribution as it is uncertain if flocculation occurs or not. The influence coefficient of flocculation can not be determined because the Bernoulli distribution is a discrete probability distribution which can not be approximated by a continuous normal distribution, as required in the FORM.

[3] http://www.windfinder.com/windstats/windstatistic_hoek_van_holland.htm

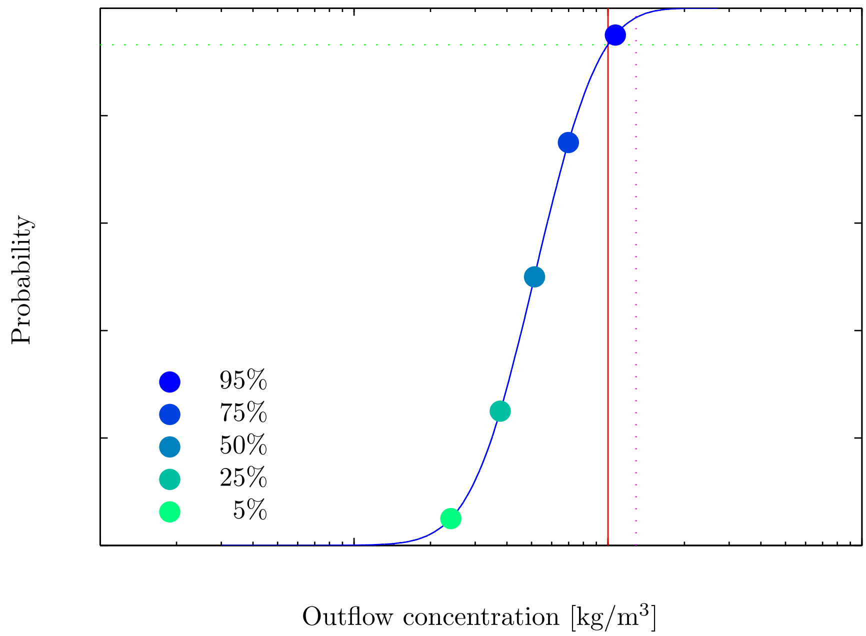


Figure 4.1: Cumulative distribution function of the outflow concentration for the case study

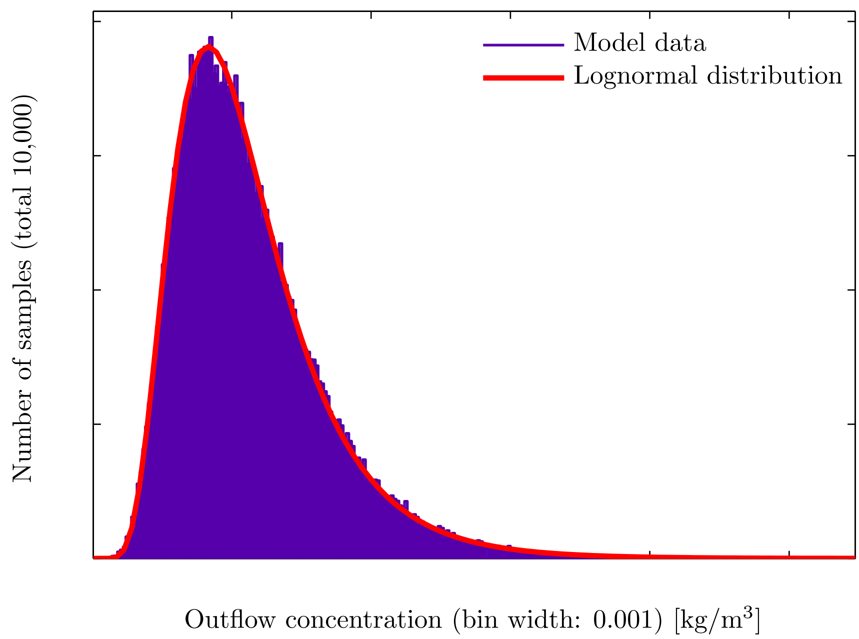


Figure 4.2: Curve fitting for distribution of the outflow concentrations of the case study

The input parameters of Table 4.1 are also used in a Monte Carlo simulation with 10,000 independent simulations. This gives a very good insight in the distribution of the outflow concentration. This distribution is visualized in Figure 4.1 and shows that in only 7% of the cases the outflow concentration is higher than the limit value of 100 mg/l. The deterministic design value of 129 mg/l is exceeded in less than 2% of the cases, showing that the assumptions in the deterministic design are very conservative. Especially when it is considered that the wind speed, that has a large influence on the outflow concentration, is distributed over the full spectrum in the Monte Carlo simulation. The distribution of the outflow concentration fits very good with a lognormal distribution , as shown in Figure 4.2. The lognormal distribution has the largest value for the log likelihood value, compared to other distributions. Therefore this distribution is the best fit statistically. The maximum likelihood estimation results in the following parameters: $\mu = -2.97454$ and $\sigma = 0.454072$. According to this parameters, $P(Z > 0) = 0.9305$ which corresponds very good with the failure probability of the Monte Carlo simulation. The lognormal distribution is often used for variables that cannot assume negative values on physical grounds. This is exactly the case for the suspended sediment concentration. According to the central limit theory the product of a large number of random variables is lognormally distributed. Taking into account the suspended transport equation (Equation 2.4), the outflow concentration can be considered as a product of a number of random variables. Therefore the lognormal distribution appears to be a good choice for the distribution of the outflow concentration of suspended sediments.

### 4.2.1 The weighted sensitivity for Monte Carlo simulations

The FORM provides the influence coefficients in a analytical way, based on a linearisation of the reliability function (Equation 4.1) in the design point (point in the failure space $Z < 0$ with the greatest probability density). This design point is based on minimization of the distance between the reliability function and the origin of the normalized basic variables (CUR, 1997, Section 5.3). Meeuws (1997) provides methods to determine the design point for a Monte Carlo simulation. Within this project the method *centre of gravity* is used the determine the design point. First the center of gravity of each parameter for the 'failed' simulations ($Z < 0$) is determined. Thereafter, a linearisation is applied between the center of gravity and the mean values. The point of intersection between this linearisation and the reliability function ($Z = 0$) is a approximation of the design point. The two determined design points are given in Table 4.2. The design point of both methods is more or less the same. The design point of the flocculation parameter is 0 as it is discreetly distributed and cannot be interpolated between 0 and 1. The design point of the Monte Carlo simulation is used to calculate the derivative of the reliability function of each parameter. If the parameters are assumed to be normally distributed, the influence coefficients can also be determined in the design point on a analytical way (CUR, 1997). This latter method is similar to the influence coefficients of the FORM, except the location of the design point and the determination of the distance between the reliability function and the origin of the normalized basic variables. This distance is based on the probability of failure of the Monte Carlo simulation.

The influence coefficients can also be determined by calculating the covariance between the realizations of a certain input parameter $X_i$ and the resulting value of the reliability function $Z$. This approach is based on the linear regression analysis and gives an expected value for the correlation coefficient of $X_i$ and $Z$ (Vrijling and van Gelder, 2006). Table 4.3 gives a overview of the calculated influence coefficients for the various methods. It gives indications of the influence of each parameter. The differences come from the way the influence is determined. The covariance-method takes into account all realizations and is not concentrated on the design point, whereas the third column assumed normally distributed variables. Contrary to the FORM, the Monte Carlo based influence coefficients gives more reliable values for the influence coefficient of the flocculation parameter. Appendix D gives an overview of the derivation of the influence coefficients for the various methods.

| input | distribution | parameters | | design point ($Z = 0$) FORM | Monte Carlo |
|---|---|---|---|---|---|
| $Q_{in}$ | normal | $\mu =$ [redacted] | $\sigma =$ [redacted] | 1.5294 | 1.5314 |
| $C_{in}$ | normal | $\mu = 1.0$ | $\sigma = 0.10$ | 1.0652 | 1.0580 |
| $k_s$ | normal | $\mu = 0.25$ | $\sigma = 0.05$ | 0.2521 | 0.2523 |
| $S$ | normal | $\mu = 35$ | $\sigma = 2$ | 35.0004 | 34.9734 |
| $U_{10}$ | Weibull | $\lambda = 7.896$ | $k = 2$ | 8.4008 | 8.2172 |
| $angle$ | uniform | $a = 0$ | $b = 360$ | 162.5377 | 179.4903 |
| $Part_{Out}$ | normal | $\mu = 0.45$ | $\sigma = 0.05$ | 0.4501 | 0.4595 |
| $floc$ | Bernoulli | $p = 0.25$ | | 0.0000 | 0 |
| $w_{s,min}$ | normal | $\mu = 7 \cdot 10^{-5}$ | $\sigma = 7 \cdot 10^{-6}$ | $6.8241 \cdot 10^{-5}$ | $6.8335 \cdot 10^{-5}$ |

Table 4.2: Design point for both FORM and the Monte Carlo simulation

| parameter | $\alpha_i = \frac{Cov(X_i,Z)}{\sigma_{X_i}\sigma_Z}$ | $\alpha_i = \frac{-\frac{\partial Z}{\partial X_i}\sigma_{X_i}}{\sigma_z}$ | $\alpha_i = \frac{X_i^* - \mu_{X_i}}{\beta\sigma_{X_i}}$ | FORM |
|---|---|---|---|---|
| $Q_{in}$ | -0.3637 | -0.4252 | -0.1375 | -0.2966 |
| $C_{in}$ | -0.4073 | -0.7250 | -0.1991 | -0.4932 |
| $k_s$ | -0.0778 | -0.0938 | -0.0351 | -0.0646 |
| $S$ | 0.0091 | -0.0002 | -0.0036 | -0.0001 |
| $U_{10}$ | -0.2929 | -0.9105 | -0.2227 | -0.6972 |
| $angle$ | 0.0054 | -0.0207 | 0.0016 | 0.1844 |
| $Part_{Out}$ | 0.0060 | 0.0000 | -0.0007 | -0.0033 |
| $floc$ | 0.3167 | 0.4997 | 0.3865 | 0.0000 |
| $w_{s,min}$ | 0.3757 | 0.5672 | 0.1724 | 0.3801 |

Table 4.3: Weighted sensitivity analysis for Monte Carlo simulation

## 4.3 Modifications in the Case Study

The influence of the previous section of mostly based on the design point. In order to get a better insight in larger variations of certain parameter, a number of modifications is applied on the case study. These are: discharge, wind angle, probability of flocculation and water depth.

### 4.3.1 Change of the mean discharge

The distribution of the outflow concentration of suspended sediments is simulated for various mean discharges for the case study. These mean discharges are varying from [redacted] m$^3$/s up to [redacted] m$^3$/s which represent different types of equipment. Each discharges has again a standard deviation of 10% and is simulated 10,000 times. Figure 4.3 gives an overview of the various cumulative distribution functions. It clearly shows that the risks of excedance of the limit value increases drastically by increasing the discharge, which can be explained by the increased flux through the vertical column. Decreasing the mean discharge reduces the risk of exceedance to a few promille.

### 4.3.2 Influence of the direction of the wind

The direction of the wind in the case study is assumed to be uniformly distributed. The FORM already showed that the direction of the wind can be a significant parameter in the determination of the outflow condition. To visualize this influence, the case study in modelled for various fixed wind directions. Figure 4.4 shows the probability of an outflow concentration as a function of the wind direction. It clearly shows that a wind direction opposite to the flow direction gives a higher risk of exceedance of the limit value. As only the secondary flow is influenced by the wind angle, this effect had to be caused by the higher flow velocity near the higher concentrated bottom and the vertical upwelling. Extra information on the dominant wind direction creates possibilities to

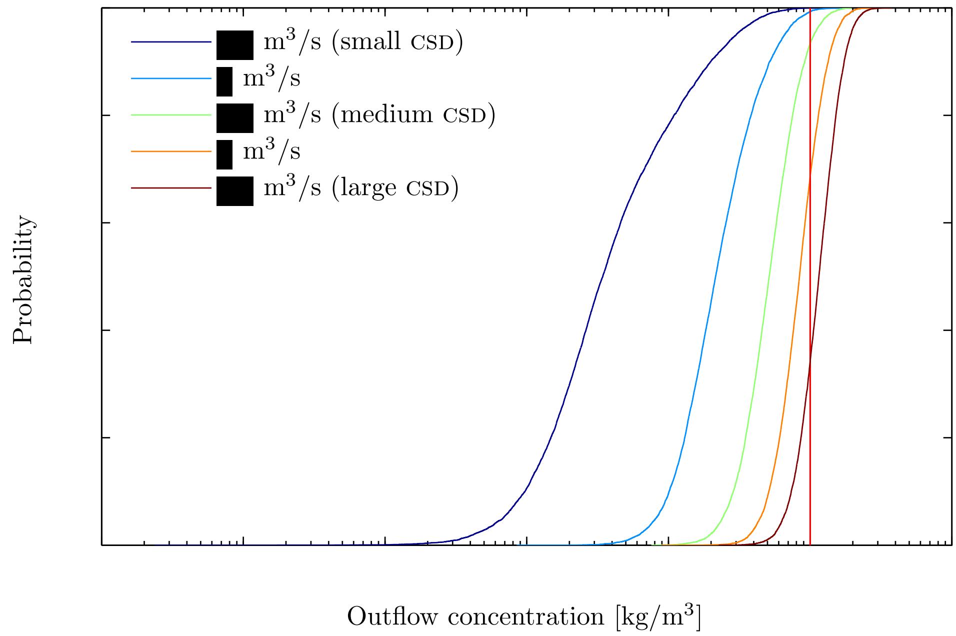


Figure 4.3: Cumulative distribution function of the outflow concentration for the case study for various mean discharges (CSD: cutter suction dredger)

design a settling basin in the most optimum way and gives also a better insight in the increased risk if this optimum design is not possible. The markers in Figure 4.4 represent all simulations and approaches the simulation with a uniform distribution that is given in Figure 4.1 and the markers in the latter figure correspond with these markers.

### 4.3.3 Influence of flocculation

The change on flocculated fines is determined on 25%. These kind of assumptions are based on expert judgement. The influence of this parameter on the outflow concentration is important to get insight on the sensitivity of this parameter. This influence is analyzed with a Monte Carlo simulation with a varying probability of occurance of flocculation. This probability of flocculation varies from 0% (never flocculated fines) to 100% (always flocculated fines). Figure 4.5 shows the results of this simulation and shows that the distribution of the outflow concentration of suspended sediments is moving towards lower concentrations with a increasing probability of flocculation. The spreading of the outflow concentration also decreases for flocculated fines, indicating that a system with full flocculated fines has a lower sensitivity.

### 4.3.4 Influence of the basin depth

In Section 3.2 the influence of the water depth is already mentioned. The basin depth has various influences on the outflow concentration. First of all it has a direct influence on the flow velocity and the residence time. A longer residence time gives particles more time to settle and would therefore result in a lower outflow concentration. Although deeper basins are also more turbulent, as the turbulent kinetic energy is related to the mixing length which is assumed to be proportional to the basin depth (Equation C.29). At some point the turbulent mixing over the vertical is dominant compared to the settling of the particles, which results is very small vertical gradients in the suspended sediment concentration. Therefore in deep basins the effect of the longer residence time is eliminated by the increased turbulence. In Figure 4.6 the effect of the dominant turbulence

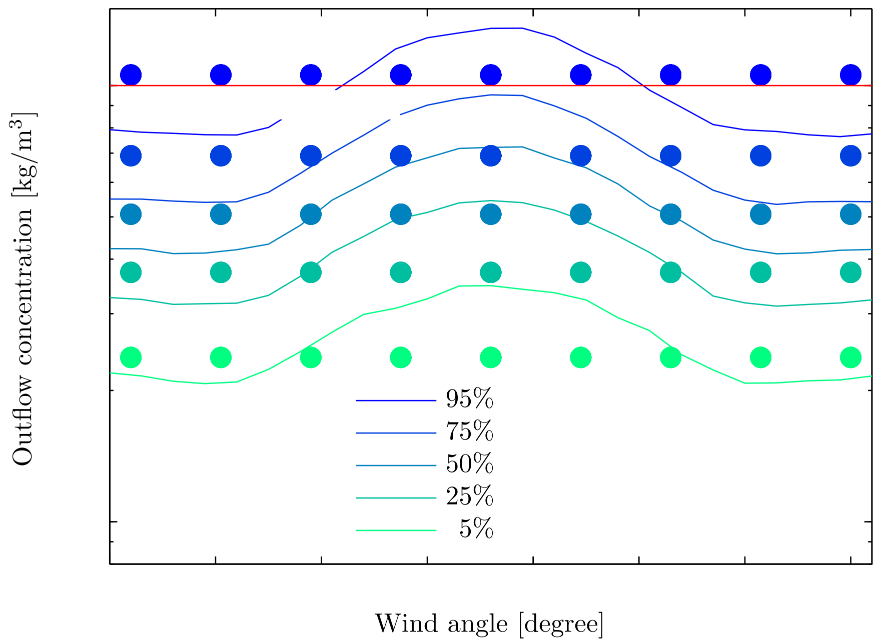


Figure 4.4: Probability of an outflow concentration for various wind directions; the markers take in account all simulations, which corresponds with the markers in the cumulative distribution function Figure 4.1

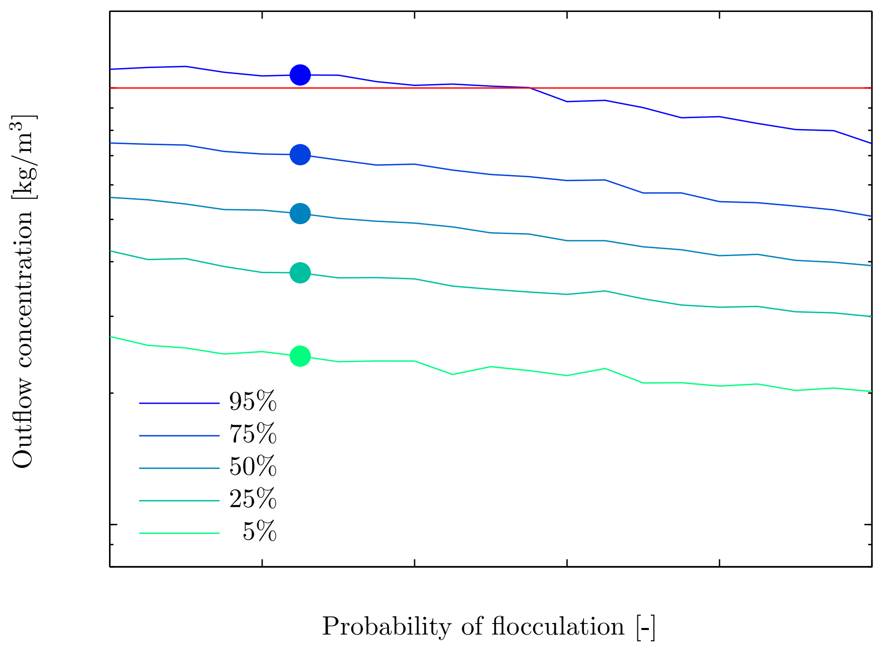


Figure 4.5: Probability of an outflow concentration for various probabilities of flocculated fines; the markers correspond with the markers in cumulative distribution function Figure 4.1

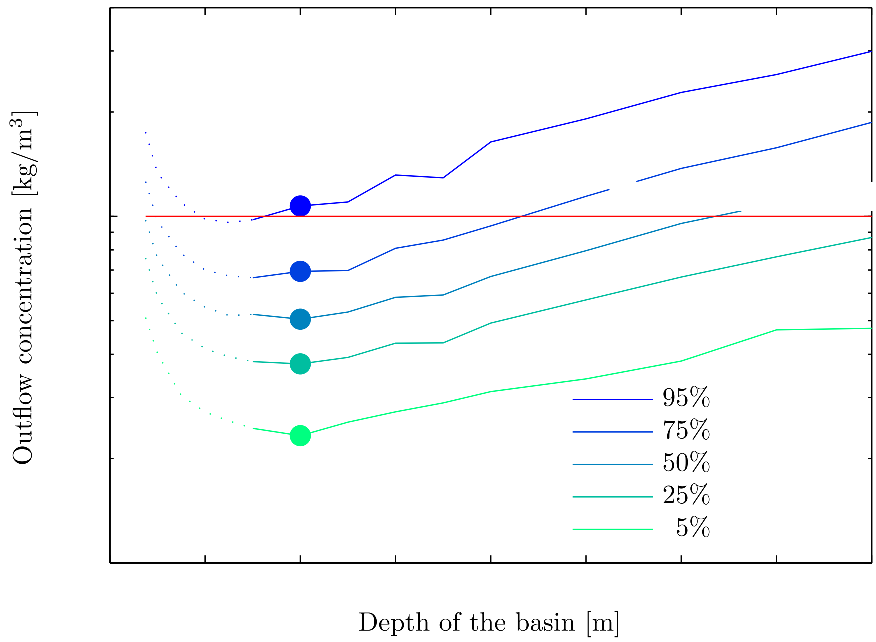


Figure 4.6: Probability of an outflow concentration for various basin depths; the markers correspond with the markers in cumulative distribution function Figure 4.1

is clearly visible. For certain depths also the horizontal turbulent mixing starts to play a role, which can be seen in the figure by the increased outflow concentration for larger depths. The optimum basin depth can be found in the trough of the graph. The dotted graphs are outside the applicability of the project model as the influence of wind waves near the bed cannot be neglected. Neglecting this influence is only allowed if the water depth is significant higher than the wave length. Typical calculations for the case study give wave lengths in the order of [redacted] meter for wind speeds of 10-15 m/s.

### 4.3.5 Influence of the mean wind speed

Already in Figure 4.6 the influence of the wind can be noticed, as its influence on turbulence increases with the depth of the basin. Figure 4.7 shows directly the influence of wind of the distribution of the outflow concentration by varying the annual mean wind speed. The actual wind speed is still modeled as a Weibull distribution, but the mean wind speed is varied. Besides the influence in the wind speed, it implicitly shows the influence of the wind-drag coefficient $C_d$ which translate the wind speed into a surface shear stress (see also Equation B.45). This wind-drag coefficient is influenced by waves and appears to be hardly determinable. The figure shows the importance of the wind induced effects as the outflow concentration for a mean wind speed of zero (no wind at all as negative wind speeds do not occur) is of a lower order. Although the outflow concentrations for the more realistic annual mean wind speeds are in the same order of magnitude, the influence is still significant. The case study has a annual mean wind speed of 7 m/s resulting in a probability of failure of 7% (Figure 4.1). Decreasing this annual mean wind speed to [redacted] m/s by using for instance wind protection screens reduces the probability in failure to less than 1% (magenta coloured marker in Figure 4.7).

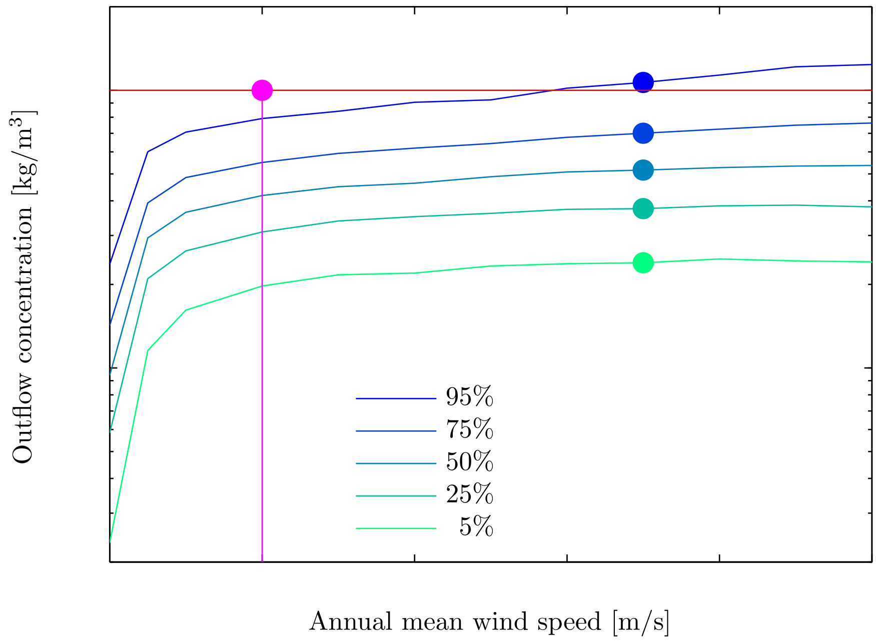


Figure 4.7: Probability of an outflow concentration for various annual mean wind speeds; the markers correspond with the markers in cumulative distribution function Figure 4.1

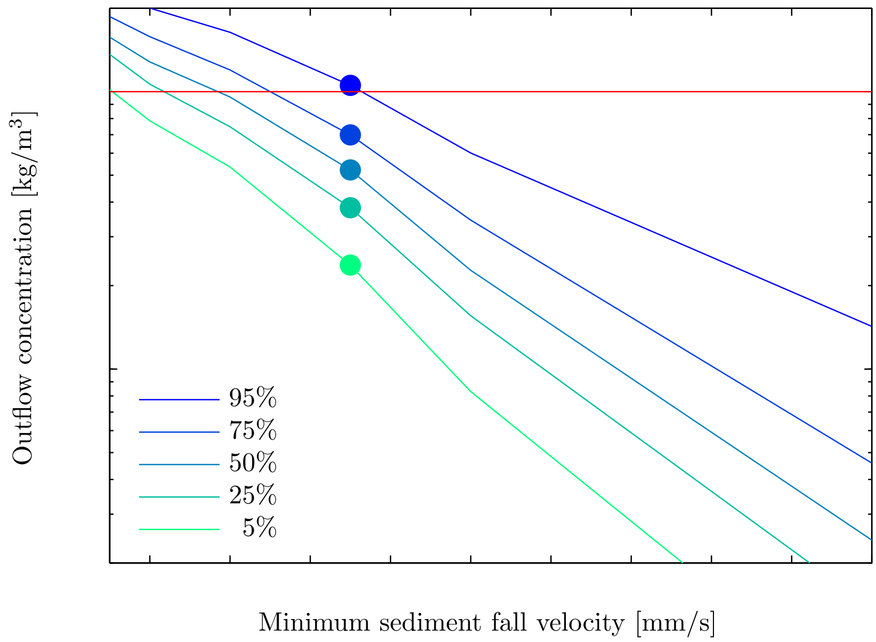


Figure 4.8: Probability of an outflow concentration for various minimum sediment fall velocities; the markers correspond with the markers in cumulative distribution function Figure 4.1

### 4.3.6 Influence of the minimum fall velocity

The minimum fall velocity is an important parameter in the modelling of a settling basin as it represents the minimum floc size which 'survices' the dredging process (see autorefmodelling-floc. In the FORM and the Monte Carlo simulations, this parameter is assumed to be 0.07 mm/s, representing a particle size of about 8 $\mu m$. A standard deviation of 10% is included to deal with uncertainties in the determination of the minimum fall velocity and to represent the model uncertainty as mentioned in Section 4.1.1. To get insight in the importance of this determation a number of different minimum fall velocities is modelled, showing large variations due to this minimum fall velocity (Figure 4.8).

## 4.4 Conclusions

The determination of the influence coefficients with both the Monte Carlo simulation and the FORM, clearly show the influence of the different parameters on the design point. These influences result in the a lognormal distribution of the outflow concentration of suspended sediments.

Several Monte Carlo simulations show the importance of the wind induced effects and identify an optimum basin depth. Limiting these wind induced effects can be a effective measure to reduce the probability of failure (exceedance of the limit value). Optimization of the basin orientation compared to the dominant wind direction also appears to be an effective measurement.

Finally it can be concluded that the outflow concentration is largely dependent on the flocculation effects and the minimum floc size. Careful determination of the latter parameter is extremely important to get useful information from the simulations.

# Chapter 5

# Probabilistic design

## 5.1 Goal variable

From a contractors point of view, the design of a settling basin in the most economic way is the main objective he wants to be achieved. Therefore he wants to fulfil the environmental requirements in a economic way with an acceptable financial risk. This chapter will only threat the economic optimization as the environmental requirements are assumed to fulfill the social and environmental objectives.

## 5.2 Decision variables

The search for the most economic basin design is started with the identification of the so called decision variables. These are the parameters which can vary between a certain range in order to find either the economic optimum or a required level of safety. In case of a settling basin these parameters involve the basin design and the choice of the equipment. Based on practical experience from the past it is concluded that the area available for a settling basin can hardly vary within a certain project. Especially in the stage of the design of the settling basin the available space is already specified. Although this practice can change in the future, this project will focus on possible decision variables for a given available area.

### 5.2.1 Basin depth

A first decision variable is the depth of the basin, which enlarges the basin volume and therefore the residence time in the basin. This give the particle more time to settle. A larger depth gives also rise to turbulence due to the larger mixing length. This mixing length is only limited by both bottom and surface and therefore a deeper basin is more turbulent. Because of the very low flow velocity in the basin, turbulence is in most cases dominated by the wind shear stress. A deeper basin also include higher construction costs. These opposing influences indicate a certain economic optimum between residence time, additional turbulent mixing and construction costs.

### 5.2.2 Choice of equipment

The second decision variable which is identified is the choice of the equipment and therefore the discharge of the water sediment mixture. This discharge is directly related to the residence time in the basin. A higher discharge decreases the residence time and will result in higher sediment concentrations over the basin is most cases. This will increases the risk of exceeding a certain concentration limit at the outflow of the basin. However in most cases a higher discharge will save time and will be financial beneficial in most cases. These competing interests also give rise to a certain economic optimum depending on the financial risk of increased sediment concentrations in the outflow.

### 5.2.3 Unconventional decision variables

Wind dominates the generation of turbulence in most cases, due to the low mean flow velocities. Therefore in potential critical cases, with high wind speeds, it might be attractive to protect a settling basin against these influence by changing the orientation of the basin or by protecting to basin with wind break nets. Especially in critical cases, where interrupting the dredging process is unacceptable costly this can be an economic acceptable alternative.

A possible way to change the orientation of the basin is the manipulation of the flow pattern with the use of multiple inflow and outflow constructions. Depending on the wind direction and the actual suspended sediment concentration it is possible to choose the most optimal flow direction. In that case the angle between the flow direction and the wind direction is no longer completely unpredictable.

## 5.3 Risks and variable costs

The design of a settling basin has to include all costs and financial risks that are involved during construction and execution. The quantification of the financial risk is fully project based as the environmental requirements are site specific and set in contract document. Therefore the financial risks of the case study are based on assumptions for downtime and fining.

For the determination of an economic optimum it is necessary to get insight the variable cost of a settling basin. Based on practical experience (J.A. van den Herik, personal communication, January 6, 2011) a number of variable costs is identified. The costs of the construction of the basin are mainly determined by earthmoving and are quantified by a price per cubic meter in the order of € [redacted] As stated above the amount of available space is given in almost all projects so no significant variable costs are involved.

The financial risks of downtime are identified for three different types of equipments with increasing production capacities. Therefore typical working and idle costs of this equipment are made available (W.G. van Poele, personal communication, February 16, 2011). The risks of fining are assumed to be a percentage of the contract price. Therefore the product of probability of failure and the contract price is used the identify a fine, which is considered as a conservative assumption.

## 5.4 Time effects

Time effects play an important role as some parameters vary during the execution of a project. The statistical distribution of the wind speed and wind direction is a good example of parameters which vary within the execution of a project, but also the realizations of uncertain parameters as discharge and inflow concentration can vary within a project. Therefore a correlation time is defined. This is a time step for which a realization of the outflow concentration is assumed to be independent of the previous realization. The correlation time can be determined by calculating the correlation over time. This can be done with both time varying model results and measurement data, which are both not available. Therefore the residence time in the basin is used as a first approximation of the correlation time for the case study. This residence time is approximately one day, which also is assumed to be a realistic value for the correlation time of the wind. The modelling of the time effects of a project will be done by simulation the execution of a project with $n$ independent realizations of the outflow concentration. Herein, $n$ is the total working time divided by the residence time.

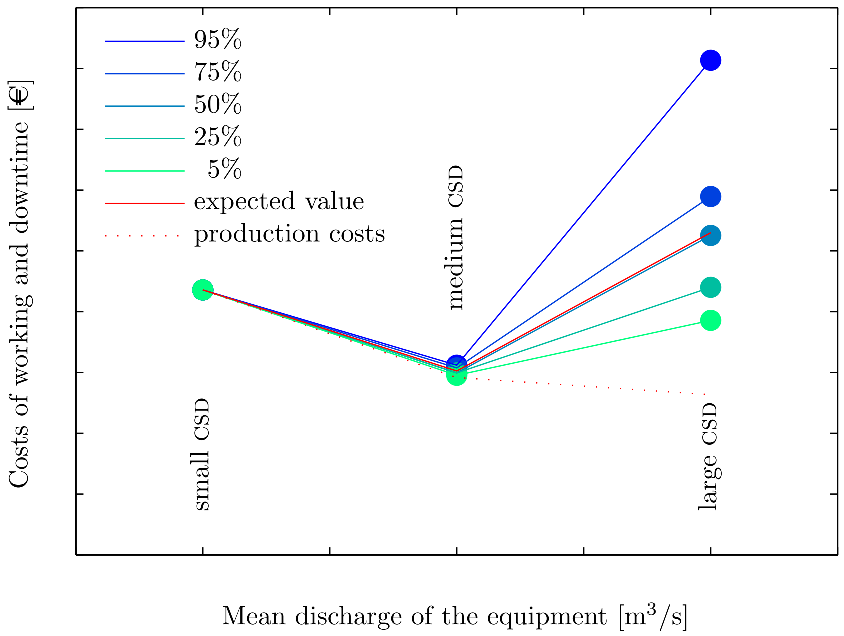


Figure 5.1: Cost of production and downtime for different types of equipment (CSD: cutter suction dredger)

## 5.5 Most economic choice of equipment

The economic optimal choice for the equipment will be determined in the following way. Again the case study of Section 3.2 is taken into account and the contractor has three different types of equipment available with weekly productions of [redacted] $m^3$. The total contract volume is [redacted] $m^3$ with takes respectively about [redacted] working days. The contract forces the contractor to stop the dredging activities when the limit value for the suspended sediment concentration is exceeded. This exceedance is defined as failure. In order to take into account the time effects, the project is simulated with a number of independent realizations which is equal to the number of working day (correlation time is assumed to be one day). Each project simulation results in a failure rate. These project simulations are done several times resulting in a distribution of the failure rate. This failure rate can be transformed into the downtime and costs due to downtime. Together with the fixed production costs this results in the total costs. Figure 5.1 gives an overview of the costs and its uncertainty for different types of equipment. The figure clearly shows that the medium CSD is the best choice. The production costs are low and the risk of downtime is very limited. The small CSD appears to be to conservative as there is no downtime at all. The large CSD has a too great risk of downtime (the validity of the latter simulation is decreased as the total project time becomes significant longer than the working time due to the large downtime).

## 5.6 Risk portfolio

The way time effects have to be taken into account depends on the risk portfolio of the contractor. When the contractor concerns the risks on a project scale, they might be significant due to the large uncertainties. Taking into account a larger time scale will result in a reduction of the uncertainties of the risk. If for example the above mentioned case study is executed on many similar locations, the overall costs will finally approach the expected value in Figure 5.1. Assuming that the

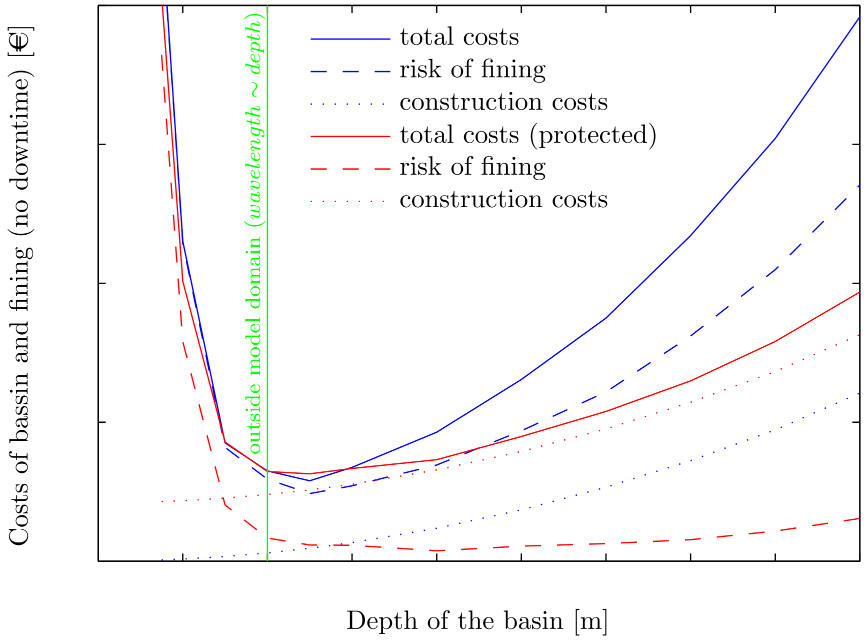


Figure 5.2: Costs of basin and fining for various basin depths in risk neutral cases, with and without wind protection screen

incidental high costs are affordable and acceptable for the contractor, the economic optimal design is the minimum of the expected costs. In the case when incidental high costs are unaffordable or unacceptable for the contractor, he is willing to pay a certain amount of money in order the reduce the risk. The first risk concept describes a risk neutral attitude while the latter risk attitude is called *risk aversion* The opposite attitude is *risk seeking* (e.g. gambling).

## 5.7 Most economic basin depth

The depth of a settling basin has a certain optimum for which the outflow concentration of suspended sediments will be minimal, as shown in Subsection 4.3.4. This is the optimum from a ecological point of view. It is also possible to find an optimum from a economic point of view, which might be different due to the increasing construction costs for deeper basins. The blue graphs in Figure 5.2 show the construction costs and expected fining costs for the case study. The fining costs are based on the number of failures and the contract price ($fine = P_{failure} \cdot$ € [redacted] . The graph of the total costs (construction costs and fining costs) show a minimum around [redacted] meter basin depth for risk neutral conditions. Investigation of the uncertainty is irrelevant as both the risk of fining and the construction costs increase for deeper basins. This basin depth therefore also appears to be the optimal basin dept for risk averse contractors

## 5.8 Profitability of wind protection

In the previous section it is concluded that the risk cannot be decreased by deepening the basin, as the risk increases for deeper basin. Already in Subsection 4.3.5, the high influence of the mean wind speed is mentioned. Therefore the influence of a reduced mean wind speed is investigated. A possible way to reduce the influence of the wind is the coverage of the basin with wind break nets. Identical calculations show that for the case study with an optimal basin depth the expected costs for risk neutral cases are more or less the same for both protected and unprotected conditions. The uncertainty under unprotected conditions is much larger as the main part of the costs is the expected cost for fining. Under protected conditions these costs are largely come form the construction costs which are more or less fixed. Therefore the use of a wind break net can be a attractive measurement to reduce the risk.

## 5.9 Conclusions

In order to come to the most economic basin design a number of decision variables can be changed. The choice of equipment has a interesting propagation in the total project costs. Based on the working and idle cost of three cutter suction dredgers, the most economic choice for the case study is determined for a policy in which exceedance of the limit value results in downtime. Also the uncertainties of the costs due to downtime on a project time scale are visualized.

As already concluded in Chapter 4, there is a certain optimal basin depth. Including the construction costs of a basin does not have a significant effect an this optimal depth as the construction costs are low compared to the financial risk. For the conditions of the case study, a wind protection net has a strong risk reducing effect but the expected costs are more a less the same as for unprotected conditions. For more critical cases with high financial risks, a wind protection net might be beneficial from an economic point of view as well. The feasibility of wind break nets is subject of discussion, because there are no known practical experiences.

# Chapter 6

# Conclusions and recommendations

## 6.1 Conclusions

The objective of this study is the development and evaluation of a probabilistic approach to quantify the outflow concentration of settling basins on dredging and reclamation works, in order to enable environmental risk based design optimization. On the basis of the study results, a number of conclusions are drawn for each of the research questions.

**I How can the outflow concentration of suspended sediments (TSS) at settling basins be determined?**

Quantification of the outflow concentration of settling basins and its uncertainty is an important element to investigate the environmental risk of dredging and reclamation works. This outflow concentration can be determined in a simplified way with the 1DH-modelling of the flow and the 2DV-modelling of the suspended sediment concentration. The project model, developed for this study, is an efficient tool that contains the relevant processes for the determination of the outflow concentration of suspended sediment at settling basins. The model is only appropriate for low concentrated sediment mixtures, due to the simplifications that are required for computational efficiency.

The settling of the finest particles dominates the outflow concentration. This settling is determined by the turbulent mixing and the fall velocity of these finest particles. The fall velocity of the finest particles is determined by the minimum floc size (size of agglomerated clay particles) and is defined as the minimum fall velocity. The minimum floc size is assumed to be mainly determined by the dredging process. It is unlikely that flocculation (agglomeration of clay particles) occurs in the settling basin as the time for flocculation seems to be too short. Therefore the minimum floc size is assumed to be constant over the basin. The minimum fall velocity is an important parameter for calibration and can easily be determined in the field by simple equipment and a trained eye.

**II How does the project model perform for measurement data and compared to existing solutions?**

The performance of the project model is evaluated by comparison with measurement data and existing solutions. The results of this evaluation are promising. The comparison with measurement data gave results of the same order of magnitude for [redacted]

The comparison with the [redacted] also gave outflow concentrations which were of the same order of magnitude. The distribution of the suspended sediment concentration over the vertical differs from each other. The project model is considered to provide a more useful representation of reality than [redacted] The process based approach resulted in a generic framework in which a number of physical processes have been implemented that were not included in the [redacted] before. Especially the vertical resolution in the suspended sediment concentrations is considered to be an important improvement.

The distribution of the suspended sediment concentration in the vertical plane corresponds with the analytical solution in a very good way. Despite some differences due to horizontal mixing, the results can be considered as equivalent.

**III What are the main sources of uncertainties in case of probabilistic calculation of the outflow concentration of suspended sediments?**

The probabilistic method enables the investigation of the main sources of uncertainties. For the case study, this resulted in a lognormal distribution of the outflow concentration with a probability of failure of 7% whereas the deterministic calculation shows failure. This distribution gives a realistic picture of the actual risks of exceedance of the limit value.

Determination of the design point with both the FORM and the Monte Carlo based *center of gravity* method enables the determination of the influence coefficients in different ways. Due to non-normal and discreet distributions, this resulted in discrepancies between the different methods, although it gives a good impression of the influence of each parameter. To investigate these discrepancies in the influence coefficients, several Monte Carlo simulations were executed for various parameters.

The influence coefficients and the results of the several Monte Carlo simulations show the importance of both the wind speed and the wind direction. Especially an opposite wind direction appears to cause increased outflow concentrations. Also the discharge has a very large effect as it directly influences the flux of suspended sediments. The same holds for the inflow concentration, which is in low concentrated mixtures linear related to the outflow concentration. The minimum fall velocity has a very large influence and the determination of its mean value and uncertainty is a important calibration parameter. The probability of flocculation also is an important calibration parameters, as it influences the fall velocity of the finest particles. This has a significant influence on the outflow concentration as well. The basin depth appears to have a certain optimum, because the benefit of a longer residence time in deeper basins is eliminated by the increased turbulence due to the increased depth. This causes additional mixing in both the vertical and horizontal direction.

**IV What is the economic optimal design of a settling basin accounting for uncertainties?**

The economic optimal design of a settling basin can be found by defining the inability to meet the environmental requirements as an environmental risk in terms of money. The basin depth and the choice of equipment are the main decision variables. For both decision variables an economic optimum can be found. Due to the limited construction costs of the basin, the economic optimal basin depth is almost equal to the optimal basin depth without taking into account the construction costs and the environmental risk.

For the choice of equipment also time effects are taken into account. These effects consider the variation of certain parameters over time and are taken into account for the time scale of a project, because from a contractors point of view the environmental risk of a single project can be decisive. This resulted in a spreading of the costs of both working time and downtime for various discharges (this can be considered as various type of equipment). Based on the expected costs and the uncertainty, the contractor can decide which equipment he wants to use. In risk neutral cases this will be the equipment with the lowest expected costs but a risk averse contractor is willing to accept higher expected costs with a lower uncertainty.

An extra investment in the construction of the settling basin by using wind protection nets can be profitable in critical cases. In the case study this resulted in a reduction of the risk which was more or less the same as the assumed costs for the wind protection nets. For risk averse contractor this might be a good option as it results in a lower risk for more or less the same expected costs. In critical cases with high environmental risks a wind protection screen can result in lower expected costs and would be beneficial is all cases.

## 6.2 Recommendations for the use in practice

The project model gives optima for both basin depth and basin orientation. For future basin design projects it is advised the identify the optimal basin depth for the expected discharge and wind conditions. If possible, the orientation of the basin should be optimized depending on the dominant wind direction. Depending on the availability of equipment and the environmental risks, the project model can identify the most economic choice of equipment.

Investigation of sediment samples and experiences of similar dredging projects is required for the determination of the minimum sediment fall velocity and the probability of flocculation. For calibration purposes is it advised to determine the minimum sediment fall velocity and the occurrence of flocculation with water samples. The minimum floc size in the inflow of the basin is assumed to be mainly determined by the dredging process. Shear stresses on the scale of the floc size can break up the flocs in the water-sediment mixture. Decreasing these shear stresses would be very attractive for the settling of the flocs as larger flocs settle far more faster than smaller flocs and individual silt particles. Therefore, in case of critical environmental requirements, it can be beneficial to reduce the shear stresses by the use of different equipment in order to prevent break up of small flocs. Investigation of the financial consequences of reduction of the shear stresses is advised.

## 6.3 Recommendations for economic optimization

The environmental risk is defined in terms of downtime and penalties for the inability to meet the environmental requirements. Further investigation is required to investigate the environmental related financial risks for the contractor. Especially when contractors are liable for environmental damage caused by their activities, which is the case in design and construct contracts, this can be a serious risk.

The risk policy of contractors can be an important criterion in the determination of the most economic choice. Especially when risks are considered on a project time scale, risk neutral approach is not always appropriate and time effects have to be investigated in more detail.

## 6.4 Recommendations for model improvements

There are a number of elements in the project model which can be improved if it appears to be necessary for future use of the model.

The influence of the wind is significant and therefore the wind-drag coefficient becomes a important uncertainty which is already visualized in Subsection 4.3.5. In the project model this uncertainty is assumed to be included in the uncertainty of the wind speed. Investigation of this uncertainty separately would gives more insight in this quantity, and perhaps confirm the above mentioned assumption.

Secondary flow is only taken into account in the vertical flow plane. Secondary flows perpendicular to this plane are assumed to not influence the vertical flow plane or the vertical mixing. Three dimensional modelling should verify this assumption and create more insight in the consequences of the secondary flow.

The influence of a vertical current due to the weir box is modelled as a part of the vertical concentration profile that is representative for the outflow concentration. Although the vertical gradients in the suspended sediment concentration are small, further research is advised to calibrate this parameter for different flow conditions.

As already visualized in Figure E.8 the model has the ability to update the bed level by using the change in sediment flux. For silt ponds which only contain low concentrations of fines, the influence of the settled fines on the bed is neglected. For the use in dumping sites this update of the bed level is essential, as the dimensions of the basin change drastically over the time. Further research into the change of the bed level at dumping sites is necessary to ensure realistic simulations of the fill up of these basins.

An important assumption in the project model is the neglect of sediment-fluid interactions, as for instance density currents. For low concentrated silt ponds this assumption is defensible, but in the more concentrated dumping sites, gradients in density can not be neglected anymore. Therefore the influence of possible density currents has to be investigated in order the valuate potential use of the project model for dumping sites.

Within this project all parameters were stationary for each individual simulation. An advisable next step would be the variation of for instance wind and flow conditions within a single simulation to better mimic the reality. [redacted]

The project model simulates a settling basin is a simplified way, which is considered to be appropriate for application in probabilistic calculations. The modelling of a settling basin in more detail reduces the model uncertainties and can be very useful to provide more insight in the processes of a settling basin. Delft3D-FLOW (Deltares, 2010) in a powerful tool for this application.

## 6.5 Recommendations for environmental impacts assessments

The availability of a probabilistic method to determine the distribution of the outflow concentration of settling basins creates the opportunity to use this information in sediment spreading models and ecosystem models. Further research into the applicability of probabilistic methods for environmental impact assessments is recommended. Application of these methods enables the user to directly investigate the effects on the environment without the use of environmental requirements in terms of suspended sediment emissions. Therefore, the project model can be an important element for probabilistic analysis of environmental impacts at dredging and reclamation projects.

# Bibliography

[redacted]

[redacted]

[redacted]

ASCE (2008). *Sedimentation Engineering: Processes, Measurements, Modeling, and Practice.* ASCE Manuals and Report on Engineering Practice No. 110.

Battjes, J. A. (2002a). *Fluid Mechanics.* Lecture notes, Faculty of Civil Engineering and Geosciences, Delft University of Technology. (in Dutch: Vloeistofmechanica).

Battjes, J. A. (2002b). *Open Channel Flow.* Lecture notes, Faculty of Civil Engineering and Geosciences, Delft University of Technology. (in Dutch: Stroming in Waterlopen).

Begon, M., Townsend, C. R., and Harper, J. L. (2006). *Ecology: From Individuals to Ecosystems.* Blackwell Publishing.

CUR (1997). *Probability in Civil Engineering Part 1: The Theory of Probabilistic Design.* Number 190. CUR, Gouda.

Deltares (2010). *Delft3D-FLOW User Manual.* Latest version downloadable at http://www.delftsoftware.com.

Hjelmfelt, A. T. and Lenau, C. W. (1970). Nonequilibrium Transport of Suspended Sediment. *Journal of the Hydraulic Division*, HY 7:1567–1586.

Holthuijsen, L. H. (2007). *Waves in Oceanic and Coastal waters.* Cambridge University Press.

Hutter, K., Wang, Y., and Chubarenko, I. P. (2011). *Physics of Lakes.* Springer.

IADC/CEDA (2008). *Environmetal Aspects of Dredging.* Taylor & Francis.

IAHR (1991). Hydraulics and the Environment: Publication of the IAHR Workshop on Matching Hydraulics and Ecology in Water Systems. *Journal of Hydraulic Research*, 29:extra issue.

Jansen, P. P., editor (1979). *Principles of River Engineering. The non-tidal alluvial river.* Delftse Uitgevers Maatschappij, Delft.

Meeuws, P. (1997). The design point in Monte Carlo simulation (Het ontwerppunt bij Monte Carlo simulatie). Master's thesis, Delft University of Technology. In Dutch.

Nieuwaal, M. (2001). Requirements for sediment plumes caused by dredging. Master's thesis, Delft University of Technology.

van Gelder, P. H. A. J. M. (2000). *Statistical methods for the risk-based design of civil structures.* PhD thesis, Delft University of Technology.

van Koningsveld, M. (2003). *Matching specialist knowledge with end user needs. Bridging the gap between coastal science and coastal management.* PhD thesis, University of Twente.

van Koningsveld, M. (2010). Basic Mathematical Physics applied to Hydraulic Engineering Problems. under construction.

van Koningsveld, M., de Boer, G. J., Baart, F., Damsma, T., den Heijer, C., van Geer, P., and de Sonneville, B. (2010). OpenEarth - Inter-Company Management of: Data, Models, Tools & Knowledge. In *Proceedings WODCON XIX Conference*, Beijing, China.

van Kruchten, Y. J. G. (2008). A probabilistic analysis of the ecological effects of sand mining for Maasvlakte 2. Master's thesis, Delft University of Technology.

van Rijn, L. C. (1984). Sediment Transport, Part II: Suspended Load Transport. *Journal of Hydraulic Engineering*, 110(11):1613–1641.

van Rijn, L. C. (1993). *Principles of Sediment Transport in Rivers, Estuaries and Coastal Seas.* Aqua Publications, Amsterdam.

van Rijn, L. C. (2006). *Principles of Sediment Transport in Rivers, Estuaries and Coastal Seas, Supplement 2006.* Aqua Publications.

van Rijn, L. C. (2007). Unified View of Sediment Transport by Currents and Waves II: Suspended Transport. *Journal of Hydraulic Engineering*, 133(6):668–689.

Vrijling, J. K. and van Gelder, P. H. A. J. M. (2006). *Probabilistic Design in Hydraulic Engineering.* Lecture notes, Faculty of Civil Engineering and Geosciences, Delft University of Technology.

Wang, Z. B. (1989). *Mathematical Modelling of Morphological Processes in Estuaries.* PhD thesis, Faculty of Civil Engineering, Delft University of Technology.

Wiering, J. and Rijkoort, P. J. (1983). *Windklimaat in Nederland.* KNMI.

Winterwerp, J. C. and van Kesteren, W. G. M. (2004). *Introduction to the Physics of Cohesive Sediment in the Marine Environment.* Elsevier.

# Appendix A

# Frame of reference

In Chapter 1 a brief description is given about the origin of the environmental requirements. Also the practical implementation for the environmental impacts of suspended sediments is described. For the analyses of the problem the *Frame of reference* is used (van Koningsveld, 2003).

The framework starts which the a strategic objective. In case of the environmental impacts of dredging and reclamation works, this strategic objective can be described a societal request for sustainable conservation of the local ecosystem. This results in a number of operational objective in order to achieve the strategic objective. Within this study only the operational objective related to the emission of suspended sediments is taken into account.

In order to achieve the operational objective a decision recipe is required. This starts with a quantitative state concept to enable objective and reproducible decision making. For the emission of suspended sediments, this is the actual suspended sediment concentration and the turbidity. Also the total release of suspended sediment could be taken into account. To evaluate the achievement of the operational objective, a benchmarking procedure is required. Therefore, within this study a fixed limit value is defined for to outflow concentration of suspended sediments.

Exceedance of this limit results in a intervention. For the case of a settling basin, this was the stop of the construction activities and the payment of a fine. The way these intervention procedures enable the achievement of both the operational objective and the strategic objective has to be evaluated. Is the operational objective is not achieved the decision recipe has the be modified. Ounce the operational objective is achieved, the way it fulfills the stategic objective has to be evaluated, which can results in modifications of the operational objective.

Figure A.1 gives the frame of reference as it was used within this project to analyse the problem related to the environmental impacts of suspended sediments and the mitigation of these impacts by the use of settling basins.

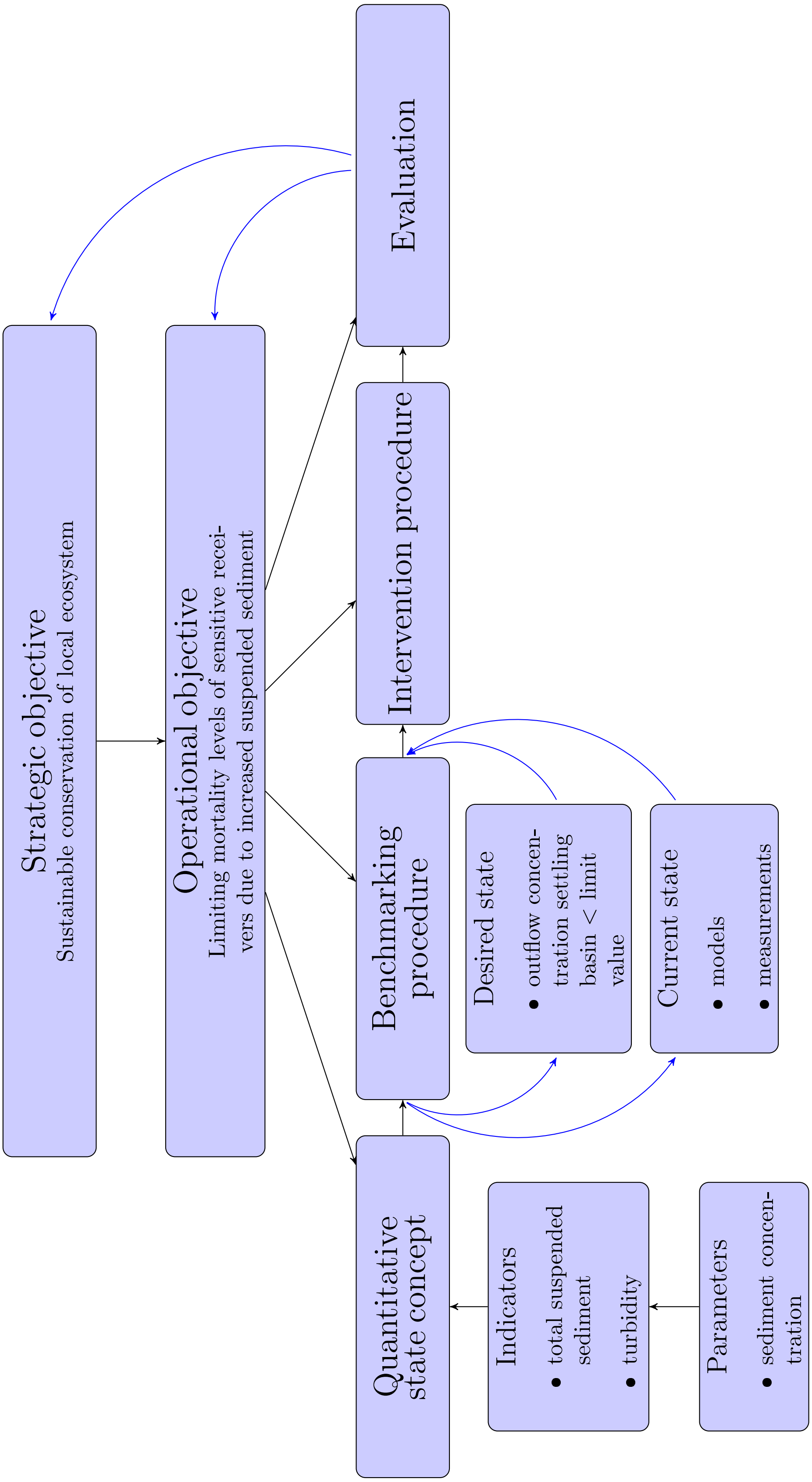


Figure A.1: Frame of reference (van Koningsveld, 2003)

# Appendix B

# Shallow water equations

The derivations in this appendix are taken from van Koningsveld (2010) and are slightly modified for application within this project.

## B.1 Formal integration of NS-equations

In this chapter we derive the 1DH Saint-Venant equations from the 3D Navier-Stokes equations by systematic introduction of assumptions and formal integration (over depth and width). The remaining dimension that is resolved is the horizontal one along the main stream direction (e.g. along a river, estuary etc.), in this case defined as the $x$-direction. We start by presenting the 3D Navier-Stokes equations:

**The continuity equation**

$$\frac{\partial u}{\partial x} + \frac{\partial v}{\partial y} + \frac{\partial w}{\partial z} = 0 \tag{B.1}$$

**The equations of motion in three dimensions**

$$\frac{\partial u}{\partial t} + u\frac{\partial u}{\partial x} + v\frac{\partial u}{\partial y} + w\frac{\partial u}{\partial z} - fv = g_x - \frac{1}{\rho}\frac{\partial p}{\partial x} + \epsilon\left(\frac{\partial^2 u}{\partial x^2} + \frac{\partial^2 u}{\partial y^2} + \frac{\partial^2 u}{\partial z^2}\right) \tag{B.2}$$

$$\frac{\partial v}{\partial t} + u\frac{\partial v}{\partial x} + v\frac{\partial v}{\partial y} + w\frac{\partial v}{\partial z} + fu = g_y - \frac{1}{\rho}\frac{\partial p}{\partial y} + \epsilon\left(\frac{\partial^2 v}{\partial x^2} + \frac{\partial^2 v}{\partial y^2} + \frac{\partial^2 v}{\partial z^2}\right) \tag{B.3}$$

$$\frac{\partial w}{\partial t} + u\frac{\partial w}{\partial x} + v\frac{\partial w}{\partial y} + w\frac{\partial w}{\partial z} = g_z - \frac{1}{\rho}\frac{\partial p}{\partial z} + \epsilon\left(\frac{\partial^2 w}{\partial x^2} + \frac{\partial^2 w}{\partial y^2} + \frac{\partial^2 w}{\partial z^2}\right) \tag{B.4}$$

With:

| | |
|---|---|
| $x$ | = horizontal coordinate [m] |
| $y$ | = horizontal coordinate [m] |
| $z$ | = vertical coordinate [m] |
| $u, v, w$ | = velocity in $x$, $y$ and $z$-direction respectively [m/s] |
| $f$ | = Coriolis acceleration [$s^{-1}$] |
| $p$ | = pressure ($N/m^2$) |
| $\rho$ | = mass density of the fluid [$kg/m^3$] |
| $\mu$ | = dynamic viscosity [Pa s)] |
| $\epsilon$ | = kinematic viscosity ($= \mu/\rho$) [$m^2/s$] |
| $g_{(x,y,z)}$ | = gravitational accelerations in $x$, $y$ and $z$-direction [$m/s^2$] |

### B.1.1 First assumptions

Given our focus in this chapter on 1DH Shallow Water Motion we can make a number of assumptions to simplify the 3D Navier-Stokes equations. First of all we will limit the gravitational accelerations on the fluid to the downward pull by the earths gravitation in this case. Other gravitational forces that could act on the fluid, like gravitational pull by the moon and sun, will be ignored. As a result $g_x = g_y = 0$ and $g_z = -g$ (NB: $z$ is defined as positive in the upward direction so the earth's gravitational pull acts in negative direction). We shall also ignore Coriolis forces ($-fv$ and $fu$), as they have been shown to be unimportant for rivers and estuaries not exceeding several kilometers in width. We shall furthermore assume uniform flow in the horizontal direction perpendicular to the stream direction (in this case the $y$-direction). This basically eliminates the momentum equation in $y$-direction (Eq. B.3) as all derivatives of $v$ and all derivatives in $y$-direction are reduced to zero. In the continuity equation $\frac{\partial v}{\partial y}$ is reduced to zero, yielding:

$$\frac{\partial u}{\partial x} + \frac{\partial w}{\partial z} = 0 \tag{B.5}$$

We furthermore assume that vertical accelerations ($\frac{\partial w}{\partial t}$; $\frac{\partial w}{\partial x}$; $\frac{\partial w}{\partial y}$ and $\frac{\partial w}{\partial z}$) and vertical velocity gradients ($\frac{\partial^2 w}{\partial x^2}$; $\frac{\partial^2 w}{\partial y^2}$ and $\frac{\partial^2 w}{\partial z^2}$) are negligible compared to gravity. This allows us to simplify the vertical momentum equation (Eq. B.4) to:

$$0 = -g - \frac{1}{\rho}\frac{\partial p}{\partial z} \tag{B.6}$$

Integrating this equation over depth yields:

$$\int \frac{\partial p}{\partial z}\, dz = \int -\rho g\, dz \tag{B.7}$$

$$p = -\rho g z + c_1 \tag{B.8}$$

Solving with the pressure boundary condition at the still water level ($z = \eta$) and taking $p|_{z=\eta} = 0$ (zero pressure at the still water level) we find integration constant $c_1$ to be:

$$c_1 = \underbrace{p\Big|_{z=\eta}}_{=0} + \rho g z\Big|_{z=\eta} = \rho g z\Big|_{z=\eta} \tag{B.9}$$

which combined with Eq. B.8 yields the hydrostatic pressure distribution:

$$p = \rho g\,(\eta - z) \tag{B.10}$$

With the hydrostatic pressure distribution (taking into account that the $z$ in Eq. B.10 is independent of $x$) the pressure *gradient* in the momentum equation in $x$-direction (Eq. B.2) can be rewritten to:

$$-\frac{1}{\rho}\frac{\partial p}{\partial x} = -\frac{1}{\rho}\rho g\frac{\partial \eta}{\partial x} = -g\frac{\partial \eta}{\partial x} \tag{B.11}$$

If we further assume that velocity gradients in $x$-direction $\left(\frac{\partial^2 u}{\partial x^2}\right)$ are much smaller than those in $z$-direction $\left(\frac{\partial^2 u}{\partial z^2}\right)$ (bottom friction!) we can further simplify Eq. B.2 to:

$$\frac{\partial u}{\partial t} + u\frac{\partial u}{\partial x} + w\frac{\partial u}{\partial z} = -g\frac{\partial \eta}{\partial x} + \epsilon\left(\frac{\partial^2 u}{\partial z^2}\right) \tag{B.12}$$

With the continuity equation this equation can be rewritten in conserving form:

$$\frac{\partial u}{\partial t} + \frac{\partial}{\partial x}\left(u^2\right) + \frac{\partial}{\partial z}(uw) = -g\frac{\partial \eta}{\partial x} + \epsilon\left(\frac{\partial^2 u}{\partial z^2}\right) \tag{B.13}$$

(applying the chain rule and the simplified continuity equation) as:

$$\frac{\partial}{\partial x}\left(u^2\right) + \frac{\partial}{\partial z}(uw) = u\frac{\partial u}{\partial x} + u\frac{\partial u}{\partial x} + u\frac{\partial w}{\partial z} + w\frac{\partial u}{\partial z} = \tag{B.14}$$

$$u\frac{\partial u}{\partial x} + w\frac{\partial u}{\partial z} + u\underbrace{\left(\frac{\partial u}{\partial x} + \frac{\partial w}{\partial z}\right)}_{=0\ \ (See Eq. B.5)} \tag{B.15}$$

Our initial system of equations Eq.'s B.1 to B.4 has now reduced to the continuity equation containing the velocity gradients in $x$ and $z$ direction:

$$\frac{\partial u}{\partial x} + \frac{\partial w}{\partial z} = 0 \tag{B.16}$$

and one conserving equation of motion in $x$ direction containing the hydrostatic pressure term:

$$\frac{\partial u}{\partial t} + \frac{\partial}{\partial x}\left(u^2\right) + \frac{\partial}{\partial z}(uw) = -g\frac{\partial \eta}{\partial x} + \epsilon\left(\frac{\partial^2 u}{\partial z^2}\right) \tag{B.17}$$

### B.1.2 Integrating over depth

Equations B.16 and B.17 can now be integrated over depth. A useful tool in this integration process is Leibniz' Integral Rule, named after Wilhelm Gotfried Leibniz[1] (1646 - 1716), that provides a formula for differentiation of a definite integral whose limits are functions of the differential variable[2]. For our purpose of integration, the Leibniz Integral Rule (or in short the Leibniz Rule) can be re-written in general terms as:

$$\int_{a(z)}^{b(z)} \frac{\partial f}{\partial z}dx = \frac{\partial}{\partial z}\int_{a(z)}^{b(z)} f(x,z)dx - f(b(z),z)\frac{\partial b}{\partial z} + f(a(z),z)\frac{\partial a}{\partial z} \tag{B.18}$$

Beside the Leibniz Rule we also need the boundary conditions at the bed ($z = z_b$) and free surface ($z = \eta$) to successfully complete the integration process. At the bed the vertical velocity component must vanish:

$$u\Big|_{z=z_b}\frac{\partial z_b}{\partial x} - w\Big|_{z=z_b} = 0 \tag{B.19}$$

Also the tangential velocity component must vanish (the kinematic boundary condition). No water can cross the water surface, so:

$$\frac{\partial \eta}{\partial t} + u\Big|_{z=\eta}\frac{\partial \eta}{\partial x} - w\Big|_{z=\eta} = 0 \tag{B.20}$$

#### The continuity equation

Depth integrating the continuity equation the Leibniz rule can be used to integrate the velocity gradients in $x$-direction as in this case the integration limits are a function of the differential variable. This is not the case for the velocity in $z$-direction. To avoid confusion (and errors) it is important to carefully use the general form of Leibniz's rule and apply the relevant aspects of the to-be-integrated argument at hand. For the velocity gradient in $x$-direction, part of the continuity

[1]See also: http://en.wikipedia.org/wiki/Gottfried_Leibniz

[2]See also: http://mathworld.wolfram.com/LeibnizIntegralRule.html - Weisstein, Eric W. "Leibniz Integral Rule." From MathWorld–A Wolfram Web Resource.

equation (Eq. B.16), for example, the arguments of Eq. B.18 should be taken as follows: $f = u$, $z = x$, $x = z$, $a(z) = z_b$ and $b(z) = \eta$. Applying these arguments yields:

$$\int_{z=z_b}^{z=\eta} \frac{\partial u}{\partial x} dz = \frac{\partial}{\partial x} \int_{z=z_b}^{z=\eta} u\ dz - u|_{z=\eta} \frac{\partial \eta}{\partial x} + u|_{z=z_b} \frac{\partial z_b}{\partial x} \tag{B.21}$$

The velocity gradient in $z$-direction can be integrated using the normal approach. The total depth integrated continuity equation then yields:

$$\int_{z=z_b}^{z=\eta} \left( \frac{\partial u}{\partial x} + \frac{\partial w}{\partial z} \right) dz = 0 \tag{B.22}$$

$$\frac{\partial}{\partial x} \int_{z=z_b}^{z=\eta} u\ dz - u\Big|_{z=\eta} \frac{\partial \eta}{\partial x} + u\Big|_{z=z_b} \frac{\partial z_b}{\partial x} + w\Big|_{z=\eta} - w\Big|_{z=z_b} = 0$$

Rearranging the terms yields:

$$\frac{\partial}{\partial x} \int_{z=z_b}^{z=\eta} u\ dz \underbrace{-u\Big|_{z=\eta} \frac{\partial \eta}{\partial x} + w\Big|_{z=\eta}}_{=\frac{\partial \eta}{\partial t}\ \ (See\ Eq.\ B.20)} \underbrace{+u\Big|_{z=z_b} \frac{\partial z_b}{\partial x} - w\Big|_{z=z_b}}_{=0\ \ (See\ Eq.\ B.19)} = 0$$

Applying the pre-mentioned boundary conditions, Eq.'s B.19 and B.20, and performing the remaining integrations yields (where $\overline{u}$ is the now depth averaged velocity):

$$\frac{\partial}{\partial x}(\overline{u}h) + \frac{\partial \eta}{\partial t} = 0 \tag{B.23}$$

### The equation of motion

Depth integrating the momentum equation in $x$-direction (Eq. B.17) the Leibniz Rule can be used to integrate the local acceleration term, the convective acceleration term in $x$-direction and the pressure term (although the latter is a special case), as also in these cases the integration limits are functions of the differential variable. Applying the Rule of Leibniz to the local acceleration term (with: $f = u$, $z = t$, $x = z$, $a(z) = z_b$ and $b(z) = \eta$) yields:

$$\int_{z=z_b}^{z=\eta} \frac{\partial u}{\partial t} dz = \frac{\partial}{\partial t} \int_{z=z_b}^{z=\eta} u dz - u\Big|_{z=\eta} \frac{\partial \eta}{\partial t} + u\Big|_{z=z_b} \frac{\partial z_b}{\partial t}$$

For the convective acceleration term in $x$-direction a similar operation (with: $f = u^2$ and $z = x$) yields:

$$\int_{z=z_b}^{z=\eta} \left( \frac{\partial}{\partial x} \left(u^2\right) \right) dz = \frac{\partial}{\partial x} \int_{z=z_b}^{z=\eta} u^2\ dz - u^2\Big|_{z=\eta} \frac{\partial \eta}{\partial x} + u^2\Big|_{z=z_b} \frac{\partial z_b}{\partial x}$$

Depth integration of the other terms yields (notice the introduction of $\tau_\eta$ and $\tau_{z_b}$):

$$\int_{z=z_b}^{z=\eta} \frac{\partial}{\partial z}(uw) dz = \Big[uw\Big]_{z=z_b}^{z=\eta} = u\Big|_{z=\eta} w\Big|_{z=\eta} - u\Big|_{z=z_b} w\Big|_{z=z_b}$$

$$\int_{z=z_b}^{z=\eta} \left( \epsilon \left( \frac{\partial^2 u}{\partial z^2} \right) \right) dz = \left[ \epsilon \frac{\partial u}{\partial z} \right]_{z=z_b}^{z=\eta} = \epsilon \frac{\partial u}{\partial z}\Bigg|_{z=\eta} - \epsilon \frac{\partial u}{\partial z}\Bigg|_{z=z_b} = \frac{\tau_\eta}{\rho} - \frac{\tau_{z_b}}{\rho}$$

Finally the pressure term may also be subjected to the normal integration procedure as, introducing the hydrostatic pressure earlier, $\eta$ is independent of $z$.

$$\int_{z=z_b}^{z=\eta} \left(-g\frac{\partial \eta}{\partial x}\right) dz = -g\frac{\partial \eta}{\partial x}\int_{z=z_b}^{z=\eta} dz = -g\frac{\partial \eta}{\partial x}\Big[z\Big]_{z=z_b}^{z=\eta} = -g\Big(\underbrace{\eta - z_b}_{=h}\Big)\frac{\partial \eta}{\partial x} = -gh\frac{\partial \eta}{\partial x}$$

Combining and rearranging the above results yields:

$$\frac{\partial}{\partial t}\int_{z=z_b}^{z=\eta} u dz - u\Big|_{z=\eta}\frac{\partial \eta}{\partial t} + u\Big|_{z=z_b}\frac{\partial z_b}{\partial t} + \frac{\partial}{\partial x}\int_{z=z_b}^{z=\eta} u^2\, dz \cdots$$

$$-u\Big|_{z=\eta}\Big(\underbrace{u\Big|_{z=\eta}\frac{\partial \eta}{\partial x} - w\Big|_{z=\eta}}_{=-\frac{\partial \eta}{\partial t}\ \ (See\ Eq.\ B.20)}\Big) + u\Big|_{z=z_b}\Big(\underbrace{u\Big|_{z=z_b}\frac{\partial z_b}{\partial x} - w\Big|_{z=z_b}}_{=0\ \ (See\ Eq.\ B.19)}\Big) = -gh\frac{\partial \eta}{\partial x} + \frac{\tau_\eta}{\rho} - \frac{\tau_{z_b}}{\rho} \tag{B.24}$$

Rearranging, applying the boundary conditions (Eq.'s B.19 and B.20) and performing the remaining integrations yields:

$$\frac{\partial}{\partial t}(\overline{u}h) + \underbrace{u\Big|_{z=\eta}\frac{\partial \eta}{\partial t} - u\Big|_{z=\eta}\frac{\partial \eta}{\partial t}}_{=0} + \underbrace{u\Big|_{z=z_b}}_{=0}\frac{\partial z_b}{\partial t} + \frac{\partial}{\partial x}(\alpha_1\overline{u}^2 h) = -gh\frac{\partial \eta}{\partial x} + \frac{\tau_\eta}{\rho} - \frac{\tau_{z_b}}{\rho}$$

Finally assuming the velocity at the bed to be zero ($u\big|_{z=z_b} = 0$), yields the depth averaged momentum equation in $x$-direction:

$$\frac{\partial}{\partial t}(h\overline{u}) + \frac{\partial}{\partial x}(\alpha_1\overline{u}^2 h) = -gh\frac{\partial \eta}{\partial x} + \frac{\tau_\eta}{\rho} - \frac{\tau_{z_b}}{\rho} \tag{B.25}$$

**Resulting equations**

The coefficient $\alpha_1$ is a correction factor for the fact that the mean of a product of two variables is not equal to the product of the means of these variables. Depending on the velocity profiles the value of $\alpha_1$ varies between 1 and 1.1 and usually it is assumed to be 1 (Jansen, 1979). With the introduction of first assumptions, the integration of all equations over depth and assuming $\alpha_1 = 1$ the resulting system of equations reads:

$$\frac{\partial}{\partial x}(\overline{u}h) + \frac{\partial \eta}{\partial t} = 0 \tag{B.26}$$

$$\frac{\partial \overline{u}h}{\partial t} + \frac{\partial \overline{u}^2 h}{\partial x} = -gh\frac{\partial \eta}{\partial x} + \frac{\tau_\eta}{\rho} - \frac{\tau_{z_b}}{\rho} \tag{B.27}$$

With:

$$\tau_\eta = \rho\epsilon\frac{\partial u}{\partial z}\Big|_{z=\eta} \tag{B.28}$$

$$\tau_{z_b} = \rho\epsilon\frac{\partial u}{\partial z}\Big|_{z=z_b} \tag{B.29}$$

### B.1.3 Integrating over width

When we assume vertical shores at the river edges, a constant waterlevel over the river width and momentum to be conveyed through the streaming channel only (see also Fig. B.1) we can integrate Equations B.26 and B.27 over width:

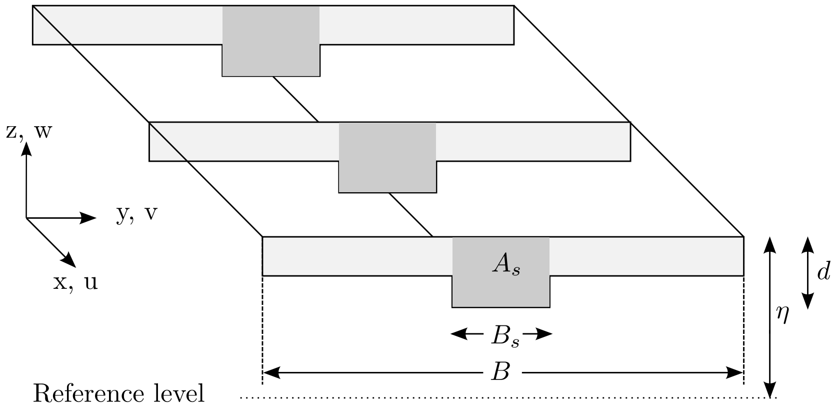


Figure B.1: River transect

**The continuity equation:**

The entire crosssection (of width $B$) is included in the continuity equation:

$$\int_{-\frac{1}{2}B}^{\frac{1}{2}B} \Big(\frac{\partial}{\partial x}\left(\overline{u}h\right) + \frac{\partial \eta}{\partial t}\Big) dy = 0 \tag{B.30}$$

$$\frac{\partial}{\partial x}\left(\overline{u}h\right)\Big[y\Big]_{-\frac{1}{2}B}^{\frac{1}{2}B} + \frac{\partial \eta}{\partial t}\Big[y\Big]_{-\frac{1}{2}B}^{\frac{1}{2}B} = 0 \tag{B.31}$$

$$B\frac{\partial}{\partial x}\left(\overline{u}h\right) + B\frac{\partial \eta}{\partial t} = 0 \tag{B.32}$$

$$\frac{\partial Q}{\partial x} + B\frac{\partial \eta}{\partial t} = 0 \tag{B.33}$$

**The equation of motion:**

For the equation of motion it is assumed that only the streaming channel (of width $B_s$ and depth $h_s$) contributes momentum.

$$\int_{-\frac{1}{2}B_s}^{\frac{1}{2}B_s} \Big(\frac{\partial \overline{u}h_s}{\partial t} + \frac{\partial u^2 h_s}{\partial x}\Big) dz = \int_{-\frac{1}{2}B_s}^{\frac{1}{2}B_s} \Big( - gh_s\frac{\partial \eta}{\partial x} + \frac{\tau_\eta}{\rho} - \frac{\tau_{z_b}}{\rho}\Big) dz \tag{B.34}$$

$$\frac{\partial Q}{\partial t} + \frac{\partial}{\partial x}\Big(\alpha_2\frac{Q^2}{A_s}\Big) = -gA_s\frac{\partial \eta}{\partial x} + \frac{\tau_\eta}{\rho} - \frac{\tau_{z_b}}{\rho} \tag{B.35}$$

With:

$$\alpha_2 = \frac{\overline{u^2}}{\overline{u}^2} \tag{B.36}$$

$$\tau_b = \rho\frac{g}{C^2}\frac{Q|Q|}{A_s R} = \rho c_f B_s\frac{Q|Q|}{A_s^2} \tag{B.37}$$

$$\tau_\eta = -B_s F_w \tag{B.38}$$

**NB:** the above formulations of $\tau_\eta$ and $\tau_{z_b}$ are width averaged!

The bed shear stress $\tau_b$ in this formula is expressed as a function of the bottom friction coefficient $c_f$. For logarithmic velocity profiles under hydraulic rough conditions, the dimensionless resistance coefficient can be approximated by (Battjes, 2002a):

$$\frac{1}{\sqrt{c_f}} = 5.75 \cdot log \frac{12R}{k} \tag{B.39}$$

With:

| | |
|---|---|
| $c_f$ | = bottom friction coefficient [-] |
| $R$ | = hydraulic radius [m] |
| $k$ | = roughness height (Nikuradse) [m] |

**Resulting equations**

With the integration over width we now arrived at the well-known form of the 1DH Shallow Water Equations (Battjes, 2002b) also known as the 1DH Saint-Venant equations (Eq. B.40 and B.41).

$$\frac{\partial Q}{\partial x} + B\frac{\partial \eta}{\partial t} = 0 \tag{B.40}$$

$$\frac{\partial Q}{\partial t} + \frac{\partial}{\partial x}(\alpha_2 \frac{Q^2}{A_s}) = -gA_s\frac{\partial \eta}{\partial x} - c_f B_s \frac{Q|Q|}{A_s^2} \tag{B.41}$$

Equations B.40 and B.41 include the concept that not the entire cross section contributes to the flow, e.g. when there are floodplains with high flood resistance (perhaps caused by the presence of obstructions such as groins) essentially serving as storage only (see also Figure B.1). Such areas do contribute to the equation of continuity, but not to the momentum equation. The Saint-Venant equations are named after Adhémar Jean Claude Barré de Saint-Venant (1797-1886), who was the first to develop the one-dimensional unsteady open channel flow shallow water equations.

## B.2 Velocity profile

A general expression for the velocity profile (i.e. the velocity distribution over depth) is:

$$u(z) = \frac{u_*}{\kappa} \ln\left(\frac{z}{z_0}\right) \tag{B.42}$$

With $\kappa$ being the constant of Von Karman ($\kappa = 0.4$). Parameter $z_0$ is the level of zero-velocity, indicating at what level the logarithmic profile should start. As such it is a mathematical parameter rather than one with actual physical meaning. According to van Rijn (1993), $z_0$ depends in the following manner on the hydraulic flow regime. As stated in chapter 3, hydraulic rough conditions are assumed. This results in a $z_0$-level of $z_0 = 0.033 \cdot k_s$ Averaging Eq. B.42 over depth yields:

$$\overline{u} = \frac{1}{h}\int_{z_0}^{h} \frac{u_*}{\kappa} \ln\left(\frac{z}{z_0}\right) dz = \frac{u_*}{\kappa}\left[\frac{z_0}{h} - 1 + \ln\left(\frac{z}{z_0}\right)\right] \tag{B.43}$$

Inserting Eq. B.43 into Eq. B.42, the velocity distribution over the vertical can be expressed as (see figure 2.3):

$$u = \left[\frac{\overline{u}}{\frac{z_0}{h} - 1 + \ln\left(\frac{h}{z_0}\right)}\right] \ln\left(\frac{z}{z_0}\right) \tag{B.44}$$

## B.3 Wind-induced currents

The horizontal flow due to wind in a homogeneous lake is determined with the following equations as taken from Hutter et al. (2011).

$$\hat{u} := \frac{u}{\left(\frac{h\tau_s}{4\rho\nu}\right)} = \frac{(1-\Gamma)(1-3\Gamma+4\delta)-2\delta}{(1+\delta)} \tag{B.45}$$

$$\hat{w} := \frac{w}{\left(\frac{h^2\tau_s'}{4\rho\nu}\right)} = \frac{\Gamma(1-\Gamma)(1-\Gamma+2\delta)}{(1+\delta)} \tag{B.46}$$

in which:

| | | |
|---|---|---|
| $\Gamma$ | $= 1 - z/h$ | Relative vertical position $[-]$ |
| $h$ | | water depth [m] |
| $z$ | | vertical position (bottom: $z = 0$) |
| $u$ | | horizontal flow velocity [m/s] |
| $w$ | | vertical flow velocity [m/s] |
| $\nu$ | | turbulent viscosity [$m^2/s$] (assumed to be constant) |
| $\rho$ | | density of the fluid [$kg/m^3$] |
| $\tau_s$ | $= \rho_{air} \cdot C_d \cdot {U_{10}}^2$ | surface shear stress [$N/m^2$] |
| $\tau_s'$ | $= \frac{d\tau_s}{dx} \approx \frac{\tau_s}{\Delta x}$ | linear relation over boundary grid cells [$N/m^3$] |
| $\Delta x$ | | width of the boundary grid cells [m] |
| $\rho_{air}$ | | density of air [$kg/m^3$] |
| $C_d$ | | drag coefficient [-] |
| $C_d$ | $= 1.2875 \cdot 10^{-3}$ | for $U_{10} < 7.5$ m/s (Holthuijsen, 2007, eq. 9.3.6) |
| $C_d$ | $= (0.8 + 0.065 U_{10}) \cdot 10^{-3}$ | for $U_{10} \geq 7.5$ m/s |
| $U_{10}$ | | wind speed at 10 meters above the surface [m/s] |
| $\delta$ | | non-dimensional parameter for slip condition [-] |

For consistency reasons a no-slip condition at the bottom is applied in order to be consistent which the no-slip condition of the mean flow. This results in $\delta = 0$.

# Appendix C

# Sediment transport

The derivations in this appendix are partly taken from van Koningsveld (2010) and are both extended and revised for application within the project.

## C.1 Basic equations

The shallow water equations we need were already derived in Appendix B, viz. Equation B.26 and B.27. Details on translating depth integrated velocities to a vertical logarithmic profile are provided in Appendix B.2. This section focuses on the description and implementation of the suspended sediment transport model. The time varying mass balance for suspended sediment is given below.

$$\frac{\partial c}{\partial t} + u\frac{\partial c}{\partial x} + v\frac{\partial c}{\partial y} + w\frac{\partial c}{\partial z} + \frac{\partial s_x}{\partial x} + \frac{\partial s_y}{\partial y} + \frac{\partial s_z}{\partial z} = 0 \tag{C.1}$$

This indicates that a change in sediment concentration is caused by a combination of flow induced sediment convection and gradients in the sediment transport flux. When we assume uniform flow in the horizontal direction perpendicular to the stream direction (in this case the $y$-direction) we can eliminate all derivatives in $y$-direction. The sediment transport flux in $x$-direction is assumed to be proportional to the concentration gradient in $x$-direction:

$$s_x = -\epsilon_{s,x}\frac{\partial c}{\partial x} \tag{C.2}$$

The sediment transport flux in $z$-direction is assumed to be a composite consisting of a generally downward directed flux related to sediment precipitation (NB: as the positive $z$ is directed upward, the scalar settling velocity $w_s$ should be negative for it to act in downward direction) and a generally upward directed flux that is proportional to the concentration gradient:

$$s_z = w_s \cdot c - \epsilon_{s,z}\frac{\partial c}{\partial z} \tag{C.3}$$

In which:

| | |
|---|---|
| $c$ | suspended sediment concentration [kg/m$^3$] |
| $t$ | time [s] |
| $x$, $y$ and $z$ | Cartesian coordinates in three dimensions |
| $u$, $v$ and $w$ | flow velocity in x, y and z direction [m/s] |
| $s_x$, $s_y$, and $s_z$ | suspended sediment flux in x, y and z direction [kgm$^{-2}$s$^{-1}$] |
| $\epsilon_{s,x}$ and $\epsilon_{s,z}$ | sediment mixing coefficient [m$^2$/s] |
| $w_s$ | sediment fall velocity [m/s] |

Combining Eq.'s C.1, C.2 and C.3 and removing all derivatives in $y$-direction yields:

$$\frac{\partial c}{\partial t} + u\frac{\partial c}{\partial x} + w\frac{\partial c}{\partial z} - \frac{\partial}{\partial x}\left(\epsilon_{s,x}\frac{\partial c}{\partial x}\right) + \frac{\partial w_s c}{\partial z} - \frac{\partial}{\partial z}\left(\epsilon_{s,z}\frac{\partial c}{\partial z}\right) = 0 \tag{C.4}$$

The flow is assumed to be horizontal ($w \ll u$) with a velocity distribution $u(z)$. This allows us to to simplify Equation C.4 to:

$$\frac{\partial c}{\partial t} + u\frac{\partial c}{\partial x} + \frac{\partial w_s c}{\partial z} - \frac{\partial}{\partial x}\left(\epsilon_{s,x}\frac{\partial c}{\partial x}\right) - \frac{\partial}{\partial z}\left(\epsilon_{s,z}\frac{\partial c}{\partial z}\right) = 0 \tag{C.5}$$

To solve Equation C.5 initial and boundary conditions are needed. An initial condition requires $c = f(x,z)$ at $t = 0$. An initial condition could be a concentration of $c = 0$ throughout the model domain. The value of $\epsilon_{s,x}$, $\epsilon_{s,z}$ are related to the flow conditions and are treated in Section C.5. The particle fall velocity $w_s$ is treated in Section C.4.

## C.2 Boundary conditions

At the inflow boundary a vertical concentration profile $c = f(z,t)$ is needed. Sediment should be able to flow out of the model domain freely. No sediment enters or leaves the region across the water surface, resulting in the following surface boundary condition:

$$w_s c - \epsilon_{s,z}\frac{\partial c}{\partial z} = 0 \text{ @ } z = \eta \tag{C.6}$$

In other words, the net sediment flux at the water surface is zero. The bed boundary for suspended load transport is located at a small height $a$ above the bed level. The transport of sediment below this level is assumed to be bed load transport. Level $a$ is called the reference level and is located at half the bed form height above the bed level with a minimum of $0.01 \cdot h$ (van Rijn, 1984). Sediment may leave (sediment settling) or enter (sediment pickup) the model region through the bed boundary. Two types of boundary may be applied to achieve this: a concentration type boundary or a gradient type boundary (Wang, 1989). The former requires the indication of a fixed, albeit potentially time-varying, concentration value at the bed. The latter assumes that the bed concentration adjusts itself such that the concentration gradient near the bed at all times is equal to the concentration gradient under equilibrium conditions. The gradient type boundary is generally considered to be the most appropriate, because the bed concentration can be different from the equilibrium concentration, but it still has the tendency to adapt to the equilibrium concentration profile. For numerical reasons, the reference level for a gradient type boundary is located halfway the two lowest vertical points grid points , as the gradient is approximated here the best (see Equation C.19). The following formulation for a gradient type boundary, stating that the concentration at reference level $a$ is equal to that under equilibrium conditions, is applied:

$$\frac{\partial c}{\partial z} = \frac{\partial c_e}{\partial z} = \frac{w_s c_e}{\epsilon_{s,z}} \text{ @ } z = z_a \tag{C.7}$$

Herein $c_e$ is a dimensionless volume concentration. Multiplication with $\rho_s$ leads to a concentration in mass per unit volume. The value of $c_e$ needs to be derived from a sediment transport formula. For settling basins it is desirable to get insight in the behaviour or more than one fraction. Therefore the multi-fraction method of van Rijn (2006) is selected for implementation. This method provides a reference concentration for each individual sediment fraction for a given sediment distribition:

$$c_{e,i} = 0.015 \cdot f_{silt} \cdot (1 - p_{clay}) \cdot p_i \cdot \frac{d_i}{a} \cdot \frac{T_{cw,i}^{1.5}}{D_{star,i}^{0.3}} \tag{C.8}$$

In which:

| | | |
|---|---|---|
| $c_{e,i}$ | | equilibrium volume concentration of each fraction [-] |
| $f_{silt}$ | $= \frac{d_{sand}}{d_i}$ | silt factor of individual sediment fraction [-] |
| $d_{sand}$ | $= 62e^{-6}\ m$ | particle diameter of sand [m] |
| $p_{clay}$ | | fraction of clay in the sediment fraction) [-] |
| $p_i$ | | volumic fraction percentage [-] |
| $d_i$ | | fraction diameter [m] |
| $a$ | | reference level [m] |
| $h$ | | water depth [m] |
| $k_s$ | | overall roughness height [m] |
| $T_{cw,i}$ | | bed-shear stress parameter [-] |
| $D_{star,i}$ | $= \left(\frac{d_i(s-1)g}{\nu^2}\right)^{\frac{1}{3}}$ | particle parameter[-] |
| $s$ | $= \frac{\rho_s}{\rho}$ | relative density [-] |
| $\nu$ | $= [4/(20+Te)] \cdot e^{-5}$ | kinematic viscosity [m$^2$/s] |
| $Te$ | | water temperature [°C] |
| $g$ | | gravitational acceleration [m/s$^2$] |

$$T_{cw,i} = \lambda_i \frac{\tau'_{b,cw,i} - r \cdot \tau_{cr} \cdot \frac{d_i}{d_{50}} \cdot \xi_i}{\tau_{cr} \cdot \frac{d_i}{d_{50}}} \tag{C.9}$$

In which:

| | | |
|---|---|---|
| $\lambda_i$ | $= \frac{d_i}{d_{50}}^{0.25}$ | correction factor of effective bed-shear stress [-] |
| $\tau'_{b,cw,i}$ | | effective bed-shear stress current and waves [N/m$^2$] |
| $r$ | $= 0.8 + 0.2[(\frac{\tau'_{b,cw}}{\tau_{cr}} - 0.8)/1.2]$ | correction factor (risk of movement) |
| $r_{min}$ | $= 0.8$ $\quad r_{max}$ | $= 1$ |
| $\xi_i$ | $= \frac{\log 19}{\log \frac{19 d_i}{d_{50}}}^2$ | hiding factor of Egiazaroff |
| $\tau_{cr}$ | | critical bed shear stress [N/m$^2$] |

$$\tau_{cr} = FCR \cdot f_{clay} \cdot f_{ch} \cdot f_{pack} \cdot (\rho_s - \rho) \cdot g \cdot d_{50} \cdot \theta_{cr} \tag{C.10}$$

In which:

| | | |
|---|---|---|
| $\theta_{cr}$ | | initiation of motion [-] |
| $FCR$ | | linear scaling factor [-] (default = 1) |
| $f_{clay}$ | $= (1 + p_{clay})^3$ | influence of cohesion [-] |
| $f_{clay,max}$ | $= 2$ | |
| $f_{ch}$ | $= \frac{d_{sand}}{d_{50}}^{1.5}$ | silt factor [-] |
| $f_{ch,max}$ | $= 1$ | |
| $f_{pack}$ | $= \frac{c_{max}}{c_{max,s}}$ | packing effects [-] |
| $f_{pack,max}$ | $= 1$ | |
| $c_{max}$ | $= \frac{d_{50}}{d_{sand}} \cdot c_{max,s}$ | gelling mass concentration [-] |
| $c_{max,s}$ | $= 0.65$ | gelling mass concentration for sand [-] |
| $\rho_s$ | | density of sediment particle [kg/m$^3$] |
| $\rho$ | | density of the fluid [kg/m$^3$] |

The effective bed-shear stress ($\tau'_{b,cw,i}$) is caused by both current and waves. Because the basin is small compared to the fetch length needed to get a measurable effect at the bottom, the wave effect on the bed-shear stress is neglected and only the effect of the current is taken into account. The effective bed-shear stress due current is defined as follows:

$$\tau'_b = \rho g \left(\frac{\overline{u}}{C'}\right)^2 \tag{C.11}$$

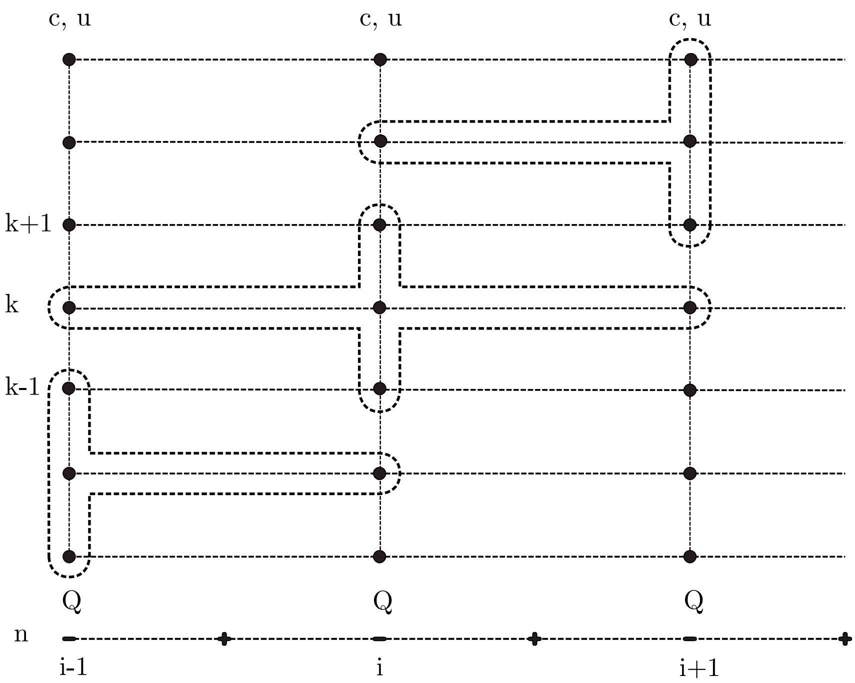


Figure C.1: Grid suspended sediment. Upper panel: 2DV grid with $c$ and $u$ as a function of $x$ and $z$. Lower panel: 1DH staggered grid for flow calculation. Indicated are the $\theta$ scheme stencils: full stencil in central area, reduced stencils at the left and right boundaries. NB: $c$ is only defined at the $Q$ points of the flow grid.

In which:

| | | |
|---|---|---|
| $\tau_b$ | | current related effective bed-shear stress [N/m$^2$] |
| $\rho$ | | density of the fluid [kg/m$^3$] |
| $g$ | | gravitational acceleration [m/s$^2$] |
| $\overline{u}$ | | depth averaged flow velocity [m/s] |
| $C'$ | $= 18\log\left(12h/d_{90}\right)$ | grain-related Chézy coefficient [m$^{1/2}$/s] |
| $h$ | | water depth [m] |
| $d_{90}$ | | grain diameter of 90th percentile [m] |

## C.3 Discretization of the equations

We use the $\theta$ scheme to discretize the balance equation for suspended sediment. Figure C.1 shows the grid that is used and the positioning of the various discretizations thereon (upper panel). It also shows the link between the depth average discharge and water level information (lower panel) and 2DV flow field that is generated using the vertical logarithmic profile approximation and the secondary flow approximation(upper panel - using an arbitrary number of seven vertical grid points). The grid is selected such that concentration information is available at the $Q$ points. For practical reasons we choose here to develop special discretizations for the boundaries. Most important reason is that this 2DV case encounters problems at the corner points of the computational domain.

For the case of a settling basin example we assume $\epsilon_{s,x}$ to be constant in horizontal direction but $\epsilon_{s,z}$ *not* to be constant in vertical direction. The value of the sediment fall velocity $w_s$ will be allowed to vary over the whole domain as processes like flocculation and hindered settling can influence it. As a result Equation C.5 is changed mildly to the following form that will be used for the discretization process:

$$\frac{\partial c}{\partial t} + u\frac{\partial c}{\partial x} + \frac{\partial w_s c}{\partial z} - \epsilon_{s,x}\frac{\partial^2 c}{\partial x^2} - \frac{\partial}{\partial z}\left(\epsilon_{s,z}\frac{\partial c}{\partial z}\right) = 0 \tag{C.12}$$

Discretization of Equation C.12 using the $\theta$ scheme yields:

$$\frac{c^{n+1}_{i,k} - c^n_{i,k}}{\Delta t} + \theta u^{n+1}_{i,k}\frac{c^{n+1}_{i+1,k} - c^{n+1}_{i-1,k}}{2\Delta x} + (1-\theta)u^n_{i,k}\frac{c^n_{i+1,k} - c^n_{i-1,k}}{2\Delta x}\cdots$$

$$+\theta w^{n+1}_{s,i,k}\frac{c^{n+1}_{i,k+1} - c^{n+1}_{i,k-1}}{2\Delta z} + (1-\theta)w^n_{s,i,k}\frac{c^n_{i,k+1} - c^n_{i,k-1}}{2\Delta z}\cdots$$

$$+\theta c^{n+1}_{i,k}\frac{w^{n+1}_{s,i,k+1} - w^{n+1}_{s,i,k-1}}{2\Delta z} + (1-\theta)c^n_{i,k}\frac{w^n_{s,i,k+1} - w^n_{s,i,k-1}}{2\Delta z}\cdots$$

$$-\theta\epsilon^{n+1}_{s,x,i,k}\frac{c^{n+1}_{i-1,k} - 2c^{n+1}_{i,k} + c^{n+1}_{i+1,k}}{\Delta x^2} - (1-\theta)\epsilon^n_{s,x,i,k}\frac{c^n_{i-1,k} - 2c^n_{i,k} + c^n_{i+1,k}}{\Delta x^2}\cdots$$

$$-\theta\epsilon^{n+1}_{s,z,i,k}\frac{c^{n+1}_{i,k-1} - 2c^{n+1}_{i,k} + c^{n+1}_{i,k+1}}{\Delta z^2} - (1-\theta)\epsilon^{n+1}_{s,z,i,k}\frac{c^n_{i,k-1} - 2c^n_{i,k} + c^n_{i,k+1}}{\Delta z^2}\cdots$$

$$-\theta\frac{\epsilon^{n+1}_{s,z,i,k+1} - \epsilon^{n+1}_{s,z,i,k-1}}{2\Delta z}\cdot\frac{c^{n+1}_{i,k+1} - c^{n+1}_{i,k-1}}{2\Delta z} - (1-\theta)\frac{\epsilon^n_{s,z,i,k+1} - \epsilon^n_{s,z,i,k-1}}{2\Delta z}\cdot\frac{c^n_{i,k+1} - c^n_{i,k-1}}{2\Delta z} = 0 \tag{C.13}$$

Rearranging to separate implicit and explicit terms yields:

$$\frac{1}{\Delta t}c^{n+1}_{i,k} + \theta\frac{u^{n+1}_{i,k}}{2\Delta x}c^{n+1}_{i+1,k} - \theta\frac{u^{n+1}_{i,k}}{2\Delta x}c^{n+1}_{i-1,k} + \theta\frac{w^{n+1}_{s,i,k}}{2\Delta z}c^{n+1}_{i,k+1} - \theta\frac{w^{n+1}_{s,i,k}}{2\Delta z}c^{n+1}_{i,k-1} + \theta\frac{w^{n+1}_{s,i,k+1} - w^{n+1}_{s,i,k-1}}{2\Delta z}c^{n+1}_{i,k}\cdots$$

$$-\theta\frac{\epsilon^{n+1}_{s,x,i,k}}{\Delta x^2}c^{n+1}_{i-1,k} + \theta\frac{2\epsilon^{n+1}_{s,x,i,k}}{\Delta x^2}c^{n+1}_{i,k} - \theta\frac{\epsilon^{n+1}_{s,x,i,k}}{\Delta x^2}c^{n+1}_{i+1,k} - \theta\frac{\epsilon^{n+1}_{s,z,i,k}}{\Delta z^2}c^{n+1}_{i,k-1} + \theta\frac{2\epsilon^{n+1}_{s,z,i,k}}{\Delta z^2}c^{n+1}_{i,k} - \theta\frac{\epsilon^{n+1}_{s,z,i,k}}{\Delta z^2}c^{n+1}_{i,k+1}\cdots$$

$$-\theta\frac{\epsilon^{n+1}_{s,z,i,k+1} - \epsilon^{n+1}_{s,z,i,k-1}}{(2\Delta z^2)}c^{n+1}_{i,k+1} + \theta\frac{\epsilon^{n+1}_{s,z,i,k+1} - \epsilon^{n+1}_{s,z,i,k-1}}{(2\Delta z^2)}c^{n+1}_{i,k-1} = \frac{1}{\Delta t}c^n_{i,k} - (1-\theta)\frac{u^n_{i,k}}{2\Delta x}c^n_{i+1,k} + (1-\theta)\frac{u^n_{i,k}}{2\Delta x}c^n_{i-1,k}\cdots$$

$$-(1-\theta)\frac{w^n_{s,i,k}}{2\Delta z}c^n_{i,k+1} + (1-\theta)\frac{w^n_{s,i,k}}{2\Delta z}c^n_{i,k-1} - (1-\theta)\frac{w^n_{s,i,k+1} - w^n_{s,i,k-1}}{2\Delta z}c^n_{i,k}\cdots$$

$$+(1-\theta)\frac{\epsilon^n_{s,x,i,k}}{\Delta x^2}c^n_{i-1,k} - (1-\theta)\frac{2\epsilon^n_{s,x,i,k}}{\Delta x^2}c^n_{i,k} + (1-\theta)\frac{\epsilon^n_{s,x,i,k}}{\Delta x^2}c^n_{i+1,k}\cdots$$

$$+(1-\theta)\frac{\epsilon^n_{s,z,i,k}}{\Delta z^2}c^n_{i,k-1} - (1-\theta)\frac{2\epsilon^n_{s,z,i,k}}{\Delta z^2}c^n_{i,k} + (1-\theta)\frac{\epsilon^n_{s,z,i,k}}{\Delta z^2}c^n_{i,k+1}\cdots$$

$$+(1-\theta)\frac{\epsilon^n_{s,z,i,k+1} - \epsilon^n_{s,z,i,k-1}}{(2\Delta z)^2}c^n_{i,k+1} - (1-\theta)\frac{\epsilon^n_{s,z,i,k+1} - \epsilon^n_{s,z,i,k-1}}{(2\Delta z^2)}c^n_{i,k-1} \tag{C.14}$$

Finally grouping coefficients per unknown, we get the following discrete approximation to implement into software:

$$\theta\left(-\frac{u_{i,k}^{n+1}}{2\Delta x}-\frac{\epsilon_{s,x,i,k}^{n+1}}{\Delta x^2}\right)c_{i-1,k}^{n+1}\cdots$$

$$+\theta\left(-\frac{w_{s,i,k}^{n+1}}{2\Delta z}+\frac{\epsilon_{s,z,i,k+1}^{n+1}-\epsilon_{s,z,i,k-1}^{n+1}}{(2\Delta z)^2}-\frac{\epsilon_{s,z,i,k}^{n+1}}{\Delta z^2}\right)c_{i,k-1}^{n+1}\cdots$$

$$+\left(\frac{1}{\Delta t}+\theta\left(\frac{2\epsilon_{s,x,i,k}^{n+1}}{\Delta x^2}+\frac{w_{s,i,k+1}^{n+1}-w_{s,i,k-1}^{n+1}}{2\Delta z}+\frac{2\epsilon_{s,z,i,k}^{n+1}}{\Delta z^2}\right)\right)c_{i,k}^{n+1}\cdots$$

$$+\theta\left(\frac{w_{s,i,k}^{n+1}}{2\Delta z}-\frac{\epsilon_{s,z,i,k+1}^{n+1}-\epsilon_{s,z,i,k-1}^{n+1}}{(2\Delta z)^2}-\frac{\epsilon_{s,z,i,k}^{n+1}}{\Delta z^2}\right)c_{i,k+1}^{n+1}\cdots$$

$$+\theta\left(\frac{u_{i,k}^{n+1}}{2\Delta x}-\frac{\epsilon_{s,x,i,k}^{n+1}}{\Delta x^2}\right)c_{i+1,k}^{n+1}=\cdots$$

$$(1-\theta)\left(\frac{u_{i,k}^{n}}{2\Delta x}+\frac{\epsilon_{s,x,i,k}^{n}}{\Delta x^2}\right)c_{i-1,k}^{n}\cdots$$

$$+(1-\theta)\left(\frac{w_{s,i,k}^{n}}{2\Delta z}-\frac{\epsilon_{s,z,i,k+1}^{n}-\epsilon_{s,z,i,k-1}^{n}}{(2\Delta z)^2}+\frac{\epsilon_{s,z,i,k}^{n}}{\Delta z^2}\right)c_{i,k-1}^{n}\cdots$$

$$+\left(\frac{1}{\Delta t}+(1-\theta)\left(-\frac{2\epsilon_{s,x,i,k}^{n}}{\Delta x^2}-\frac{w_{s,i,k+1}^{n}-w_{s,i,k-1}^{n}}{2\Delta z}-\frac{2\epsilon_{s,z,i,k}^{n}}{\Delta z^2}\right)\right)c_{i,k}^{n}\cdots$$

$$+(1-\theta)\left(-\frac{w_{s,i,k}^{n}}{2\Delta z}+\frac{\epsilon_{s,z,i,k+1}^{n}-\epsilon_{s,z,i,k-1}^{n}}{(2\Delta z)^2}+\frac{\epsilon_{s,z,i,k}^{n}}{\Delta z^2}\right)c_{i,k+1}^{n}\cdots$$

$$+(1-\theta)\left(-\frac{u_{i,k}^{n}}{2\Delta x}+\frac{\epsilon_{s,x,i,k}^{n}}{\Delta x^2}\right)c_{i+1,k}^{n} \tag{C.15}$$

**Left boundary:**

At the left boundary, the $i-1$ concentration variables are given as a boundary condition. The $i-1$ terms thus can be moved to the right lid. Terms with second derivatives in the horizontal are neglected as they are impossible to be discretized between two points. The vertical velocity term, which is the third term in Equation C.4, cannot be neglected at the vertical boundaries, as the vertical flow is assumed to go through these boundary grids to ensure continuity. This is mentioned in Subsection 2.2.1. Therefore the left and right boundary both contain extra terms in de discretization.

$$+\theta\left(-\frac{w_{s,i,k}^{n+1}+w_{i,k}^{n+1}}{2\Delta z}+\frac{\epsilon_{s,z,i,k+1}^{n+1}-\epsilon_{s,z,i,k-1}^{n+1}}{(2\Delta z)^2}-\frac{\epsilon_{s,z,i,k}^{n+1}}{\Delta z^2}\right)c_{i,k-1}^{n+1}\cdots$$

$$+\left(\frac{1}{\Delta t}+\theta\left(\frac{2\epsilon_{s,x,i,k}^{n+1}}{\Delta x^2}+\frac{w_{s,i,k+1}^{n+1}-w_{s,i,k-1}^{n+1}}{2\Delta z}+\frac{2\epsilon_{s,z,i,k}^{n+1}}{\Delta z^2}\right)\right)c_{i,k}^{n+1}\cdots$$

$$+\theta\left(\frac{w^{n+1}_{s,i,k}+w^{n+1}_{i,k}}{2\Delta z}-\frac{\epsilon^{n+1}_{s,z,i,k+1}-\epsilon^{n+1}_{s,z,i,k-1}}{(2\Delta z)^2}-\frac{\epsilon^{n+1}_{s,z,i,k}}{\Delta z^2}\right)c^{n+1}_{i,k+1}\cdots$$

$$+\theta\left(\frac{u^{n+1}_{i,k}}{2\Delta x}-\frac{\epsilon^{n+1}_{s,x,i,k}}{\Delta x^2}\right)c^{n+1}_{i+1,k}=\cdots$$

$$\theta\left(\frac{u^{n+1}_{i,k}}{2\Delta x}+\frac{\epsilon^{n+1}_{s,x,i,k}}{\Delta x^2}\right)c^{n+1}_{i-1,k}\cdots$$

$$(1-\theta)\left(\frac{u^{n}_{i,k}}{2\Delta x}+\frac{\epsilon^{n}_{s,x,i,k}}{\Delta x^2}\right)c^{n}_{i-1,k}\cdots$$

$$+(1-\theta)\left(\frac{w^{n}_{s,i,k}+w^{n}_{i,k}}{2\Delta z}-\frac{\epsilon^{n}_{s,z,i,k+1}-\epsilon^{n}_{s,z,i,k-1}}{(2\Delta z)^2}+\frac{\epsilon^{n}_{s,z,i,k}}{\Delta z^2}\right)c^{n}_{i,k-1}\cdots$$

$$+\left(\frac{1}{\Delta t}+(1-\theta)\left(-\frac{2\epsilon^{n}_{s,x,i,k}}{\Delta x^2}-\frac{w^{n}_{s,i,k+1}-w^{n}_{s,i,k-1}}{2\Delta z}-\frac{2\epsilon^{n}_{s,z,i,k}}{\Delta z^2}\right)\right)c^{n}_{i,k}\cdots$$

$$+(1-\theta)\left(-\frac{w^{n}_{s,i,k}+w^{n}_{i,k}}{2\Delta z}+\frac{\epsilon^{n}_{s,z,i,k+1}-\epsilon^{n}_{s,z,i,k-1}}{(2\Delta z)^2}+\frac{\epsilon^{n}_{s,z,i,k}}{\Delta z^2}\right)c^{n}_{i,k+1}\cdots$$

$$+(1-\theta)\left(-\frac{u^{n}_{i,k}}{2\Delta x}+\frac{\epsilon^{n}_{s,x,i,k}}{\Delta x^2}\right)c^{n}_{i+1,k} \tag{C.16}$$

**Right boundary:**

At the right boundary a modified scheme has to be applied as the $i+1$ concentration variable is not available there. Again the vertical velocity terms are not neglected to ensure continuity.

$$\theta\left(-\frac{u^{n+1}_{i,k}}{\Delta x}\right)c^{n+1}_{i-1,k}\cdots$$

$$+\theta\left(-\frac{w^{n+1}_{s,i,k}+w^{n+1}_{i,k}}{2\Delta z}+\frac{\epsilon^{n+1}_{s,z,i,k+1}-\epsilon^{n+1}_{s,z,i,k-1}}{(2\Delta z)^2}-\frac{\epsilon^{n+1}_{s,z,i,k}}{\Delta z^2}\right)c^{n+1}_{i,k-1}\cdots$$

$$+\left(\frac{1}{\Delta t}+\theta\left(\frac{w^{n+1}_{s,i,k+1}-w^{n+1}_{s,i,k-1}}{2\Delta z}+\frac{2\epsilon^{n+1}_{s,z,i,k}}{\Delta z^2}+\frac{u^{n+1}_{i,k}}{\Delta x}\right)\right)c^{n+1}_{i,k}\cdots$$

$$+\theta\left(\frac{w^{n+1}_{s,i,k}+w^{n+1}_{i,k}}{2\Delta z}-\frac{\epsilon^{n+1}_{s,z,i,k+1}-\epsilon^{n+1}_{s,z,i,k-1}}{(2\Delta z)^2}-\frac{\epsilon^{n+1}_{s,z,i,k}}{\Delta z^2}\right)c^{n+1}_{i,k+1}=\cdots$$

$$(1-\theta)\left(\frac{u^{n}_{i,k}}{\Delta x}\right)c^{n}_{i-1,k}\cdots$$

$$+(1-\theta)\left(\frac{w^n_{s,i,k}+w^n_{i,k}}{2\Delta z}-\frac{\epsilon^n_{s,z,i,k+1}-\epsilon^n_{s,z,i,k-1}}{(2\Delta z)^2}+\frac{\epsilon^n_{s,z,i,k}}{\Delta z^2}\right)c^n_{i,k-1}\cdots$$
$$+\left(\frac{1}{\Delta t}+(1-\theta)\left(-\frac{w^n_{s,i,k+1}-w^n_{s,i,k-1}}{2\Delta z}-\frac{2\epsilon^n_{s,z,i,k}}{\Delta z^2}-\frac{u^n_{i,k}}{\Delta x}\right)\right)c^n_{i,k}\cdots$$
$$+(1-\theta)\left(-\frac{w^n_{s,i,k}+w^n_{i,k}}{2\Delta z}+\frac{\epsilon^n_{s,z,i,k+1}-\epsilon^n_{s,z,i,k-1}}{(2\Delta z)^2}+\frac{\epsilon^n_{s,z,i,k}}{\Delta z^2}\right)c^n_{i,k+1}\cdots \tag{C.17}$$

**Surface boundary:**

Discretization of the surface boundary condition (Equation C.6) between the the two highest vertical points yields:

$$\frac{w^{n+1}_{s,i,k-1}+w^{n+1}_{s,i,k}}{2}\cdot\left(c^{n+1}_{i,k-1}+c^{n+1}_{i,k}\right)-\left(\epsilon^{n+1}_{s,z,i,k}+\epsilon^{n+1}_{s,z,i,k+1}\right)\cdot\frac{c^{n+1}_{i,k}-c^{n+1}_{i,k-1}}{\Delta z}=0$$

Rearranging to separate implicit and explicit terms yields:

$$\left(\frac{w^{n+1}_{s,i,k-1}+w^{n+1}_{s,i,k}}{2}+\frac{\epsilon^{n+1}_{s,z,i,k-1}+\epsilon^{n+1}_{s,z,i,k}}{\Delta z}\right)c^{n+1}_{i,k-1}+\left(\frac{w^{n+1}_{s,i,k-1}+w^{n+1}_{s,i,k}}{2}-\frac{\epsilon^{n+1}_{s,z,i,k-1}+\epsilon^{n+1}_{s,z,i,k}}{\Delta z}\right)c^{n+1}_{i,k}=0 \tag{C.18}$$

**Bottom boundary:**

The reference concentration is calculated halfway the two lowest vertical points, as this is the best approximation for the gradient. Discretization of the bottom boundary condition (Equation C.7) yields:

$$\frac{1}{\Delta z}\left(c^{n+1}_{i,k+1}-c^{n+1}_{i,k}\right)=\frac{w^{n+1}_{s,i,k}+w^{n+1}_{s,i,k+1}}{\epsilon^{n+1}_{s,z,i,k}+\epsilon^{n+1}_{s,z,i,k+1}}\cdot c_e$$

Rearranging to separate implicit and explicit terms yields:

$$c^{n+1}_{i,k+1}-c^{n+1}_{i,k}=\frac{w^{n+1}_{s,i,k}+w^{n+1}_{s,i,k+1}}{\epsilon^{n+1}_{s,z,i,k}+\epsilon^{n+1}_{s,z,i,k+1}}\cdot c_e\Delta z \tag{C.19}$$

## C.4 Particle fall velocity

### C.4.1 Spherical particle

The terminal fall velocity $w_s$ of a spherical particle is reached when the fluid drag force ($F_D = \frac{1}{2}\rho C_D \frac{\pi d^2}{4} w_s^2$) acting on the falling particle is equal to the gravity force ($F_G = (\rho_s-\rho) g \frac{\pi d^3}{6}$) acting on that particle.

$$w_s=\sqrt{\frac{4(s-1)gd}{3C_D}} \tag{C.20}$$

The drag coefficient depends on the Reynolds number ($Re = w_s\frac{d}{\nu}$). In the Stokes region ($Re < 1$) the drag coefficient is $C_D = \frac{24}{Re}$, yielding:

$$w_s=\frac{(s-1)gd^2}{18\nu} \tag{C.21}$$

For larger Reynolds numbers ($Re > 10^3$) a drag coefficient of $C_D \approx 0.4$ may be assumed, yielding:

$$w_s=\sqrt{3(s-1)gd} \tag{C.22}$$

### C.4.2 Non-spherical particle

The expressions valid for a spherical particle are not valid to natural sediment, because shape effects become relevant. The influence of shape is largest for larger particles. For small particle diameters ($1 < d \leq 100\mu m$) Eq. C.21 can still be applied:

$$w_s = \frac{(s-1)gd^2}{18\nu} \tag{C.23}$$

For intermediate particle diameters ($100 < d < 1000\mu m$) $w_s$ is given by:

$$w_s = \frac{10\nu}{d}\left[\left(1 + \frac{0.01(s-1)gd^3}{\nu^2}\right)^{0.5} - 1\right] \tag{C.24}$$

For large particle diameters ($d \geq 1000\mu m$) the following equation can be applied:

$$w_s = 1.1[(s-1)gd]^{0.5} \tag{C.25}$$

### C.4.3 Hindered settling

As described in section 2.3.4, hindered settling has a damping effect on the fall velocity of particles and is a function of the sediment concentration. The hindered settling factor is defined according to van Rijn (2007).

$$\phi_{hs} = w_s/w_{s,0} = (1 - 0.65c/c_{gel})^5 \tag{C.26}$$

With:

| | |
|---|---|
| $\phi_{hs}$ | hindered settling factor [-] |
| $w_s$ | sediment fall velocity [m/s] |
| $w_{s,0}$ | sediment fall velocity in clear water[m/s] |
| $c$ | suspended sediment concentration [kg/m$^3$] |
| $c_{gel}$ | gelling mass concentration [kg/m$^3$] |

The gelling mass concentration will be approximated using the silt factor (van Rijn, 2006).

$$c_{gel} = 1/f_{silt} \cdot c_{gel,max} \cdot \rho_p \qquad f_{silt,min} = 1 \tag{C.27}$$

With:

| | | |
|---|---|---|
| $f_{silt}$ | $= d_{sand}/d_{50}$ | hindered settling factor [-] |
| $d_{sand}$ | $= 62\ \mu m$ | particle diameter of sand [m] |
| $d_{50}$ | | grain diameter of 50$^{th}$ percentile [m] |
| $c_{gel,max}$ | $= 0.65$ | maximum mass concentration (sand) [kg/m$^3$] |
| $\rho_s$ | | density of sediment particle [kg/m$^3$] |

### C.4.4 Flocculation

As described in section 2.3.4, flocculation has an increasing effect on the fall velocity of particles and is a function of both the sediment concentration and the fraction distribution. The flocculation factor is defined according to van Rijn (2007).

$$\phi_{floc} = [4 + \log(2c/c_{gel})]^{\alpha} \tag{C.28}$$

With:

| | | |
|---|---|---|
| $\phi_{floc}$ | $\phi_{floc,min} = 1$ and $\phi_{floc,max} = 10$ | flocculation factor [-] |
| $c$ | | suspended sediment concentration [kg/m$^3$] |
| $c_{gel}$ | | gelling mass concentration (see eq. C.27) [kg/m$^3$] |
| $\alpha$ | $= \frac{d_{sand}}{d_{50}} - 1$ | $\alpha_{min} = 0$ and $\alpha_{max} = 3$ |

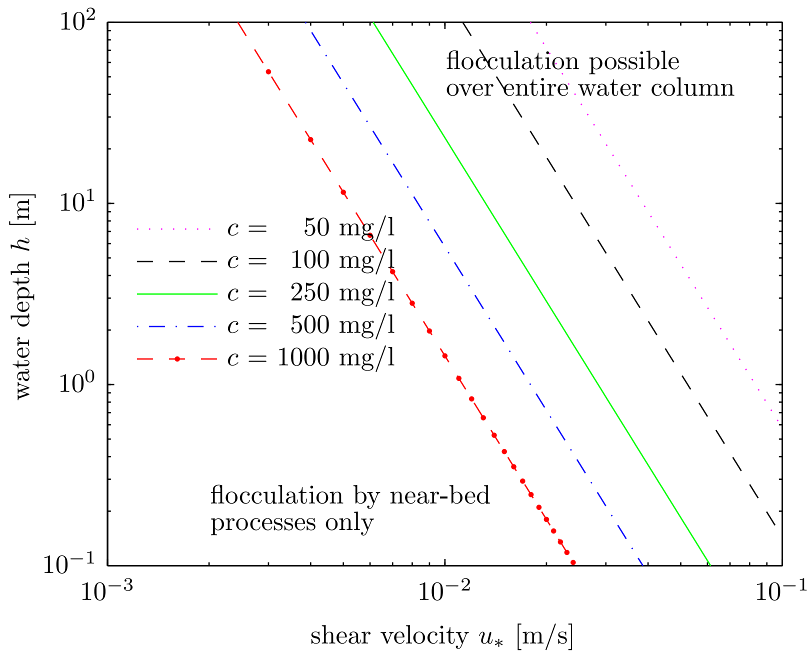


Figure C.2: Relative flocculation time of mud flocs in water column (Winterwerp and van Kesteren, 2004)

## C.5 Sediment mixing coefficient

The sediment mixing coefficient is used to include the mixing of sediment due to turbulence. This turbulence is generated by velocity gradients which are mainly caused by shear stresses at the bed or at the surface. Both shear stresses generate turbulent kinetic energy. With the use of the turbulent kinetic energy and the mixing length it is possible to determine the eddy viscosity. The eddy viscosity over the horizontal is assumed to be equal to the eddy viscosity over the horizontal. The eddy viscosity has the following form (Deltares, 2010):

$$\nu_T = c'_\mu L\sqrt{k} \tag{C.29}$$

With:

| | | |
|---|---|---|
| $c'_\mu$ | $c_\mu^{1/4}$ | a constant determined by calibration [-] |
| $L$ | $= \kappa \cdot z\sqrt{1-\frac{z}{d}}$ | mixing length [m] |
| $\kappa$ | $= 0.4$ | Von Kármán constant [-] |
| $z$ | | vertical position $[m]$ (bottom: $z = 0$) |
| $d$ | | water depth [m] |
| $k$ | | turbulent kinetic energy [m$^2$/s$^2$] |

The turbulent kinetic energy is determined with the *Algebraic closure model* for shear stresses at both bed and surface (Deltares, 2010). The surface shear stresses is caused by the wind and results in additional turbulence (see figure 2.4).

$$k = \frac{1}{\sqrt{c_\mu}}\left[\left(u_*^b\right)^2\left(1-\frac{z}{d}\right) + u_{*s}^2\frac{z}{d}\right] \tag{C.30}$$

With:

| | |
|---|---|
| $c_\mu$ | a constant determined by calibration $[-]$ |
| $k$ | turbulent kinetic energy [m$^2$/s$^2$] |

| | | |
|---|---|---|
| $u_{*b}$ | $= {c_f}^{0.5} \cdot \overline{u}$ | bed friction velocity [m/s] |
| $c_f$ | | bottom friction coefficient [-] (equation B.39) |
| $u_{*s}$ | $= \sqrt{\frac{\tau_s}{\rho_f}}$ | surface friction velocity [m/s] |
| $\rho$ | | density of the fluid [kg/m$^3$] |
| $\tau_s$ | $= \rho_{air} \cdot C_d \cdot {U_{10}}^2$ | surface shear stress [N/m$^2$] |
| $\rho_{air}$ | | density of air [kg/m$^3$] |
| $C_d$ | | drag coefficient [-] |
| $C_d$ | $= 1.2875 \cdot 10^{-3}$ | for $U_{10} < 7.5$ m/s (Holthuijsen, 2007, eq. 9.3.6) |
| $C_d$ | $= (0.8 + 0.065 U_{10}) \cdot 10^{-3}$ | for $U_{10} \geq 7.5$ m/s |
| $U_{10}$ | | wind speed at 10 meters above the surface [m/s] |
| $z$ | | vertical position [m] (bottom: $z = 0$) |
| $d$ | | water depth [m] |

The eddy viscosity generates transport of momentum. The transport mechanism of a passive tracer is called the eddy diffusivity. In many cases the transport of a passive tracer is more effective than the transport of momentum. The ratio between both properties is called the *Prandtl-Schmidt number*.

$$D_T = \frac{\nu_T}{\sigma} \tag{C.31}$$

With:

| | |
|---|---|
| $D_T$ | eddy diffusivity [m$^2$/s] |
| $\nu_T$ | turbulent eddy viscosity [m$^2$/s] |
| $\sigma$ | Prandtl-Schmidt number [-] (suspended sediment transport: $\sigma = 1.0$) |

The calculated eddy diffusivity is related to the sediment mixing coefficient by the $\beta - factor$ (van Rijn, 1984) with represents the difference in mixing between the fluid and the sediment.

$$\epsilon_s = \beta \cdot \epsilon_f \tag{C.32}$$

With:

| | | |
|---|---|---|
| $\epsilon_s$ | | sediment mixing coefficient [m$^2$/s] |
| $\beta$ | $= 1 + 2\left(\frac{w_s}{u_*}\right)^2$ | $'\beta - factor'$ (van Rijn, 1984) [-] |
| $w_s$ | | particle fall velocity [m/s] |
| $u_*$ | | bed shear stress due to currents [m/s] |
| $\epsilon_f$ | | fluid mixing coefficient ($\approx D_T$) [m$^2$/s] |

The fluid mixing coefficient is assumed to be equal to the eddy diffusion as only the mixing due to turbulence is taken into account.

# Appendix D

# Influence coefficients

## D.1 Derivative of reliability function

By definition, the influence coefficients can be calculated according to the following equation. This can be done in the design point of both the Monte Carlo simulation and the FORM. This are the so called *alpha*-values which are produced by the FORM.

$$\alpha_i = \frac{-\frac{\partial Z}{\partial X_i}\sigma_{X_i}}{\sigma_z} \tag{D.1}$$

## D.2 Covariance

The Monte Carlo simulation generates a large number of realizations of base variables and the resulting values of $Z$. By calculating the covariance between a certain base variable and the values of $Z$, and taking into account the standard deviation of both variables, it is possible to derive a approximation of the influence coefficients according to the following equation:

$$\alpha_i = \frac{Cov(X_i, Z)}{\sigma_{X_i}\sigma_Z} \tag{D.2}$$

## D.3 Normally distributed variables

In case of normally distributed variables, the influence coefficients can be determined which an estimate of the probability of failure and the design point. The probability of failure follows from the Monte Carlo simulation. The realizations of the base variables enable the approximation of both the mean value and the standard deviation. For both the Weibull and uniform distributed variables, these approximations appears to be good input parameter for the transformation of these parameter into normally distributed variables. For the Bernoulli distribution this transformation is less reliable as this is a discrete distribution.

$$P_f \approx \frac{n_f}{n} \tag{D.3}$$

$$\alpha_i = \frac{X_i^* - \mu_{X_i}}{\beta\sigma_{X_i}} \tag{D.4}$$

With:

| | |
|---|---|
| $P_f$ | probability of failure (Monte Carlo simulation) |
| $n_f$ | number of simualtions, for which $Z < 0$ |
| $n$ | number of simulations |

| | |
|---|---|
| $\alpha_i$ | influence coefficient |
| $X_i$ | base variable |
| $X_i^*$ | value of $X_i$ in the design point |
| $\sigma$ | standard deviation |
| $\mu$ | expected value |
| $\beta$ | $= \Phi^{-1}(P_f)$ reliability coefficient |
| $Z$ | reliability function (Equation 4.1) |

# Appendix E

# Model evaluation

The model is evaluated in three different ways as treated is Section 3.1. This appendix gives an overview of the input data and output data used in the model evaluations.

## E.1 Cases - [redacted]

[redacted]

```
%% Case 1: silt
%
% $Id: settling_basin01.m 2915 2011-03-30 11:06:14Z William de Lange $
% $Date: 2011-03-30 13:06:14 +0200 (Wed, 30 Mar 2011) $
% $Author: William de Lange $
% $Revision: 2915 $
%
% Input data for [redacted]model
OPT= struct(...
    [redacted] ...                               % discharge [m3/s]
    'C_in',10, ...                               % sediment concentration [kg/m3]
    'U_10',0, ...                                % wind speed at height of 10 meters [m/s]
    'angle',90, ...                              % wind angle [degree] (compared to flow)
    'B',200, ...                                 % width of the basin [m]
    'd_out',4, ...                               % water depth at the outflow [m]
    'nx',21, ...                                 % number of horizontal points
    'dx',10, ...                                 % distance between horizontal points
    'nr_vert_pts',40, ...                        % number of vertical points [-]
    'fractions',[10e-6 30e-6 50e-6], ...         % diameter of sediment fractions [m]
    'fractions_value',[0.33 0.33 0.34], ...      % distribution over fractions [m]
    'dt',3600 * 24 * 2, ...                      % time step [s]
    'nt',6, ...                                  % number of timesteps [-]
    'ws_min',2.0e-9, ...                         % minimum fall velocity [m/s]
    'S',0, ...                                   % salinity [psu]
    'T',15, ...                                  % water temperature [degree Celsius]
    'hs',0, ...                                  % include hindered settling [ 1 or 0 ]
    'floc',0, ...                                % include flocculation [ 1 or 0 ]
    'refconc', 0, ...                            % calculates reference concentration
    'morphodynamic',0, ...                       % incl. bottom update [ 1 or 0 ]
    'ks',0.02, ...                               % effective roughness height [m]
    'plotresult',1 ...                           % plot output results [ 1 or 0 ]
    );
Outflow_Conc = [redacted]instationary(OPT);      % outflow concentration [kg/m3 or g/l]
```

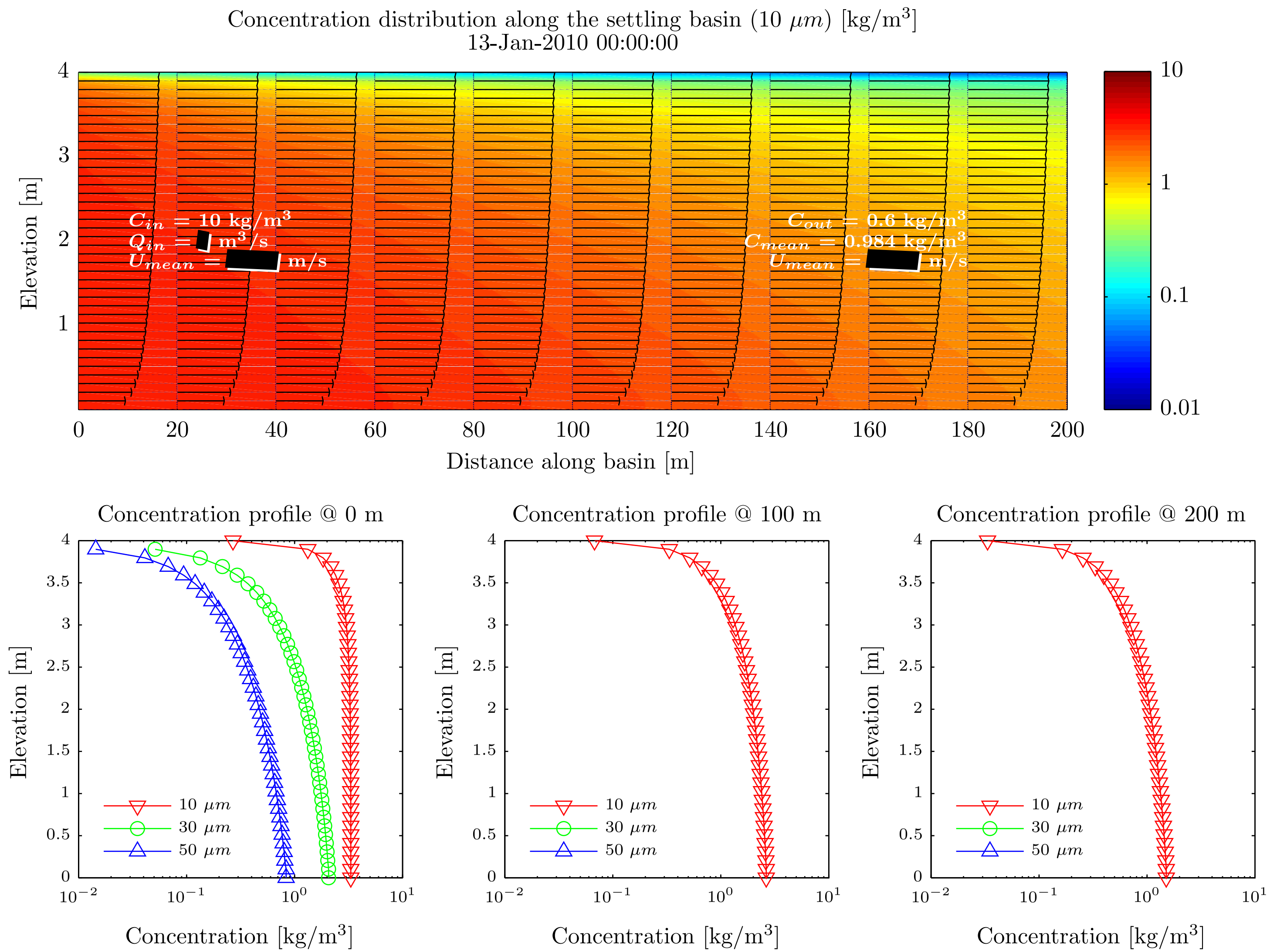


Figure E.2: Project model results Case 1

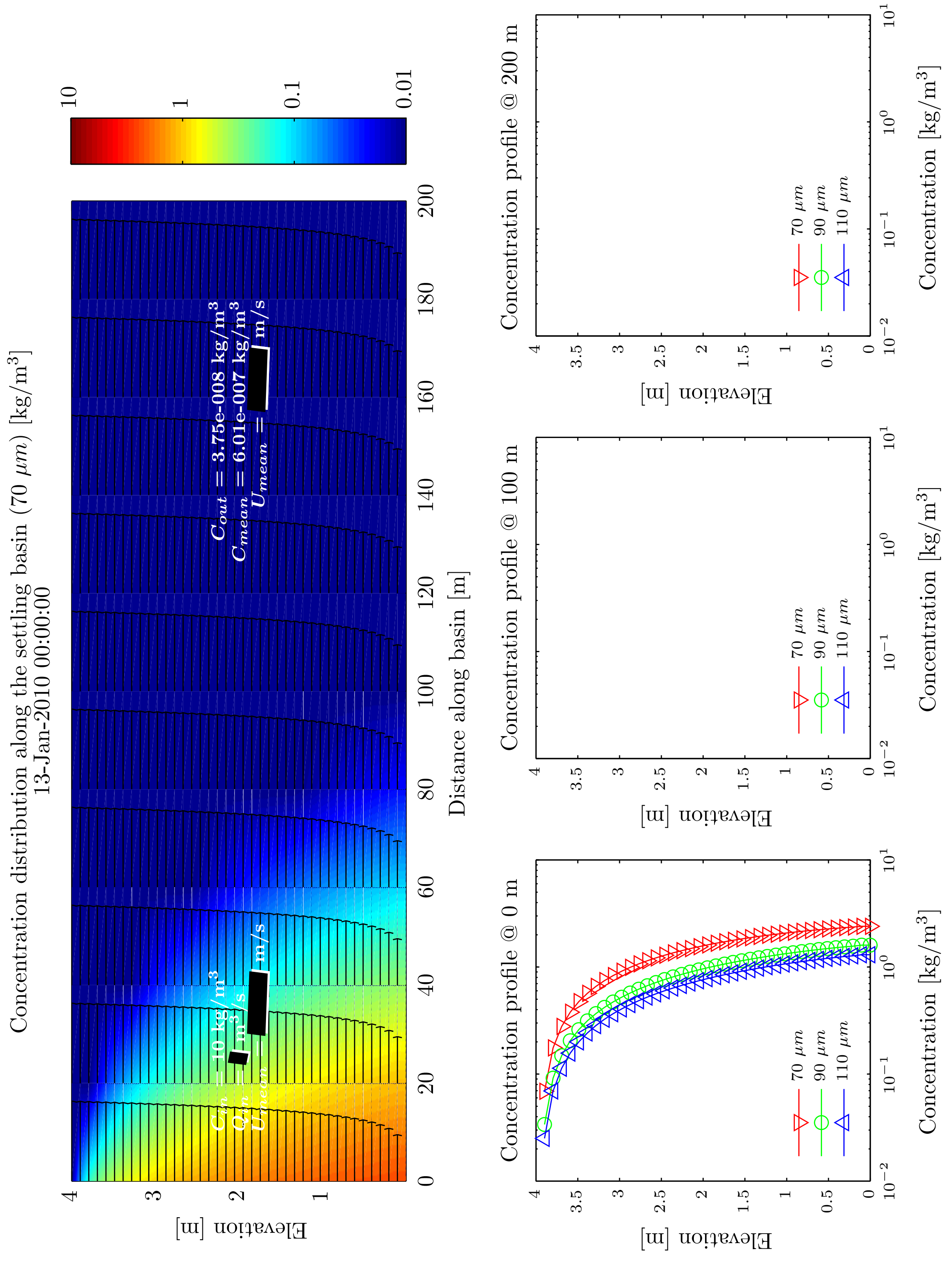


Figure E.4: Project model results Case 2

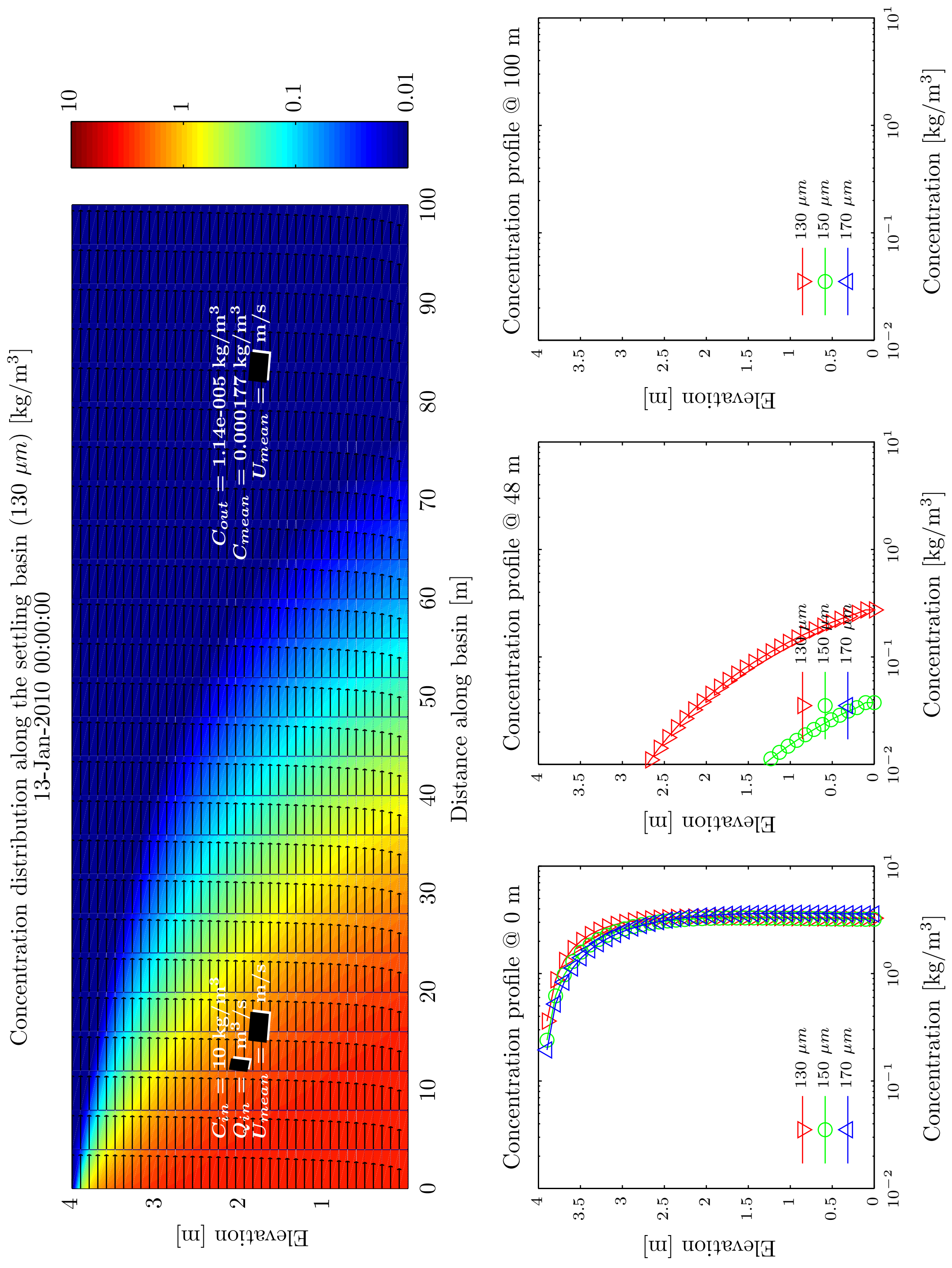


Figure E.6: Project model results Case 3

## E.2 Equilibrium sediment concentration

The bed boundary condition is compared with a analytical solution of Hjelmfelt and Lenau (1970) (Subsection 3.1.3). The upstream boundary condition for the suspended sediment concentration is 0 kg/m$^3$. After a certain distance the suspended sediment concentration reaches an equilibrium concentration of suspended sediment.

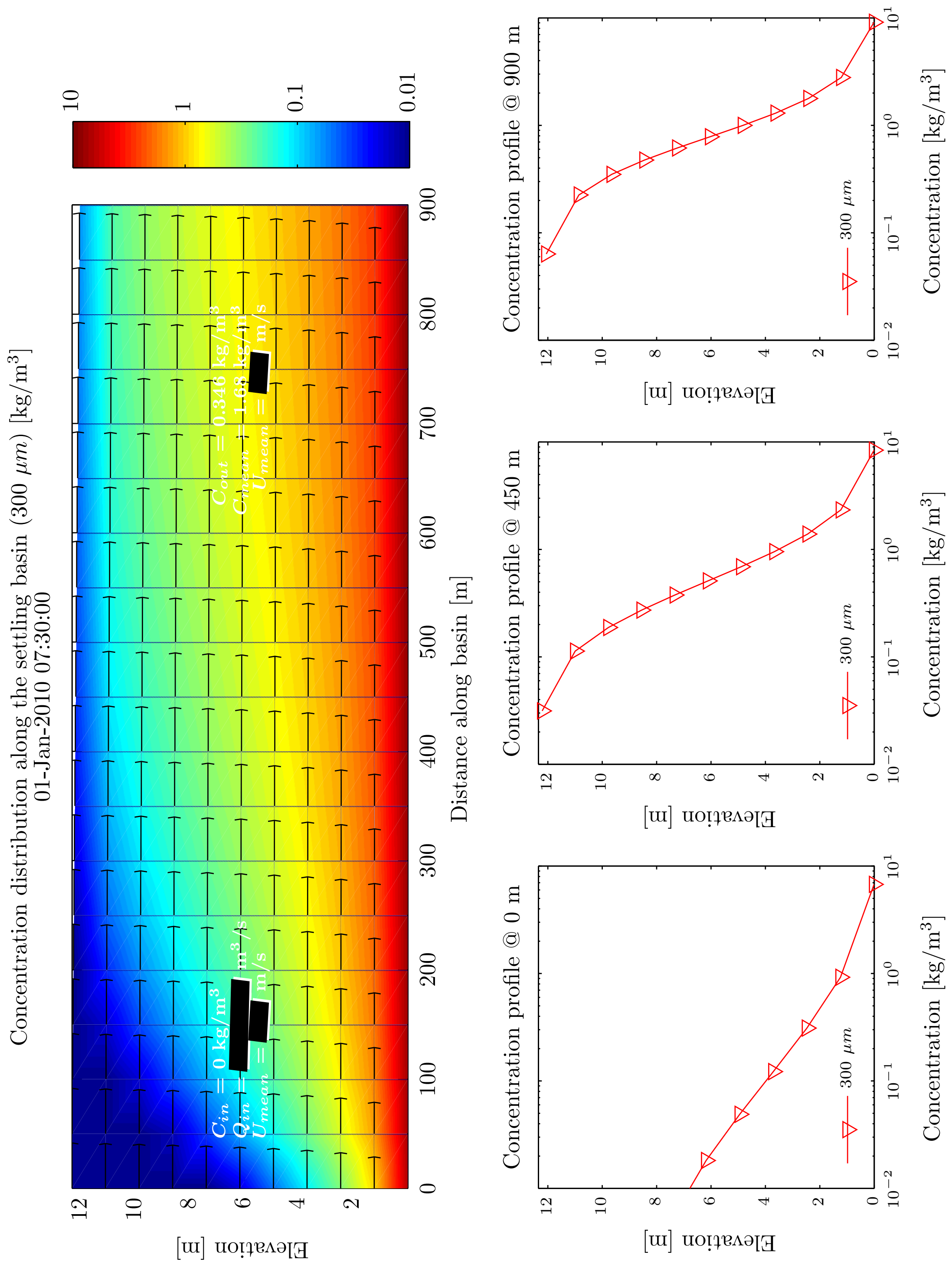


Figure E.7: Clean water which reaches equilibrium sediment concentration

## E.3 Equilibrium bed level

In order to demonstrate the general applicability of the project model, a highly suspended river is modelled. The initial bed level was at 0 m for the whole domain. After some time the bed level reaches an equilibrium bed level with a constant sediment flux.

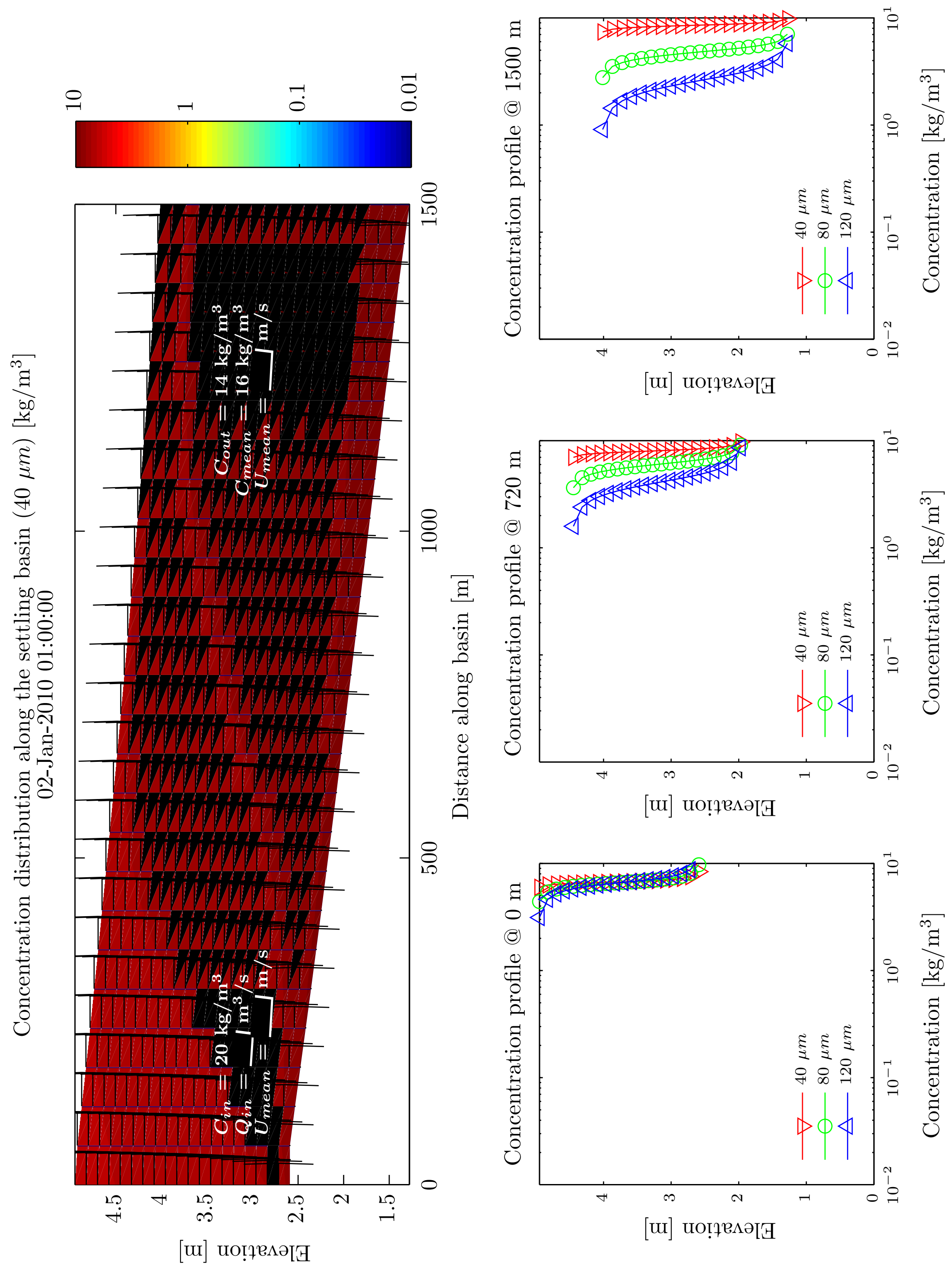


Figure E.8: Highly suspended river which reaches equilibrium bed (initial bed level: $z = 0$)